

Proteome and Phosphoproteome Analysis of Commensally Induced Dendritic Cell Maturation States

Dissertation

der Mathematisch-Naturwissenschaftlichen Fakultät
der Eberhard Karls Universität Tübingen
zur Erlangung des Grades eines
Doktors der Naturwissenschaften
(Dr. rer. nat.)

vorgelegt von
Ali Giray Korkmaz
aus Adana/Türkei

Tübingen
2022

Gedruckt mit Genehmigung der Mathematisch-Naturwissenschaftlichen Fakultät der
Eberhard Karls Universität Tübingen.

Tag der mündlichen Qualifikation:

21.11.2022

Dekan:

Prof. Dr. Thilo Stehle

1. Berichterstatter/-in:

Prof. Dr. Julia-Stefanie Frick

2. Berichterstatter/-in:

Prof. Dr. Nadine Ziemert

Table of Contents

	Page
List of Abbreviations	4
Summary	6
Zusammenfassung	7
List of Publications	8
Personal Contribution	9
1. Introduction	11
1.1. Background	11
1.2. Dendritic cells as inflammatory mediators	12
1.3. Dendritic cell maturation	15
1.4. Proteomics Study	19
2. Aims	21
3. Results and Discussion	22
3.1. Dendritic cell maturation and the resulting proteome landscape	22
3.2. Bacterial stimulation and pro-inflammatory factor expression	28
3.3. Canonical pathways and upstream regulators of dendritic cell maturation	30
3.4. Phosphoproteome analysis of dendritic cell maturation	35
3.5. Results summary and discussion	41
Acknowledgements	44
Bibliography	45
Appendix	
Full manuscript of “Proteome and phosphoproteome analysis of commensally induced dendritic cell maturation states”	
Full manuscript of “TLR Signaling-induced CD103-expressing Cells Protect Against Intestinal Inflammation”	

List of Abbreviations

ABCA1	ABC-binding cassette transporter-1
ACIN1	Apoptotic chromatin condensation inducer-1
AGC	PKA, PKC, PKG family of kinases
AKT1	AKT Serine/Threonine 1
APCs	Antigen presenting cells
CCL	Chemokine (C-C motif) ligand
CD	Cluster of differentiation
CDC42	Cell division control protein-42
CDK	Cyclin-dependent kinase
CEBPB	CCAAT enhancer binding protein beta
COX2	Cyclooxygenase-2
CX3CR1	CX3C chemokine receptor-1
CXCL	Chemokine (C-X-C motif) ligand
DCs	Dendritic cells
DOCK8	Dedicator of cytokinesis-8
DSS	Dextran sulfate sodium
DUSP1	Dual specificity phosphate-1
EGR-1	Early Growth Response-1
ELISA	Enzyme linked immunosorbent assay
FACS	Fluorescence activated cell sorting
FcR	Fc receptor
GWAS	Genome-wide association study
HDL	High-density lipoprotein
HLA	Human leukocyte antigen
IBD	Inflammatory bowel disease
IFN	Interferon
I κ B	Inhibitor of kappa-B
iNOS	Inducible nitrogen oxide synthase
IRF3	Interferon regulatory transcription factor-3
JAK/STAT	Janus kinase/signal transducers and activators of transcription

LPS	Lipopolysaccharide
LXR	Liver-X receptor
MAVS	Mitochondrial antiviral-signaling protein
MHC-II	Major histocompatibility complex II
mTOR	Mammalian target of rapamycin
MyD88	Myeloid differentiation primary response-88
NFAT	Nuclear factor of activated T-cells
NfκB	Nuclear factor kappa-B
NOD	Nucleotide-binding oligomerization domain-containing protein
NR1H3	Nuclear Receptor Subfamily-1 Group-H Member-3
NSAIDs	Nonsteroidal anti-inflammatory drugs
PPARs	Peroxisome proliferator-activated receptors
PRRs	Pattern recognition receptors
RAG1	Recombination activating gene-1
RIG1	Retinoic acid inducible gene-1
RXR	Retinoid X receptor
PI3K	Phosphoinositide-3-kinase
PTGER4	Prostaglandin E Receptor-4
PTGS2	Prostaglandin-endoperoxide synthase-2
SAMS1	S-adenosylmethionine synthase-1
SOCS1	Suppressor of cytokine signaling-1
STAT1	Signal transducer and activator of transcription-1
SWI/SNF	SWItch/Sucrose Non-Fermentable
TBK1	Serine/threonine-protein kinase TBK1
TGF	Transforming growth factor
TLRs	Toll-like receptors
TNFα	Tumor necrosis factor alpha
TREM1	Triggering receptor expressed on myeloid cells-1

Summary

Dendritic cells are integral components of the mammalian immune system, which take part in orchestrating and regulating the delicate balance of immune response. Dendritic cells are potent activators of destructive responses of the immune system, at the same time, dendritic cells also take part in activating regulatory T-cells and dampening overly destructive immune responses, as well as mediating immune tolerance. This multifaceted and at times contradictory functions of dendritic cells are, at least in part, brought about by the phenotypical differences that regulate the respective immune response. As an example of the importance of the differences in dendritic cell phenotypes, we have previously reported that feeding of *B. vulgatus* to IL-2^{-/-} mice leads to production of semi-mature dendritic cells and prevents colitis, whereas feeding of *E. coli* to IL-2^{-/-} mice leads to fully mature dendritic cells and severe intestinal inflammation (Waidmann et al., 2003). Therefore, we believe that these maturation differences in dendritic cells have an important effect on disease manifestation and progression in colitis. However, the intracellular factors and processes taking part in regulating dendritic cell maturation are not fully understood. In our project we aimed to provide a closer look at the proteome profiles of DCs and intracellular signalling pathways/processes that underlie dendritic cell maturation. Using dendritic cells generated *in vitro* from cultured mouse bone marrow, we induced semi-maturation by *B. vulgatus* stimulation and complete maturation by *E. coli* stimulation. The resulting cells were harvested and lysed for proteomic analysis. We performed comparative proteomics to analyse proteins that differ in their expression levels, and shotgun phosphoproteomics to detect proteins that are differentially phosphorylated. Thereby we aimed to catalogue proteins, processes, and signalling pathways that lead to the observed phenotypical differences between the semi-mature and fully-mature dendritic cells. To this end, subsequent to the mass spectrometry runs we have employed bioinformatical tools i.e. pathway analysis, upstream regulator analysis and kinase analysis. We have determined various pathways and regulators, many of which have key roles in immunity and inflammation. We hope that our results provide a more systematic and comprehensive information on factors governing different states of dendritic cell maturation, as well as the effects of commensal and pathogenic bacteria on dendritic cell mediated immune regulation.

Zusammenfassung

Dendritische Zellen sind essentielle Komponenten des Säugtier Immunsystems, die eine instrumentierende und eine regelnde Rolle bei der Balancierung der Immunantwort spielen. Dendritische Zellen sind wirkmächtige Aktivatoren von zerstörerischen Antworten des Immunsystems, zugleich können die Dendritische Zellen regulatorische T-Zellen aktivieren und auf diese Weise die übermäßige Immunantwort schwächen und Immuntoleranz vermitteln. Diese vielseitige und zuweilen widersprechende Dendritische Zell Funktionen sind, mindestens teilweise, von phänotypischen Differenzen die entsprechende Immunantwort regulieren, herbeigeführt. Als ein Beispiel für solche wichtige Differenzen in Dendritische Zell Phänotypen, haben wir vorher berichtet dass die Einspeisung von *B. vulgatus* zu IL-2^{-/-} Mäuse führt zu der Entsehung von semi-mature Dendritische Zellen und verhindert colitis Manifestation, im Gegenteil, die Einspeisung von *E. coli* zu IL-2^{-/-} Mäuse führt zu der Entstehung von fully-mature Dendritische Zellen und schwere colitis Manifestation (Waidmann *et al.*, 2003). Demzufolge denken wir dass die unterschiedliche Dendritische Zell maturation Zustände spielen eine wichtige Rolle in colitis Manifestation und Weiterentwicklung. Dagegen sind die Intrazelluläre Faktoren und Prozesse die Dendritische Zell maturation regulieren sind nicht ausführlich geforscht. In unserer Projekt haben wir untergenommen, ein näheres Blick auf die Proteome-Profilen von DZs und intrazelluläre Signalwege die DZ Maturation unterliegen zu verschaffen. In unserer Projekt haben wir Dendritische Zellen *in vitro* bei Maus Knochenmark isoliert und angelegt, und haben wir semi-maturation bei *B. vulgatus* Stimulation und complete-maturation bei *E. coli* Stimulation ausgeführt. Die resultierende Zellen haben wir für die Proteomeanalyse aberntet und lysiert. Die Proteine die unterschiedliche Expressionsebene aufweisen zu identifizieren, haben wir eine komparative Proteomeanalyse durchgeführt, und Proteine die unterschiedliche Phosphorylationsstatus aufweisen zu identifizieren, haben wir eine shotgun Phosphoproteomeanalyse durchgeführt. Dadurch haben wir erzielt, die Proteine, die Prozesse und die Signalwege die zu beobachtete phänotypische Differenzen zwischen semi-mature und fully-mature Zellen führen, aufzulisten. Zu diesem Zweck, nachfolglich die Massspektrometer Analysen, haben wir bioinformatische Instrumente i.e. Signalweganalyse, upstream regulator Analyse und kinase Analyse angestellt. Wir haben unterschiedliche Signalwege und Regulatoren die in der Immunität und Entzündung wichtige Rolle spielen bestimmt. Wir hoffen, dass unsere Ergebnisse eine mehr systematische und ausführliche Kenntnisse über die Faktoren die die Dendritische Zell Maturation verwalten anbieten, und auch die Effekte der kommensalen und pathogenen Bakterien über Dendritische Zell abhängige Immunregulation weiter erklären.

List of publications

1. "Proteome and phosphoproteome analysis of commensally induced dendritic cell maturation states"

Ali Giray Korkmaz, Todor Popov, Loulou Peisl, Marius Cosmin Codrea, Sven Nahnsen, Alexander Steimle, Ana Velic, Boris Macek, Martin von Bergen, Joerg Bernhardt, Julia-Stefanie Frick

PMID: 29155090

May 2018, Journal of Proteomics, Volume: 180, Print: 15.10.2017

[doi: 10.1016/j.jprot.2017.11.008]

2. "TLR Signaling-induced CD103-expressing Cells Protect Against Intestinal Inflammation"

Alexandra Wittmann, Peter A. Bron, Iris van Swam, Michiel Kleerebezem, Patrick Adam, Kerstin Gronbach, Sarah Menz, Isabell Flade, Annika Bender, Andrea Schäfer, Ali G. Korkmaz, Raphael Parusel, Ingo Autenrieth, Julia-Stefanie Frick

PMID: 25647153

Mar 2016, Inflammatory Bowel Diseases, Volume: 21 Number: 3, Print: 2.02.2015

[doi: 10.1097/MIB.0000000000000292]

Personal Contribution

Publication 1: “Proteome and phosphoproteome analysis of commensally induced dendritic cell maturation states”

All molecular biology techniques except mass spectrometry, as well as primary cell culture generation and sample collection have been performed by me, with help from group members listed in the co-authors list. These include ELISAs, FACS analysis, Western Blots, animal sacrifice, cell culture, and sample collection for mass spectrometry. I have taken part in the statistical analysis of the mass spectrometry data, generating the list of differentially expressed proteins. Ingenuity Pathway Analysis, upstream regulator analysis, reactome pathway analysis, and kinase activity analysis have been performed by me, using indicated software and with supervision from the listed co-authors. Writing of the article, figure creation and revisions were done almost exclusively by me.

Publication 2: “TLR Signaling-induced CD103-expressing Cells Protect Against Intestinal Inflammation”

I have helped with the flow cytometric analysis of TLRs and cell surface markers on lamina propria dendritic cells, including cellular staining, flow cytometry run, flow cytometry data collection and analysis. I have assisted with the representation of the data and the revision of the manuscript.



**Erklärung nach § 5 Abs. 2 Nr. 8 der Promotionsordnung der Math.-Nat. Fakultät
-Anteil an gemeinschaftlichen Veröffentlichungen-
Nur bei kumulativer Dissertation erforderlich!**

**Declaration according to § 5 Abs. 2 No. 8 of the PhD regulations of the Faculty of
Science
-Collaborative Publications-
For Cumulative Theses Only!**

Last Name, First Name: Korkmaz, Ali Giray

List of Publications

1. *Proteome and phosphoproteome analysis of commensally induced dendritic cell maturation states*
May 2018, Journal of Proteomics, Volume: 180, Print: 15.10.2017
2. *TLR Signaling-induced CD103-expressing Cells Protect Against Intestinal Inflammation*
Mar 2016, Inflammatory Bowel Diseases, Volume: 21 Number: 3, Print: 2.02.2015
- 3.

Nr.	Accepted publication yes/no	List of authors	Position of candidate in list of authors	Scientific ideas by the candidate (%)	Data generation by the candidate (%)	Analysis and Interpretation by the candidate (%)	Paper writing done by the candidate (%)
<i>Optionally, you can also declare the above-stated categories in a written statement on a separate sheet of paper.</i>							
1	Yes	See below	1	60	80	80	95
2	Yes	See below	11	5	5	5	5
3							

I confirm that the above-stated is correct.

2.3.2022

Date, Signature of the candidate

I/We certify that the above-stated is correct.

25.2.2022

Date, Signature of the doctoral committee or at least of one of the supervisors

1. Introduction

1.1. Background

Inflammatory bowel diseases, such as ulcerative colitis and Crohn's disease are complex diseases with environmental factors, with the host immune system and the patient's genetic composition all contributing to the pathophysiology of the disease. Among the environmental factors, the gut microbiota plays a crucial role. The importance of gut microbiota has been exemplified by numerous research reports focusing on the microbial composition of the intestine. Antibiotics treatments that reduce the number of anaerobic bacteria such as metronidazole (Rutgeerts et al., 1995), or long-term ciprofloxacin usage (Turunen et al., 1998) combined with conventional therapy improved disease outcome in patients with IBD. Introducing beneficial bacterial species such as *E. coli Nissle 1917* or *S. boulardii* have also shown to be beneficial by maintaining remission in IBD patients (Guslandi, Mezzi, Sorghi, & Testoni, 2000; Malchow, 1997). Shifts in the composition of the gut flora and dysbiosis are also often observed in patients with Crohn's Disease and ulcerative colitis (Frank et al., 2011; Morgan et al., 2012; Ott et al., 2004). The importance of the gut flora is further proven by various mouse models of IBD, where germ-free breeding of animals results in reduced severity of intestinal inflammation. A seminal study on this subject is done by Sellon et al.; in this study IL-10 deficient mice kept under germ-free conditions did not develop colitis, whereas IL-10 deficient mice kept under SPF conditions showed clinical signs of colitis. The same phenomenon has been observed in several other animal models that are susceptible to colitis, such as IL-2 deficient mice and $\alpha\beta$ T-cell receptor deficient mice and HLA-27/ β 2m transgenic rats which remain healthy when bred under germ-free conditions (Dianda et al., 1997; Sadlack et al., 1993; Schultz et al., 1999; Sellon et al., 1998; Taurog et al., 1994).

1.2. Dendritic Cells as Inflammatory Mediators

The gut flora found in the diseased and healthy mice is in direct contact with the host gastrointestinal tract. The gastrointestinal tract is a major immunological hub and thus a key player at every stage of IBD. The intestinal immune system has evolved to attain balance with the complex and diverse microbiota it contains and continuously interacts with. It needs to maintain tolerance to the harmless or beneficial bacterial species, at the same time, it needs to distinguish and defend against potential pathogens. All of this requires a meticulously constructed and maintained immune cell network. Dendritic cells are integral components of this immense immune network and they take part in constructing and regulating the balance of immune response. Dendritic cells (DCs) are potent activators of destructive responses of the immune system, at the same time, dendritic cells also take part in activating regulatory T-cells and dampening overly-destructive immune responses, as well as mediating immune tolerance. To perform these functions, dendritic cells survey the gut environment and actively sample the antigens they encounter. To this end, dendritic cells use numerous mechanisms to effectively take up and process antigens. Receptor mediated endocytosis, such as endocytosis via mlg and FcR molecules is a major mechanism of antigen uptake (Lanzavecchia, 1990). In addition, in order to capture soluble antigens, dendritic cells possess the ability to engulf high volumes of liquid via macropinocytosis (Sallusto & Lanzavecchia, 1994). Another interesting antigen take-up and processing mechanism is presented by CX3CR1 positive DCs in the lamina propria; these dendritic cells extend transepithelial dendrites to take up bacterial components in a CX3CR1 dependent manner (Niess et al., 2005).

Dendritic cell surveillance and antigen uptake is closely connected to the process of recognizing distinct patterns of the antigens DCs encounter. Dendritic cells sense their environment via pattern recognition receptors (PRRs) that are expressed in abundance on the cell surface. PRRs recognize the distinct structural components of the bacteria including lipopolysaccharides (LPS), cell wall peptidoglycans, lipoproteins, and unmethylated CpGs that are hallmarks of bacterial DNA. Among pattern recognition receptors are the receptor kinases, C-type lectin receptors, NOD-like and RIG-1 like receptors and Toll-like receptors (TLRs). TLRs are indispensable for proper dendritic cell function, and thus are also closely linked to

inflammatory and immune diseases. Currently there are 10 known TLRs, recognizing numerous microbial-associated molecular patterns (Akira, Takeda, & Kaisho, 2001). TLR2 recognizes bacterial wall lipoteichoic acids, lipoproteins and LPS from *P. gingivalis*, whereas TLR4 is required for recognizing LPS from many Gram-negative bacteria such as *E. coli*. TLR5 recognizes flagellin, and TLR9 binds preferentially to bacterial DNA by recognizing unmethylated CpG islands (Bron, Van Baarlen, & Kleerebezem, 2012; Kawai & Akira, 2010; Takeuchi et al., 1999). Different subsets of DCs express these TLRs in different proportions, which enable these DCs to mount a specific response to a particular type of antigen they recognize (Kadowaki et al., 2001; Jarrossay, Napolitani, Colonna, Sallusto, & Lanzavecchia, 2001).

Dendritic cell response to the antigens is dictated by the molecular machinery the dendritic cell possesses. Downstream of Toll-like receptors and other membrane-bound or intracellular pattern recognition receptors, lies an intricate molecular network that orchestrates the dendritic cell's response to the recognized antigen. Immune receptors, interleukins and cytokines, transcription factors, various phosphatases and kinases all function together to determine whether the dendritic cell response will be tolerogenic or inflammatory. The number of factors involved is overwhelming, nevertheless, there are certain master regulators to induce and direct the molecular network. The inducible nitric oxide synthase iNOS is one of the potent inflammatory regulators and its transcription is induced by TLR and CD14 signaling to the cytosol. Binding of LPS to TLR4 and CD14 inactivates I κ B and activates NF κ B, which induces iNOS expression. Under inflammatory stimuli, iNOS expression is further enhanced by STAT1 via IFN γ signaling (Du & Low, 2001; Rao, 2015; Schröder et al., 2000). In turn, iNOS has regulatory roles in cytokine production and nitric oxide acts as defensive toxin against potential pathogens (Bogdan, 2001; Coleman, 2001; Niedbala, Wei, Piedrafita, Xu, & Liew, 1999). Increased iNOS expression has been reported in patients with ulcerative colitis and Crohn's disease, additionally, inhibiting iNOS expression by quercitrin and amentoflavone reduced inflammation and disease severity in mouse DSS models of colitis and rats with colitis respectively (Boughton-Smith et al., 1993; Camuesco et al., 2004; Rachmilewitz et al., 1995; Sakthivel & Guruvayoorappan, 2013).

The inducible cyclooxygenase COX-2 is another factor that lies downstream of TLR signaling and has crucial roles regarding the regulation of inflammation. Cyclooxygenases function in prostaglandin synthesis by catalyzing the conversion of arachidonic acid to prostanoids; COX-1 is constitutively expressed in many tissues including the colon, whereas its isoform COX-2 is expressed only when induced (Baek, 2002; Kam & See, 2000). COX-2 is induced via expression of pro-inflammatory cytokines such as IL-1 β and TNF- α in the sites of inflammation, and the suppression of inflammation by blocking COX-2 by non-steroidal anti-inflammatory drugs (NSAIDs) has been proven long ago to be effective in alleviating inflammation (Seibert & Masferrer, 1994; Hawkey, 1999; Singer et al., 1998). Increased COX-2 expression has been observed in the intestinal epithelial cells of the IBD patients, and was not detected in healthy colon or ileum. In line with this data, the selective inhibition of COX-2 has been considered a promising therapy option to reduce inflammation in patients with ulcerative colitis and Crohn's disease (El Miedany, Youssef, Ahmed, & El Gaafary, 2006; Biancone, Tosti, De Nigris, Fantini, & Pallone, 2003; McCartney, Mitchell, Fairclough, Farthing, & Warner, 1999).

SOCS1 (suppressor of cytokine signaling 1), is a key regulator of cytokine signaling and its targets include IFN- α , IFN- γ , IL-4, IL-6, IL-12, and TNF- α pathways (Fujimoto & Naka, 2003). SOCS1 expression is known to be regulated upon the recognition of LPS and unmethylated CpG islands by TLRs, directly or indirectly by the activity of various signaling molecules such as EGR-1 and cytokines including IL-6 and IFN- β (Fujimoto & Naka, 2003; Mostecky, Showalter, & Rothman, 2005). The importance of the immune suppressor function of SOCS1 is observed in SOCS1 knock-out mice, which die within 3 weeks of age as a result of severe systemic inflammation (Starr et al., 1998). Macrophages from *SOCS1*^{-/-} mice are activated and readily produce high levels of nitric oxide even without LPS stimulation (Kinjyo et al., 2002). Additionally, SOCS1 has been shown to be necessary to maintain the immune tolerance in the intestine; *SOCS1*^{-/-} *RAG2*^{-/-} mice developed severe colitis which was abated by the introduction of immune suppressor T-regs expressing IL-10 (Chinen et al., 2011). Another important molecule that links LPS response, TLR signaling and dendritic cell function is ABCA1 (ATP binding cassette transporter-1) that transports cellular cholesterol and phospholipids to the membrane (Yokoyama, 1998; Oram & Yokoyama, 1996). However, the transport function of ABCA1 has a wider range of effect than solely transporting

phospholipids; ABCA1 also functions in LPS efflux from macrophages, and the regulation of ABCA1 affects many aspects of immunity and inflammation. LPS efflux is important for LPS tolerance, the rate of removal of LPS from cells affects the time-frame in which the immune cells develop reduced sensitivity to LPS. This is exemplified in ABCA1^{-/-} macrophages in which the LPS induced tolerance was prolonged, thus rendering these cells irresponsive to cytokine inducing stimuli (Thompson, Gauthier, Varley, & Kitchens, 2010). Moreover, compared to wild type murine macrophages, ABCA1^{-/-} macrophages show increased expression of IL-1 β , TNF- α , IL-6, iNOS and COX2 upon LPS stimulation (Levine, Parker, Donnelly, Walsh, & Rubin, 1993).

1.3. Dendritic cell maturation

The ability of dendritic cells to regulate immune responses is dependent on their maturation state and the maturation process. Dendritic cell maturation affects the dendritic cell's ability to uptake and process antigens, to migrate and to stimulate T-cells (Mellman & Steinman, 2001). In steady-state, the DCs are considered immature/resting, displaying low surface expression of major histocompatibility complex class II (MHC-II) and CD40, CD80, CD86 co-stimulatory molecules. Encountering potential pathogens such as LPS, viral/bacterial DNA, bacterial cell wall components as well as immunogenic stimuli from other immune cells in the form of inflammatory cytokines can direct these steady-state DCs into maturation. This results in increased surface MHC-II expression, increased co-stimulatory molecule expression, downregulation of antigen uptake, secretion of chemokines by the dendritic cell and migration to lymphoid organs. Increased MHC and co-stimulatory molecule expression is crucial for the dendritic cells' ability to present antigens, and for interacting with and stimulating immune effector T-cells and B-cells. Downregulation of antigen uptake is necessary for switching to a potent antigen presenting cell phenotype, by increasing proteolytic function of the lysosomes and preparing MHC-I and MHC-II molecules to be loaded by the processed antigen for being presented on the cell surface (Trombetta et al., 2003). Secretion of chemokines is another outreaching arm of dendritic cell function; by using various potent molecules including IL-1 α , IL-1 β , IL-6, IL-7, IL-10, IL-12, IL-17, TNF- α , TGF- β , CCLs, CXCLs, and many others, matured DCs are able to orchestrate the multifunctional T-cell and B-cell responses (de Saint-Vis et al., 1998; Jensen & Gad, 2010).

IL-1 α and IL-1 β are two pro-inflammatory cytokines that were shown to induce Th2 responses and are involved in various inflammatory diseases (Schmitz et al., 2005; Steinman, 1988). The IL-6 family of cytokines have many far reaching functions, including induction of B-cell differentiation into plasma cells, inducing T-cell proliferation, differentiation of naive CD4⁺ cells into Th17 cells, inhibiting TGF- β induced T-reg differentiation and inducing the differentiation of CD8⁺ T-cells into cytotoxic T-cells (Bettelli et al., 2006; Kishimoto, Akira, Narazaki, & Taga, 1995; Korn, Bettelli, Oukka, & Kuchroo, 2009; Okada et al., 1988; Tanaka, Narazaki, & Kishimoto, 2014). IL-6 is also known to have strong pro-inflammatory effects especially at the beginning of an inflammatory response, and its involvement in IBD and treatment options regulating its functions is well-documented (Allocca, Jovani, Fiorino, Schreiber, & Danese, 2013; Atreya & Neurath, 2005; Bernardo et al., 2012; Gabay, 2006; Mudter & Neurath, 2007).

IL-10 family of cytokines have potent anti-inflammatory effects that play a central role in regulating and dampening extensive pro-inflammatory stimuli (Sabat et al., 2010). Insufficient expression of IL-10 is directly linked to exaggerated inflammatory response, tissue damage and development of IBD (Li, Alli, Vogel, & Geiger, 2014; Siewe et al., 2006; Sturlan et al., 2001). IL-10 deficient mice raised in a germ-free environment do not develop colitis, and the *IL-10* gene is within the susceptibility locus for ulcerative colitis (Franke et al., 2008; Keubler, Buettner, Häger, & Bleich, 2015). The immunosuppressive IL-10 signal is propagated by JAK-STAT pathway in a STAT3 dependent manner, which regulates the expression of a battery of immunomodulatory genes (Ouyang, Rutz, Crellin, Valdez, & Hymowitz, 2011; Takeda et al., 1999; Wills-Karp, Nathan, Page, & Karp, 2010). Moreover, with the support of additional anti-inflammatory molecules TNF- α and IL-27, IL-10 can hamper the development of inflammatory effector cells, reduce the potency of these cells and enhance regulatory T-cell functions (Mocellin, Panelli, Wang, Nagorsen, & Marincola, 2003; Sabat et al., 2010).

IL-12 family of cytokines, commonly secreted by APCs, are key cytokines that regulate the differentiation and expansion of Th1 cells (Hsieh et al., 1993; Manetti et al., 1993). IL-12 promotes the proliferation and cytolytic activity of natural killer cells and directs the production of various interferons by these cell types (Chan et al., 1991). In mouse models, abnormally increased IL-12 secretion by APCs has been shown to predispose the animals to autoimmune

disorders (Trembleau et al., 1995), and GWAS studies identified *IL-23* gene to be associated with inflammatory bowel diseases (Duerr et al., 2006). Additionally, blocking IL-12 and IL-23 pro-inflammatory activity by a monoclonal antibody has been shown to be beneficial in inducing remission in active Crohn's disease patients (Mannon et al., 2004).

TNF- α is a major inflammatory regulator that is mainly produced by activated macrophages and monocytes during acute inflammation. Through its various receptors such as TNFRs, CD40, CD27 and FAS, it regulates numerous aspects of immunity including immune cell differentiation/proliferation and migration, expression of acute phase proteins, apoptotic response and many others. Increased production of TNF- α has been observed in intestinal biopsies from patients with IBD, and proposed to be a marker for intestinal inflammation (Braegger, Nicholls, & Murch, 1992; Reimund et al., 1996). These findings were supported by mouse models of chronic intestinal inflammation; mice with a 3' regulatory element deletion of the TNF transcript have increased production of TNF- α displayed IBD like inflammation profile (Kontoyiannis, Pasparakis, Pizarro, Cominelli, & Kollias, 1999). Similarly, dysregulated TNF- α production has been shown to be pathogenic in mouse models of IBD (Neurath et al., 1997; Mueller, 2002). In line with its profound immunological importance, TNF- α targeting molecules have been employed in a clinical setting to treat inflammatory diseases for more than 20 years. Taken together, exposure to maturing stimuli such as potential pathogens results in a dendritic cell response that is brought about by the concerted action of surface receptors, numerous cytokines and signaling pathways, which enables the cell become an immunologically active antigen presenting cell.

In their steady-state in the tissues, dendritic cells are considered immature/resting. However, the term immature or resting does not mean these dendritic cells are immunologically inactive. A subset of these cells undergo homeostatic or sometimes termed partial/semi-maturation, and are able to migrate to lymph nodes and T-cell zones to induce tolerance to self-antigens (Dalod, Chelbi, Malissen, & Lawrence, 2014; Lutz & Schuler, 2002; Ohi et al., 2004; Probst, Lagnel, Kollias, & Van Den Broek, 2003; Spörri & Reis e Sousa, 2005). This subset of dendritic cells that are considered partially mature or semi-mature are described as having a high surface expression levels of MHC-II and co-stimulatory molecules. This is in contrast to the DCs in the steady state which express low levels of these molecules,

however, it is also quite different to the dendritic cells that are fully matured and activated to mount a defensive immune response. Compared to fully mature dendritic cells, these cells do not secrete elevated levels of IL-6, IL-1 β , TNF- α or IL-12 and thus do not incite an inflammatory response. Instead, it has been reported that they induce IL-10⁺ CD4⁺ T-regs and therefore are considered tolerogenic (Dudek, Martin, Garg, & Agostinis, 2013; Lutz & Schuler, 2002).

Regardless of the terminology used to describe them, it is apparent that dendritic cells exist in distinct phenotypical and functional states which is required to react to a high number of diverse stimulants in a nondestructive but effectively protective manner. Our previous research highlighted this aspect of dendritic cell biology by studying the effects of different commensal bacterial strains on dendritic cell response and colitis induction in mice. In one of our studies (Waidmann et al., 2003), gnotobiotic IL2^{-/-} mice were co-colonized or mono-colonized either with a *B. vulgatus* mpk strain or with an *E. coli* mpk strain isolated from the fecal flora of specific pathogen-free (SPF) IL-2^{-/-} mice. Disease induction and severity were compared between different colonization groups and also between *E. coli* Nissle colonized IL2^{-/-} mice. Mono-colonization with *E. coli* mpk resulted in colitis induction whereas mono-colonization with *B. vulgatus* mpk did not, and co-colonization with both strains prevented the induction of the disease. Moreover, disease induction and severity correlated with the expression of inflammatory factors; *E. coli* mpk mono-colonized mice showed increased expression of IFN- γ , TNF- α , CD14, and IL-10 compared to *B. vulgatus* mpk mono-colonized mice. These findings prompted us to study the inflammatory effects of these two bacterial strains on dendritic cells using a dendritic cell culture system in C57BL/6 wild type mice (Frick et al., 2006). Dendritic cells stimulated with *E. coli* mpk expressed high levels of activation markers MHC-II, CD80, CD86 and CD40 compared to unstimulated DCs, suggesting dendritic cell activation and maturation. *E. coli* mpk stimulated DCs also expressed increased levels of pro-inflammatory effectors IL-12 and TNF- α . In contrast, the expression level of the activation markers and pro-inflammatory factors IL-12 and TNF- α remained unaffected in DCs stimulated with *B. vulgatus* mpk. Moreover, pretreatment of dendritic cells with *B. vulgatus* mpk prevented the dendritic cells to express IL-12 and TNF- α upon subsequent *E. coli* mpk stimulation. This study also showed differential T-helper cell polarization by different bacteria; *E. coli* mpk stimulated DCs polarized naive T-cells in Th1

direction, whereas *B. vulgatus* mpk stimulation did not produce a polarizing effect. Taken together, our previous research suggested profound differences between the two bacterial strains in the context of colitis induction and associated increase in inflammatory factors. *E. coli* mpk was observed to act as an inflammation inducer and was effective in directing the dendritic cells toward activation/maturation and T-cell polarization. In contrast, *B. vulgatus* mpk did not induce DC activation/maturation, did not elicit an inflammatory response, moreover, *B. vulgatus* mpk pretreatment in cell culture or co-colonization in mice blocked the inflammatory effects of *E. coli* mpk.

1.4. Proteomics Study

In this study, our proteomics analysis focused on three distinct dendritic cell populations; 1) steady-state DCs to serve as a control group, 2) DCs stimulated with *B. vulgatus* to obtain a semi-mature population, and 3) DCs stimulated with *E. coli* to obtain a fully-mature population, all done in cell culture. The starting point of our analyses was the pairwise proteome comparison of these three dendritic cell populations to obtain a list of proteins that exhibit a relative abundance difference. Thereby, we have determined that 301 proteins were differentially expressed among the groups of *E. coli* vs. PBS; *B. vulgatus* vs. PBS; and *B. vulgatus* vs. *E. coli* in total. For our subsequent analyses we used these 301 proteins as the input data set, and employed bioinformatical tools to elucidate the biological processes underlying the observed expression difference and in turn, the observed phenotypical difference between different DC maturation states. The first step in our analysis was to determine the effects of bacterial stimulation on cardinal cellular processes on a broader scale. Using gene ontology database, we acquired a detailed list of subprocesses, and mapped the list of differentially regulated proteins using Voronoi tessellation method. This simple method enabled us to visualize every single protein and the processes they affect. After elucidating the general patterns of difference in protein expression, we next employed functional grouping and pathway analysis to investigate the biological basis of the inflammatory response difference among dendritic cell maturation states. Our bioinformatical analyses in that step revealed how dendritic cells under bacterial influence operated their inflammatory machinery differently. Proteins belonging to signaling pathways such as TLR signaling, IRF signaling and leukocyte activation pathways showed different levels of

expression. PPAR signaling, LXR/RXR signaling and JAK/STAT signaling, which have branching immune functions were also among the pathways that were affected. Our subsequent upstream regulator analysis identified 37 factors that were predicted to have different activation states between the pairwise comparisons of steady state, *B. vulgatus* stimulated and *E. coli* stimulated DCs. Among others, these factors included PTGER4, ABCA1, DUSP1 and SOCS1 all of which have comprehensive regulatory functions in inflammation and cellular response to pathogens, thus providing hints about the cellular mechanisms behind different immune responses. After our comparative proteomics and the bioinformatical analysis that followed, we have performed an additional proteomics run targeting the phosphoproteome. In our pairwise comparisons, we have identified 465 differentially regulated phosphosites on 301 peptides. Differentially phosphorylated proteins included several major kinases such as CDK2 and CDC42, transcription factors junD and NFAT-2, cytokine regulator IRF3 and epigenetic factors SMARCC1 and SMARCC2. Taken together, we established a detailed proteomic picture of dendritic cells under distinct bacterial stimuli and maturation states, and investigated the underlying differences in cellular processes with a particular focus on inflammatory pathways.

2. Aims

The complicated process of dendritic cell maturation and its effects on immune regulation have been extensively studied in numerous mouse models and diseases including IBD. The research on the individual factors affecting dendritic cell maturation and the resulting immune-regulatory effects have also been studied. What is so far missing, however, is a more wide-scale approach to identify regulators and effectors of dendritic cell maturation. We aimed to provide information on that aspect, by performing proteomics assays on *in vitro* murine primary dendritic cell cultures stimulated with distinct bacteria. Our aims included:

1. Determining the differentially expressed proteins between distinct dendritic cell maturation states.
2. Annotating these proteins to the respective cellular processes and creating a visual catalogue of the results.
3. Predicting the effector pathways and upstream regulators of dendritic cell maturation by bioinformatical analysis.
4. Performing a quantitative phosphoproteomics analysis of distinct dendritic cell maturation states to gain insights about the phosphoproteomic landscape.

3. Results

3.1. Dendritic cell maturation and the resulting proteome landscape

In our previous study (Gronbach et al., 2014), we reported notable differences in cytokine release patterns of DCs in mice colonized with *B. vulgatus* and *E. coli*. Similar to these findings, our other study (Wittmann, Bron, Swam, & Kleerebezem, 2015, *publication 2*), reported *in vivo* differences in TLR2/TLR4 expression, the resulting proinflammatory signaling cascade and differences in the severity of colitis observed between mice treated with strains of bacteria that are weak or potent inducers of TLR2/TLR4 signaling. In this study we have aimed to replicate and build upon these *in vivo* observations in cell culture, and analyze the resulting dendritic cell populations via mass spectrometry. As obtaining sufficient biological material *in vivo* would be very difficult, we used cultured BMDCs where we have stimulated steady-state DCs with *B. vulgatus* to induce semi-maturation, with *E. coli* to induce full-maturation. Following the stimulation, we have first analyzed the resulting cytokine secretion profiles. After stimulation for 16h with either *B. vulgatus* or *E. coli*, and a restimulation following that for 24h hours with *E. coli* to assess semi/full-maturation, we have performed ELISA on cell culture supernatants for IL-6, TNF α , IL-1 β and IL-12p40 (Fig. 1a). Our results have shown that steady-state DCs secrete negligible amounts of the mentioned cytokines. When these cells are challenged by bacteria, *E. coli* stimulated cells secreted the highest level of cytokines, whereas *B. vulgatus* stimulated DCs secreted low levels of pro-inflammatory cytokines, exhibiting a profile similar to resting DCs. Restimulating *B. vulgatus* stimulated DCs with *E. coli* resulted in a different profile of pro-inflammatory cytokine secretion than restimulating the PBS controls (steady-state DCs) and *E. coli* stimulated cells, depicting their difference in the maturation spectrum. In addition to pro-inflammatory cytokine secretion levels, we have also assessed the expression levels of surface activation markers MHC-II and CD40 to provide additional information into dendritic cell activation states. In the *B. vulgatus* stimulated DC sample, MHC-II⁺ population increased from 26% to 47% compared to PBS controls, and to 70% in *E. coli* stimulated sample. CD40 expression levels were affected similarly, increasing from 9% to 25% in *B. vulgatus* stimulated cells compared to controls, and to 88% in *E. coli* stimulated dendritic cells (Fig. 1a). The observed differences in pro-inflammatory cytokine secretion and cell surface activation marker expression levels are

dependent on intact TLR2 and TLR4 signaling. When we repeated the same experiments with dendritic cells isolated from TLR2^{-/-}/TLR4^{-/-} double knockout mice, these cells showed no significant difference in cytokine secretion levels and cell surface activation markers upon bacterial stimulation (Fig 1b).

A Wild-Type C57BL/6 mice

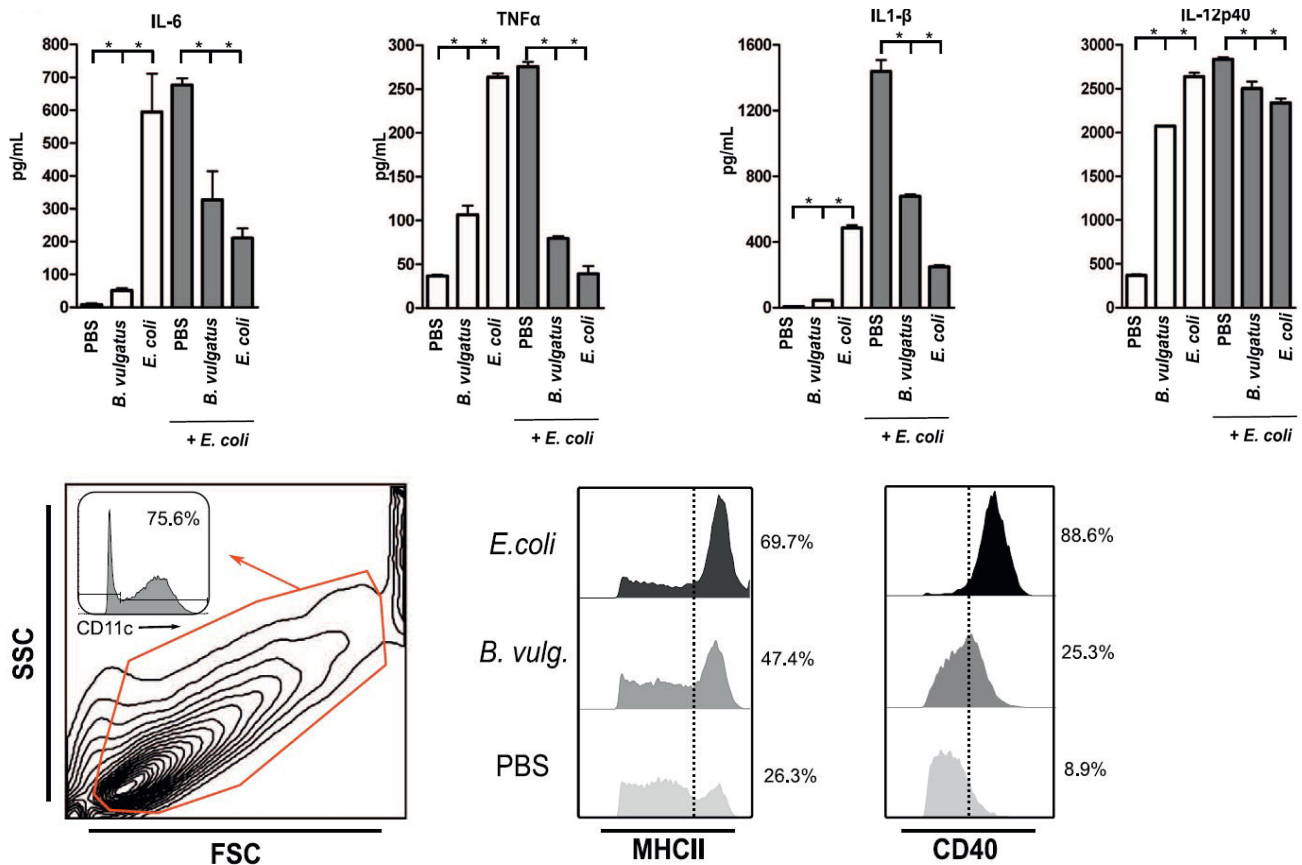


Fig1. a) Cytokine secretion and surface activation marker profiles of cultured bone marrow derived dendritic cells, isolated from wild type C57BL/6 mice. Stimulation is done after 7 days of dendritic cell culture, by incubating with bacteria for 16h for the first stimulation, and 24h for the additional *E. coli* stimulation following the first stimulation. ELISA is performed with cell culture supernatants for all cases. For flow cytometric analysis of cell surface markers, viable cell population is gated on FSC/SSC axis, which was gated again depending on CD11c expression. CD11c⁺ population was used for the assessment of MHC-II and CD40 expression. Results are representative of 3 independent experiments. *p < 0.05.

B TLR2^{-/-} TLR4^{-/-} C57BL/6 mice

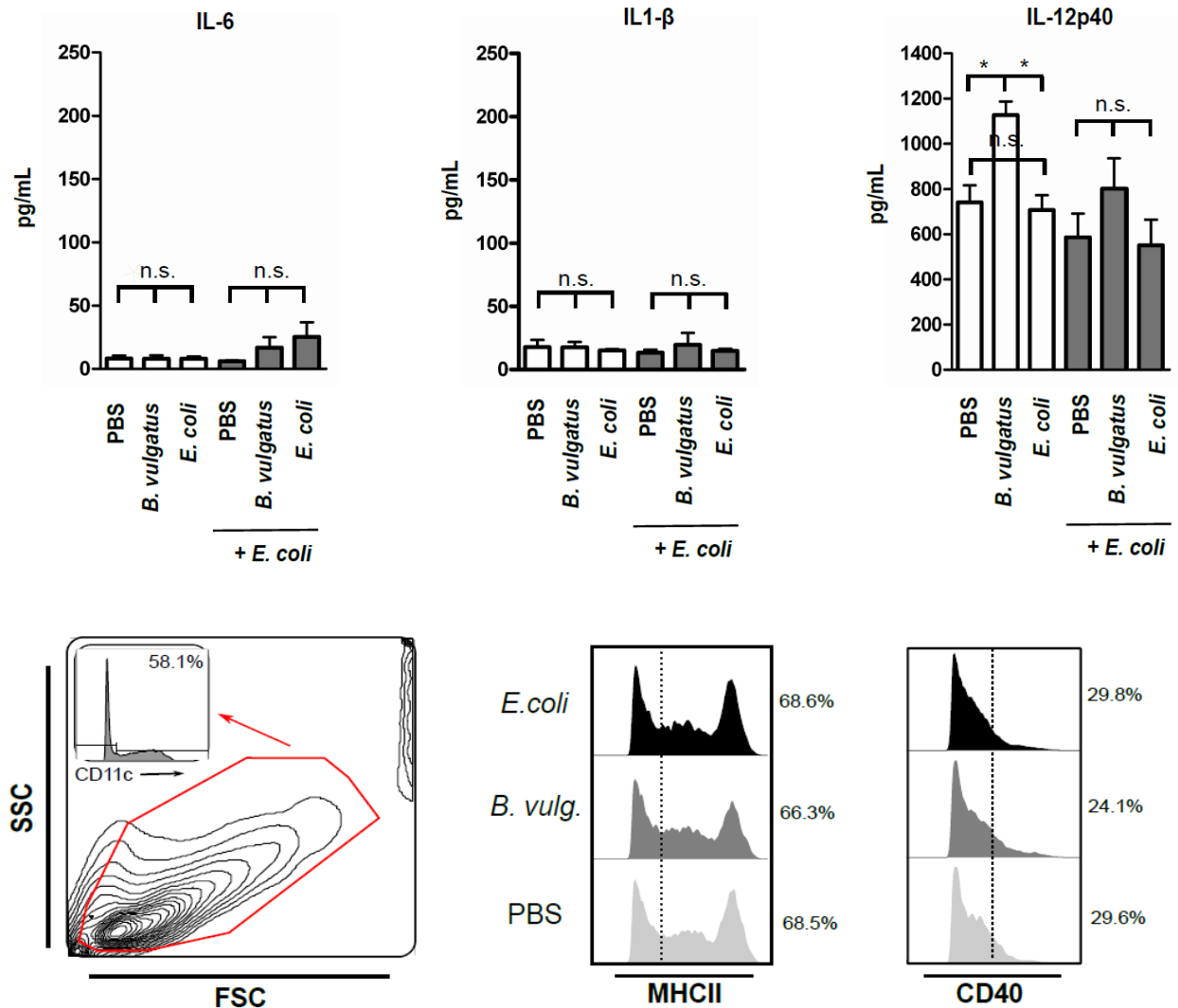


Fig1. b) Cytokine secretion and surface activation marker profiles of cultured bone marrow derived dendritic cells, isolated from TLR2+TLR4 double knockout mice on a C57BL/6 background. Stimulation is done after 7 days of dendritic cell culture, by incubating with bacteria for 16h for the first stimulation, and 24h for the additional *E. coli* stimulation following the first stimulation. ELISA is performed with cell culture supernatants for all cases. For flow cytometric analysis of cell surface markers, viable cell population is gated on FSC/SSC axis, which was gated again depending on CD11c expression. CD11c⁺ population was used for the assessment of MHC-II and CD40 expression. Results are representative of 3 independent experiments. *p < 0.05.

The levels of pro-inflammatory cytokine secretion and surface activation marker expression is regulated via a complex and overarching intracellular machinery. Therefore, in our three different experimental groups, we expected expression level differences in cellular processes concerned with immunity and inflammation as well as auxiliary processes. Accordingly, as a starting point of our proteome analysis, we aimed to determine the affected cellular processes on a general level. For this purpose, we used the online DAVID (Database for Annotation, Visualization and Integrated Discovery) website which offers various tools to functionally annotate a given set of proteins. Functional annotation is dependent on the Gene Ontology database that hierarchically organizes proteins with regard to their functions in cellular processes. As an input list, we have uploaded our set of 301 differentially regulated proteins to the DAVID server. This input list included all proteins that showed an expression difference between the comparisons; *B. vulgatus* vs. *E. coli*, *B. vulgatus* vs. PBS and *E. coli* vs. PBS. After functional annotation was performed, we organized the cellular processes into 14 major groups as can be seen in Fig. 2a. The organization of these processes into a 2D plane is shown in Fig. 2b, and their detailed hierarchical subprocesses are shown in Fig. 2f. To effectively visualize all our proteins and the cellular processes that they take part in, we chose to use the method of Voronoi tessellations. This method makes it possible to visualize multilevel data on 2D scale, at the same time representing expression levels in various intensities of color (Otto et al., 2010). Our Voronoi map for the *B. vulgatus* vs *E. coli* at 16h can be seen in Fig. 2; Fig. 2b shows the 14 major processes, Fig. 2f depicts subprocesses as smaller polygons within the bigger polygons that belong to the major processes. Fig. 2c-d-e consist of single cells that belong to single proteins together with their relative levels of expression. Relative levels of expression of a protein between a pairwise comparison is represented by varying intensities of color, with blue denoting a lower level and red denoting a higher level for that particular protein. It is important to note that as a protein can take part in more than one cellular process, several of our proteins are represented more than once in the Voronoi treemap. This way of visualizing data in 2D makes it possible to compare the expression levels of single proteins and depict the different patterns between immature, semi-mature and fully mature DCs in varying levels of detail.

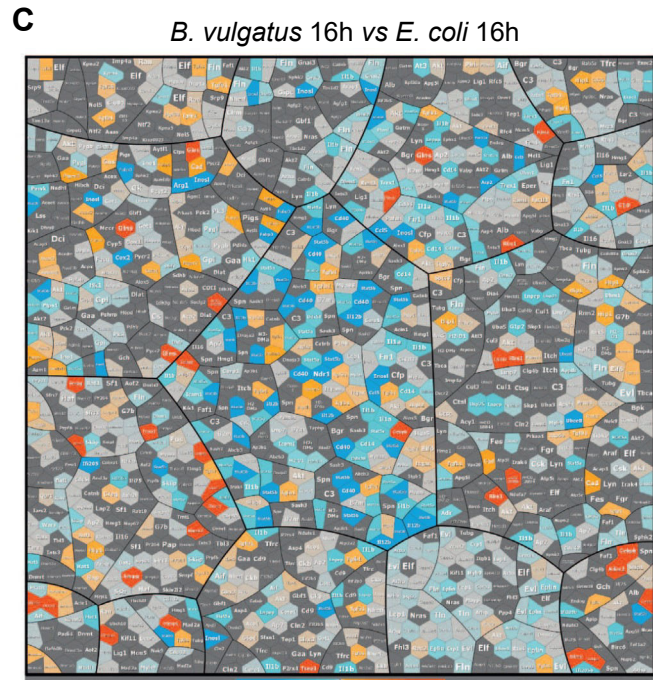
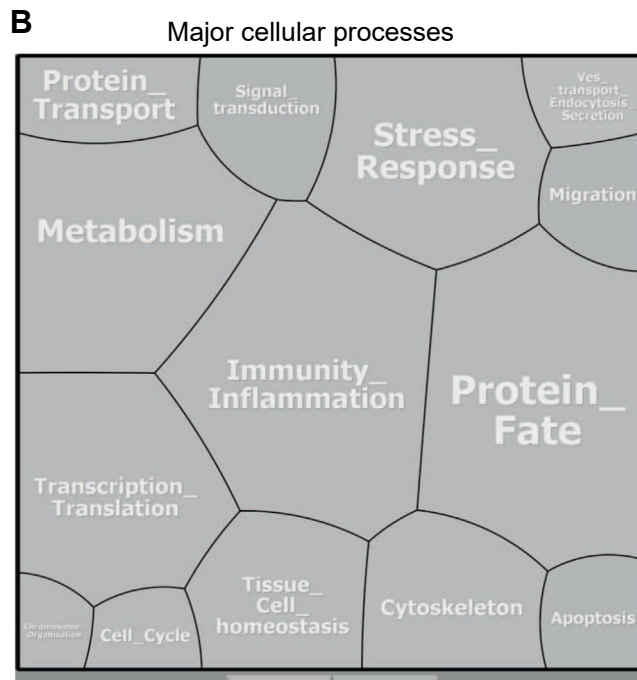
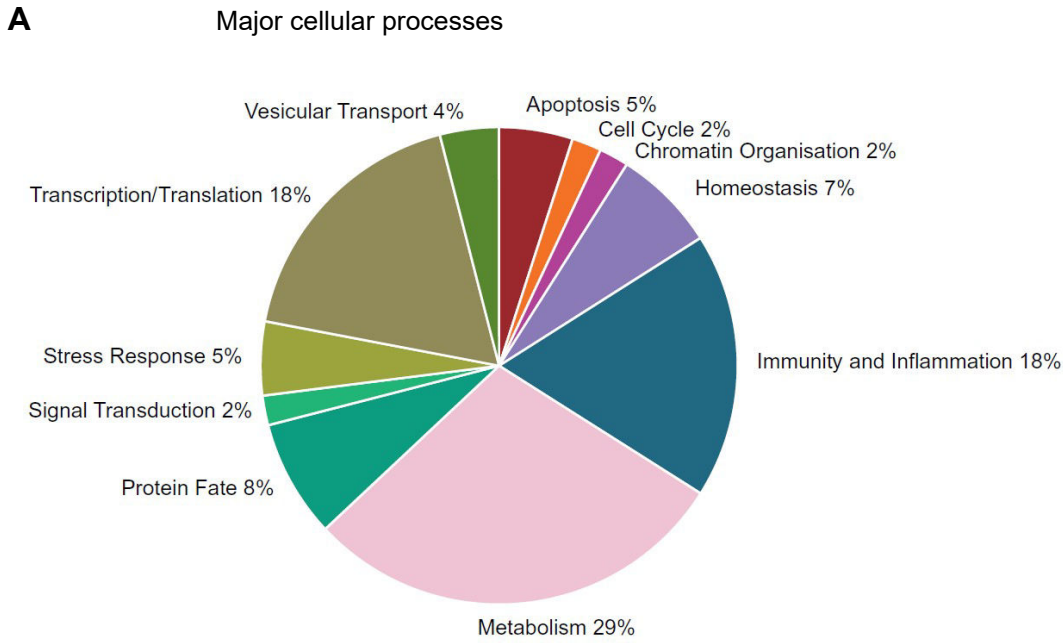


Fig2. Visual summary of differential protein expression between dendritic cell maturation states. **a)** Functional classification of all regulated proteins. Protein IDs were uploaded to DAVID website and annotated to major cellular processes according to Gene Ontology database. **b)** Voronoi treemap layout for representing major cellular processes. This layout is used for all Voronoi treemaps in our study. **c)** Expression differences of single proteins between semi-mature and fully-mature dendritic cells. Colors represent expression level differences. Orange: increased expression, Blue: decreased expression, Light grey: no change, Dark grey: protein not detected. Color intensity is adjusted to the expression level difference on log₂ scale, brighter colors indicating a higher expression level difference.

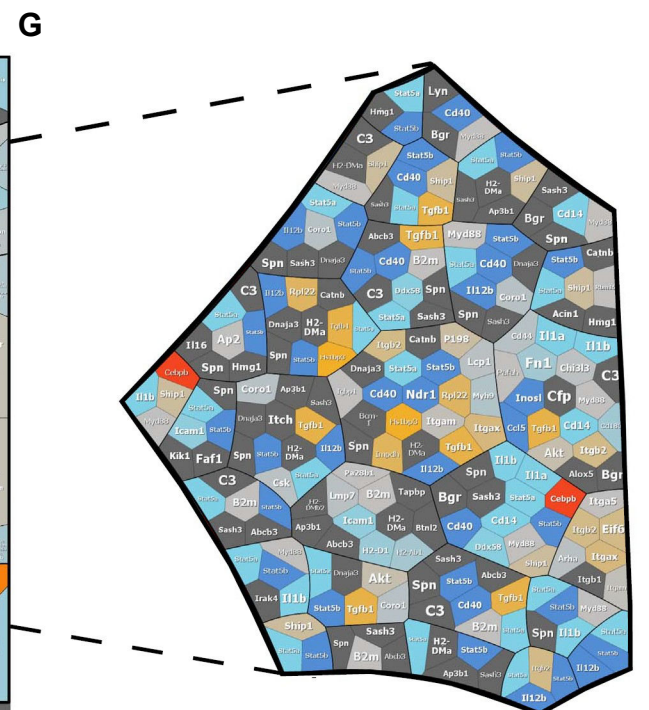
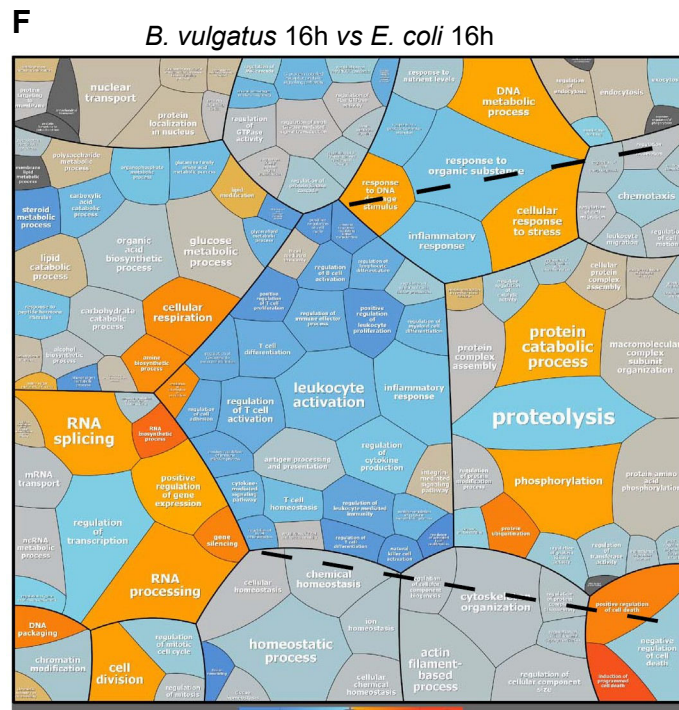
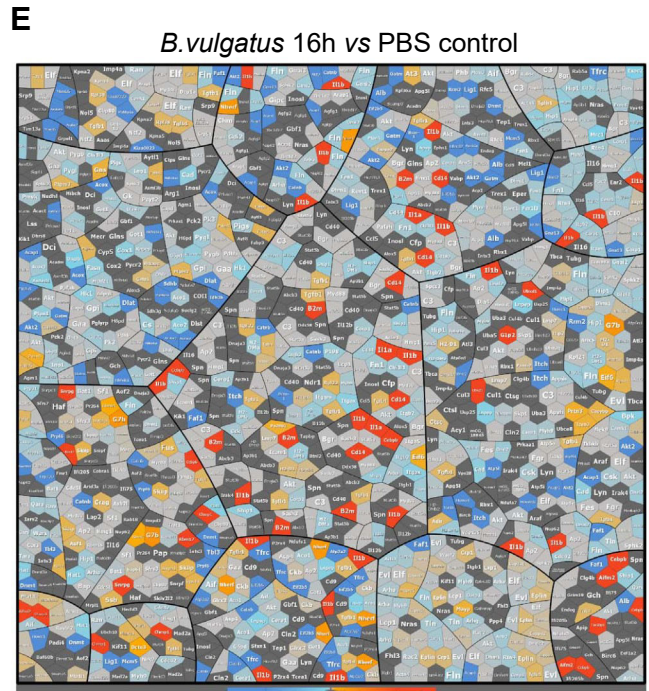
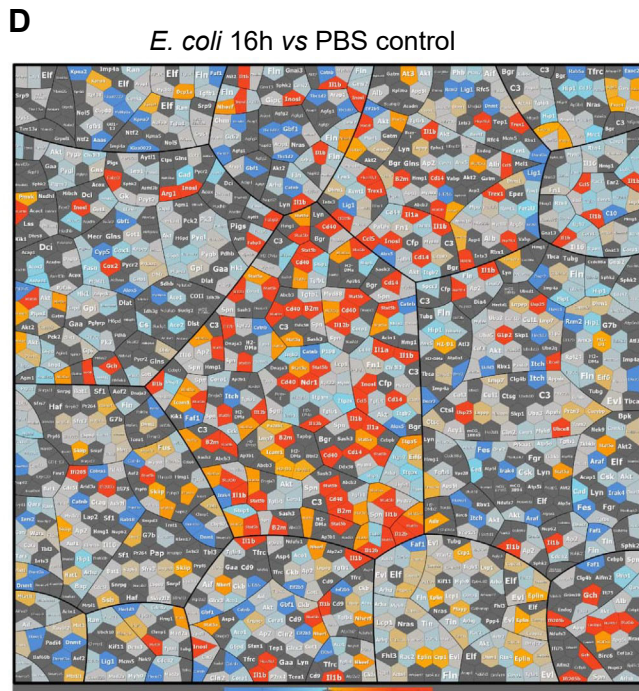


Fig2 cont. Visual summary of differential protein expression between dendritic cell maturation states. **d,e)** Expression differences of single proteins upon bacterial challenge, compared to PBS controls. **f,g)** Magnification of the immunity/inflammation cluster. At this level of detail subprocesses belonging to the cluster are shown as smaller polygons. Colors represent expression level differences. Orange: increased expression, Blue: decreased expression, Light grey: no change, Dark grey: protein not detected. Color intensity is adjusted to the expression level difference on log2 scale, brighter colors indicating a higher expression level difference.

As the Voronoi maps depict, stimulation with bacteria results in a dynamic regulation of the dendritic cell proteome. A total of 151 proteins are regulated during semi-maturation (53 are expressed more and 98 expressed less), 181 proteins are regulated during full-maturation (96 expressed more and 85 expressed less), and 103 proteins (33 expressed more and 70 expressed less) between semi-mature and fully mature DCs. Besides these expression level differences, many proteins are exclusive to a particular maturation state. 183 proteins are exclusively expressed in steady-state controls, 52 are exclusive to *B. vulgatus* stimulated sample and 61 are exclusive to *E. coli* stimulated sample. On a cellular process level, we observed that the proteins that belong to the immunity cluster and its subprocesses show increased expression in contrast with the control group and the *B. vulgatus* stimulated dendritic cells. The processes that belong to the immunity cluster are especially important for us, since they contain several proteins that are of central importance to inflammatory responses such as IL-1 α , IL1- β , iNOS, COX2, CCL5 and RIG1, all of which have lower expression levels compared to *E. coli* stimulated DCs. In contrast, TGF β 1, which has potent anti-inflammatory effects, was observed to be expressed in a higher level upon *B. vulgatus* stimulation. These suggest that there are important differences between the effects of *E. coli* and *B. vulgatus* stimulation, *E. coli* increasing the expression of pro-inflammatory factors, whereas *B. vulgatus* stimulation does not lead to such a high level of increase and may even counteract it by up-regulating anti-inflammatory factors.

3.2. Bacterial stimulation and pro-inflammatory factor expression

As our general view of dendritic cell proteomes after bacterial stimulation suggested that *E. coli* may induce or exacerbate inflammation whereas *B. vulgatus* may dampen it, we wanted to concentrate on several key inflammatory regulators to gather more information on this observation. We have picked several suitable candidates from differentially regulated inflammatory factors, namely IL1- β , iNOS, COX2 and RIG1, and we have performed ELISAs and Western Blots to determine their expression levels to confirm the mass spectrometry results. According to our mass spectrometry data, IL1- β , iNOS, COX2 and RIG1, have no detectable or have lower levels of expression in *B. vulgatus* stimulated dendritic cells. IL1- β detected in low amounts in the *B. vulgatus* stimulated sample (45 pg/mL), and iNOS

expression, which is characteristically induced under inflammatory conditions, was not detected. On the contrary, *E. coli* stimulated sample had a high amount of IL1- β (485 pg/mL), and iNOS expression was also induced as can be seen in the Western Blot imagery in Fig. 3. The inducible cyclooxygenase COX2 was another factor that behaved similarly, being detected only after *E. coli* stimulation. RIG1 also exhibited a gradual increase in expression between the untreated, *B. vulgatus* stimulated and *E. coli* stimulated samples, with the ratios being 1/2.1/3.76 in our mass spectrometry measurements and 1/1.9/ 2.53 in our Western Blot analysis (Fig. 3). As there is a concordance between the two different methods of analysis, we concluded that for the aforementioned inflammatory regulators that we have picked, there is a lack of pro-inflammatory factor expression in the *B. vulgatus* stimulated sample and the results of the mass spectrometry analysis are reproducible.

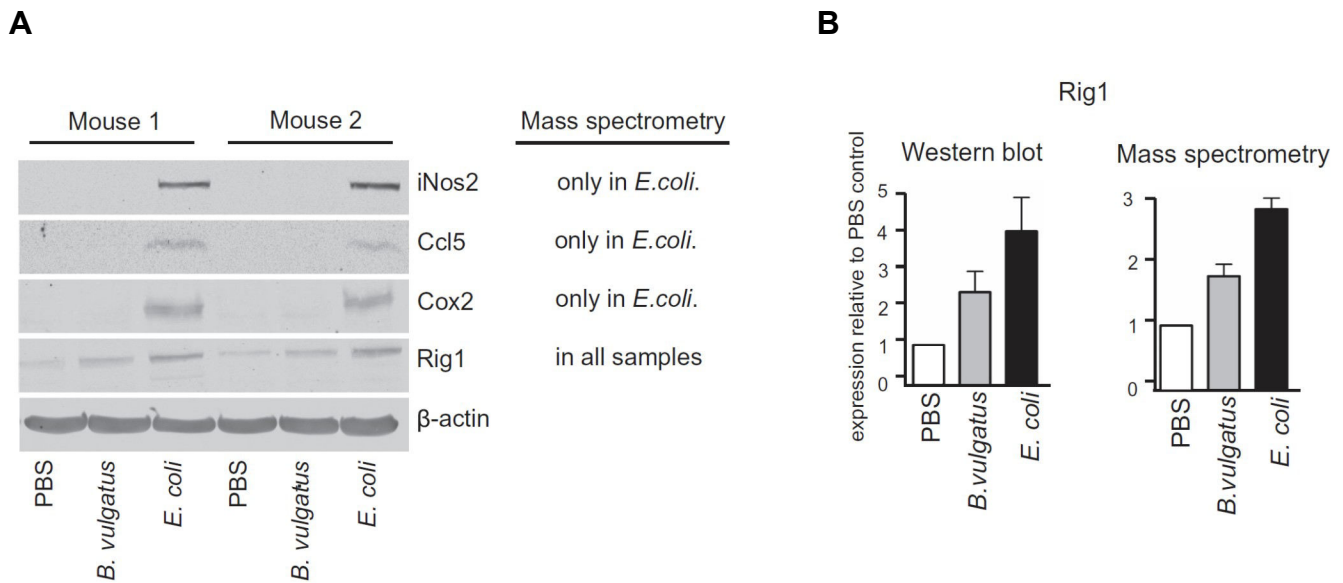


Fig. 3. a) Expression levels of several selected proteins of interest were determined by Western Blots done with whole-cell extracts prepared from BMDCs derived from two C57BL/6 mice, unstimulated (PBS) and stimulated for 16 h with *B. vulgatus* or *E. coli*. β -actin was included as a loading control. Results are representative of two independent experiments. **b)** Comparison of expression levels of RIG-1 protein by Western Blot and mass spectrometry data. Expression level in the PBS control is taken as baseline expression and set to 1. All band intensities in the Western Blot graph were normalized to β -actin.

3.3. Canonical pathways and upstream regulators of dendritic cell maturation

In this part of our study we have used bioinformatical methods to deduce which pathways and regulators took part in creating the difference between the dendritic cell populations attained after bacterial stimulation. For this purpose, we have used the IPA software (Ingenuity Pathway Analysis), which predicts the impact of major signaling pathways in creating the differences between distinct experimental groups. IPA uses an algorithm based on the enrichment values of regulated proteins in a given pathway. As previously, our input data was the list of 301 differentially regulated proteins resulting from all pair-wise comparisons. The results can be seen in Table 1, with the top 16 pathways belonging to the analysis between semi-mature and fully-mature DCs shown. Not surprisingly, dendritic cell maturation and immune signaling pathways such as IRF signaling, TREM1 and TLR signaling pathways are shown to be enriched in differentially regulated proteins. In addition, PPAR signaling, LXR/RXR activation, JAK/Stat signaling pathways also harbor numerous differentially regulated proteins. Among those proteins are STAT5a, PTGS2, iNOS, CEBPB and several interleukins and cytokines. As we already have data about the relative abundance of these proteins and under which circumstances their expression are regulated, they are potential candidates to focus our future research.

Our next bioinformatical analysis targeted the upstream regulators that govern the observed differences in protein expression levels and signaling pathways. For this purpose we have used the tools included in the IPA package which are designed for upstream regulator analysis. The analysis uses the information provided by the hand-curated literature-based information database Ingenuity® Knowledge Base, and contains extensive data on transcriptional regulators and their downstream targets (Krämer, Green, Pollard, & Tugendreich, 2014). The software requires a list of proteins provided by the experimenter with their expression values under different experimental conditions, compares it with the expected activation states determined by the Ingenuity® Knowledge Base, then generates a list of upstream regulators indicating their activation state (z-score). Additional statistical information such as an overlap p-value (threshold set as <0.01) indicating the consistency and statistical significance of the match is also included. The tabulated results of the regulator analysis between semi-mature vs. fully-mature dendritic cells are shown in Fig. 4 and their activation

states, molecular types, assessment z-scores, and targets detected by the mass-spectrometry are shown in Table 2. In line with the previous observations that proteins involved in immunity and inflammation clusters are expressed in lower levels (or not expressed at all) in the *B. vulgatus* stimulated DC population compared to the *E. coli* stimulated population, the upstream regulators and pro-inflammatory signals are also predicted to be down-regulated/inactive by the IPA software.

Several notable proteins in this group are IRF3, TLR4, TLR2 and IFN- γ which are involved in mounting an immune response against potential pathogens. In addition to detecting the aforementioned factors that we already expected to be involved, several other factors such as MAVS, SAMS1, DOCK8 and TBK1 which have not been studied in an inflammation or dendritic cell maturation context were reported to be down-regulated/inactive. Besides the low expression or inactivation of pro-inflammatory factors, it was of special interest to us to determine whether *B. vulgatus* stimulation led to the activation of factors that would dampen or reduce the inflammatory response. We have detected several such factors and they are listed in Table 2 with a positive z-score indicating that they are active in the DC population treated with *B. vulgatus*. SOCS1 (suppressor of cytokine signaling) is one of these factors which has extensively studied anti-inflammatory actions. It has been shown that conditional suppression of SOCS1 in colonic T-cells of DSS treated mice increases colitis severity (Horino et al., 2008), and SOCS1^{-/-} Rag2^{-/-} mice develop spontaneous colitis (Chinen et al., 2011). Besides SOCS1, the list includes PTGER4 (prostaglandin E receptor 4), an anti-inflammatory regulator; ABCA1, a lipid transporter with inflammation suppression function (Tang, Liu, Kessler, Vaughan, & Oram, 2009); and NR1H3, a transcription factor with inhibitory effects on pro-inflammatory cytokine expression (S B Joseph, Castrillo, Laffitte, Mangelsdorf, & Tontonoz, 2003; Sean B. Joseph et al., 2004). In summary, the IPA analysis suggested that *B. vulgatus* stimulation does not lead to robust pro-inflammatory factor expression or possibly silences pro-inflammatory factor expression by activating anti-inflammatory upstream regulators.

Affected pathways	Enrichment	Proteins detected by mass spectrometry
	Score	
Activation of IRF by cytosolic PRRs	5.81	DHX58,IFIH1,IKBKB,CD40,PPIB,DDX58,STAT2,PIN1,IRF3,IFIT2,ISG15
Dendritic cell maturation	4.12	B2M,AKT2,IL1A,ICAM1,HLA-A,MYD88,HLA-DQB1,IKBKB,AKT1,CD40,HLA-DMA,IL12B,FSCN1,HLA-DMB,IL1B,STAT2,PIK3CD,HLA-DRB5
TREM1 signaling	4.04	ITGB1,STAT5A,AKT2,ICAM1,AKT1,MPO,CD40,MYD88,ITGA5,IL1B,STAT5B,ITGAX
Communication between innate and adaptive immune cells	3.91	B2M,IL1A,CD40,HLA-A,IL12B,IL1B,CCL5,HLA-DRB5
Toll-like receptor signaling	3.91	IKBKB,IL1A,MYD88,IL12B,CD14,IL1B,IRAK4,TRAF1
Role of PRRs in recognition of bacteria and viruses	3.79	OAS1,IL1A,C3,MYD88,CCL5,IRF3,OAS3,IFIH1,CLEC7A,IL12B,TGFB1,DDX58,IL1B,CLEC6A,PIK3C,PRKCB
Retinoic acid mediated apoptosis signaling	3.55	ZC3HAV1,DAP3,PARP3,PARP9,PARP14
PPAR signaling	3.50	IKBKB,STAT5A,IL1A,NRAS,IL1B,PTGS2,STAT5B
Glucocorticoid receptor signaling	3.44	PRKACB,STAT5A,AKT2,NRAS,ICAM1,HSPA1B,SMARCD2,CEBPB,CCL5,PTGES3,PRKAG1,IKBKB,GTF2B,AKT1,POLR2A,POLR2C,PCK2,POLR2E,TGFB1,PRKAA1,IL1B,PIK3CD,PTGS2,NOS2,STAT5B
LXR/RXR activation	3.24	IL1A,ECHS1,C3,CD36,IRF3,ALB,LYZ,FASN,IL1B,CD14,ACACA,PTGS2,NOS2,HADH,MMP9
CD40 signaling	2.95	IKBKB,ICAM1,CD40,PTGS1,PIK3CD,PTGS2,MAPKAPK2,TRAF1
LPS/IL-1 mediated inhibition of RXR Function	2.82	ALDH4A1,IL1A,CPT1A,MYD88,ACOX1,GSTO1,ALDH9A1,IL4I1,ALDH1L1,ALDH3A2,ALDH1A2,CPT2,FABP4,CD14,IL1B,ALDH3B1,ALDH18A1,FABP5,FABP3,ACOX3
JAK/Stat signaling	2.73	STAT5A,AKT2,AKT1,NRAS,PTPN1,STAT2,PIK3CD,CEBPB,STAT5B
Agranulocyte adhesion and diapedesis	2.61	ITGB1,IL1A,MYH9,ICAM1,FN1,MYH14,ITGA5,CCL5,GLG1,GNAI2,ITGB2,GNAI3,IL1B,CCL6,MMP9
MAPK signaling	2.51	NRAS,ZC3HAV1,PIK3CD,PARP3,RPS6KA1,PARP9,PARP14
Death receptor signaling	2.45	ACIN1,IKBKB,ZC3HAV1,PARP3,PARP9,PARP14

Table 1. Canonical pathway analysis using IPA. Top 16 signaling pathways determined by ingenuity pathway analysis of the *B. vulgatus* vs. *E. coli* comparison at 16h are shown. The pathway with the highest enrichment score is shown at the top position, the higher the enrichment score, the more proteins that are detected by mass spectrometry are associated with the pathway compared to the background database (mouse proteome).

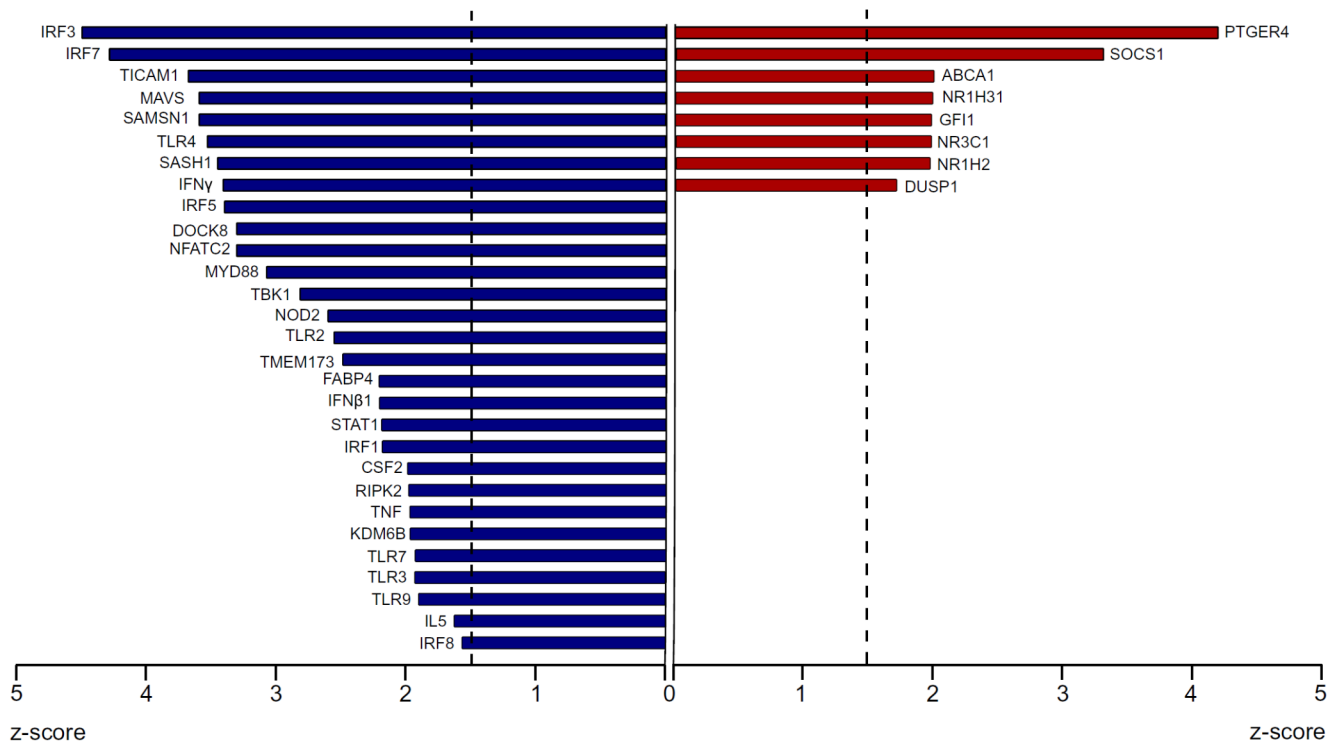


Fig.4 Upstream regulator prediction. IPA upstream regulator analysis was performed to predict key regulatory molecules that underlie the expression pattern differences observed between semi-mature and fully mature DCs. The activation z-score is used to determine the activation states of upstream factors and molecules with z-score > 1.5 are considered to be activated (red bars), whereas molecules with z-score < 1.5 are considered to be inactivated (blue bars). All listed upstream regulators have an overlap of p-value < 0.01. The overlap p-value uses Fisher's Exact Test to assess the statistical significance of the overlap between the dataset genes and the genes that are regulated by the upstream regulator.

Upstream regulator	Molecule type	z-Score	Target proteins detected by mass spectrometry
Activated			
			CD40,CMPK2,DDX58,GBP2,GBP4,IFI16,IFI47,IFIT1B,IFIT2,IGTP,IL12B,IL41I,ISG20,NOS2,PARP14,
PTGER4	G-protein coupled receptor	4.194	PTGS2,RNF213,TOR3A
SOCS1	Other	3.302	DDX58,GBP5,IFI16,IFI47,IFIT1B,IFIT2,IFIT3,IL1B,ISG15,NOS2,OAS1,PTGS2
ABCA1	Transporter	1.998	IL12B,IL1B,NOS2,PTGS2
NR1H3	Ligand-dependent nuclear receptor	1.99	CCL5,IL1B,NOS2,PTGS2
GFII	Transcription regulator	1.982	CD40,ICAM1,IL1A,IL1B
NR3C1	Ligand-dependent nuclear receptor	1.977	CCL5,GBP2,GLUL,IFIT1B,IFIT2,IL12B,IL1A,IL1B,ISG15,OASL
NR1H2	Ligand-dependent nuclear receptor	1.966	CCL5,IL1B,NOS2,PTGS2
DUSP1	phosphatase	1.71	CD40,IL1A,IL1B,PTGS2
Inhibited			
IRF3	Transcription regulator	- 4.509	CCL5,CMPK2,DDX58,DHX58,GBP5,IFI16,IFI47,IFIT1B,IFIT2,IFIT3,IGTP,ISG15,ISG20,NT5C3A, OAS1,OASL,PARP14,SLFN1,STAT2,TREX1,UBE2L6
IRF7	Transcription regulator	- 4.298	CMPK2,DDX58,DHX58,GBP5,IFI16,IFI47,IFIT2,IFIT3,IGTP,ISG15,ISG20,NT5C3A,OAS1,OASL, PARP14,SLFN1,STAT2,TREX1,UBE2L6
TICAM1	Other	- 3.69	CCL5,CD40,CFB,CMPK2,ICAM1,IFI16,IFI47,IFIT1B,IFIT2,IFIT3,IGTP,IL12B,IL1A,IL1B,ISG15,ISG20, NES,OASL,PTGS2,SLC7A2
MAVS	Other	- 3.606	CCL5,CMPK2,DDX58,DHX58,IFIT2,IFIT3,ISG15,ISG20,NT5C3A,OAS1,OASL,STAT2,UBE2L6
SAMSN1	Other	- 3.606	CD40,CMPK2,IFIT1B,IFIT2,IFIT3,IL12B,ISG15,ISG20,OASL,PTGS2,STAT2,STAT5A,USP25 CCL5,CD40,CFB,CMPK2,IFI16,IFI47,IFIT1B,IFIT2,IFIT3,IGTP,IL12B,IL1A,IL1B,ISG15,ISG20,OASL,
TLR4	Transmembrane receptor	- 3.543	PTGS2,STAT2,STAT5A,TRAF1,USP25
SASH1	OTHER	- 3.464	CD40,CMPK2,IFIT1B,IFIT2,IFIT3,IL12B,ISG15,ISG20,OASL,PTGS2,STAT2,USP25
IFNG	cytokine	- 3.421	ARG1,CCL5,CD40,GBP2,GBP4,GBP5,ICAM1,IL12B,IL1A,IL1B,NOS2,PTGS2,SLFN1
IRF5	Transcription regulator	- 3.411	CMPK2,DDX58,DHX58,IFIT2,IFIT3,ISG15,ISG20,NT5C3A,OAS1,OASL,STAT2,UBE2L6
DOCK8	Other	- 3.317	CD40,CMPK2,IFIT1B,IFIT2,IFIT3,IL12B,ISG15,ISG20,PTGS2,STAT2,USP25
NFATC2	Transcription regulator	- 3.317	CD40,CMPK2,IFIT1B,IFIT2,IFIT3,ISG15,ISG20,OASL,PTGS2,STAT2,USP25 ARG1,CCL5,CD40,CMPK2,ICAM1,IFIT1B,IFIT2,IL12B,IL1A,IL1B,ISG15,NES,NOS2,OASL,
MYD88	Other	- 3.086	PTGS2,SLC7A2
TBK1	Kinase	- 2.828	CD40,CMPK2,IFIT1B,IFIT2,IL12B,IL1A,ISG20,PTGS2
NOD2	Other	- 2.613	CD40,ICAM1,IL12B,IL1A,IL1B,NOS2,TRAF1
TLR2	Transmembrane receptor	- 2.566	ARG1,CCL5,CD40,IL12B,IL1B,NOS2,PTGS2
TMEM173	Other	- 2.499	CCL5,GBP5,IFI16,IL1B,NOS2,OASL
FABP4	Transporter	- 2.219	IL12B,IL1A,IL1B,NOS2,PTGS2
IFNB1	Cytokine	- 2.216	CCL5,CD40,CMPK2,GBP2,GBP4,GBP5,IFI16,IFI47,IFIT1B,IFIT2,IFIT3,IGTP,IL12B,NOS2,NT5C3A,STAT2
STAT1	Transcription regulator	- 2.2	CCL5,CD40,GBP2,ICAM1,IFIT1B,ISG15,NOS2,OASL
IRF1	Transcription regulator	- 2.195	CCL5,CD40,GBP2,IL12B,NOS2,PTGS2
CSF2	Cytokine	- 2	CD40,IL12B,IL1B,NOS2
RIPK2	Kinase	- 1.991	CD40,ICAM1,NOS2,TRAF1
TNF	Cytokine	- 1.982	CD40,GBP2,NOS2,PTGS2
KDM6B	Other	- 1.98	CCL5,CD40,IGTP,IL12B,OASL
TLR7	Transmembrane receptor	- 1.941	CD40,IL12B,ISG15,STAT2
TLR3	Transmembrane receptor	- 1.939	CCL5,CD40,IL12B,IL1B
TLR9	Transmembrane receptor	- 1.908	CD40,IFIT1B,IL12B,STAT2
IL5	Cytokine	- 1.633	GBP2,GBP4,NDRG1,NOS2,P4HA1,UCHL3
IRF8	Transcription regulator	- 1.573	CCL5,CD40,ICAM1,IL12B,ISG15

Table 2 List of upstream regulators and their targets that were detected as being differentially regulated between *B. vulgatus* and *E. coli* treated cells at 16h. The activation z-score is used to determine the activation states of upstream factors, with positive values indicating activation and negative values indicating inhibition. All indicated upstream regulators have an overlap p-value < 0.01. The overlap p-value uses Fisher's Exact Test to assess the statistical significance of the overlap between the dataset genes and the genes that are regulated by the upstream regulator.

3.4. Phosphoproteome analysis of dendritic cell maturation states

The regulation of protein expression, the affected pathways, and the regulators of these pathways and processes provide valuable insight into the differences in steady-state, *B. vulgatus* and *E. coli* stimulated DCs. Nevertheless, the levels of protein expression is hardly the whole picture. Post-translational modification of expressed proteins can alter their activation states, sub-cellular compartmentalization, half-lives and even their functions. Phosphorylation of the amino acids serine, tyrosine and threonine are among the most common post-translational modifications, and in this section we aimed to investigate the phosphoproteome profiles of our dendritic cell populations. As for the comparative proteome analysis experiment we have stimulated murine BMDCs with *B. vulgatus*, *E. coli*, and PBS, and collected the protein from the cellular fraction. Unlike the changes in protein expression levels, peptide phosphorylation processes are highly dynamic and occur in rapid succession (Sjoelund, Smelkinson, & Nita-Lazar, 2014). Therefore, we limited the bacterial stimulation to 30 min. instead of 16h we have done for the comparative protein expression analysis. Following stimulation and sample collection, the phosphopeptides were enriched by strong cation exchange (SCX) method and titanium oxide chromatography, and analyzed with Orbitrap XL. In total, 919 phosphosites were identified on 544 peptides, and 118 sites were differentially phosphorylated between semi-mature and fully-mature dendritic cells. It is also important to note the phosphoevents that are exclusive to one state; 283 phosphoevents were only detected in the PBS control, 120 phosphoevents were only detected in the *B. vulgatus* stimulated sample, and 18 phosphoevents in the *E. coli* stimulated DC population.

After determining the differential phosphorylation events, we have performed a kinase inference analysis to determine which kinases take part in the phosphorylation of the 465 differentially regulated phosphosites belonging to the 3 pairwise comparisons we have considered (PBS vs. *B. vulgatus*, *B. vulgatus* vs. *E. coli*, PBS vs. *E. coli*). We have used the kinase-substrate database available at PhosphositePlus (Hornbeck et al., 2015), and searched for the phosphorylated sequences detected in our experiments. The PhosphositePlus database provides lists of known *Mus musculus* kinases and their targets, and matching the phosphorylated substrates detected in our phosphoproteome analysis, we have generated a list of kinases that are responsible for the differential phosphorylation

events in our experiments (Fig. 4b). We have grouped the kinases according to their families, and observed that the majority (80/126) of phosphorylations were carried out by CMGC and AGC family of kinases, with Mapk1 and Prkaca phosphorylating the highest number of targets. Among the most active kinases are the MAP kinases, cyclin dependent kinases, AKT1 and mTOR. After the kinase analysis, we searched for differentially phosphorylated proteins that have central functions in various cellular processes such as immunity, cell division, chromatin modifications and major cellular signaling pathways. We have done this for all 3 pairwise comparisons and the results can be seen in Table 3. Upon stimulation with bacteria for 30 minutes, the cell cycle regulator CDK2 was observed to be exclusively phosphorylated in *B. vulgatus* stimulated sample at residues threonine14 and tyrosine15, which are reported to inactivate the protein. CDC42 GTPase and DOCK1 phosphorylation at indicated residues on Table 3 are also among notable phosphoevents that are observed exclusively in the *B. vulgatus* stimulated dendritic cell population. Also important to note are the phosphorylation of two factors in the epigenetic regulator complex SWI/SNF; SMARCC1 and SMARCC2, were also semi-mature DC specific, suggesting a possible involvement of epigenetic factors during the attainment of the semi-mature phenotype. Several other proteins in our differential phosphorylation list include ACIN1, a potent apoptosis effector; inositol kinase B, which is a major signal transduction relay protein found in the plasma membrane; and the transcription factor junD. The results of our phosphoproteome analysis showed that bacterial stimuli leads to post-transcriptional modification of several important cell cycle proteins, epigenetic regulators and transcriptional factors. A closer look into these factors can prove beneficial to understanding the maturation process from a different point of view.

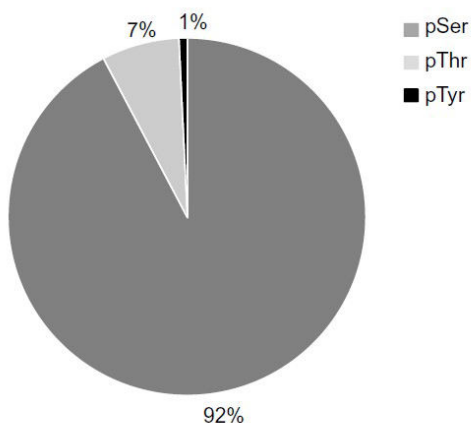
Similar to our pathway analysis for the comparative proteome experiment, after obtaining a list of proteins that showed differences in phosphorylation states, we have performed a reactome analysis on differentially phosphorylated proteins to determine the pathways that are affected by the bacterial stimulation. Reactome is an open-source, manually curated and peer-reviewed database of biological reactions and pathways (Fabregat et al., 2018). To analyze the pathways, we have used the 118 differentially phosphorylated peptides that we have detected with mass spectrometry. As the same for all our previous analyses and results, we have only included the phosphoevents of the *B. vulgatus vs E. coli*

pairwise comparison and reported the results, we have also performed the same analysis for PBS vs. *B. vulgatus* and PBS vs. *E. coli*, however chose not to report them in order to keep the focus. The reactome analysis of semi-mature vs. fully-mature dendritic cells showed that the processes and pathways concerning cell division, mTOR pathway, stress response pathways and signaling pathways such as PI3K pathway are enriched in differentially phosphorylated proteins (Table 4). Considering the importance of these pathways, it appears that *B. vulgatus* and *E. coli* stimulation do not only affect cellular processes regarding immunological functions, but also various other cellular processes such as cell cycle, cell growth and apoptosis. As our analyses subsequent to the mass spectrometry are purely bioinformatical, any conclusions regarding thereof should be confirmed experimentally in order to determine whether the predicted differential regulation of processes and the observed phosphorylation differences in fact have direct biological relevance and contribute to the difference in pathogenicity between *B. vulgatus* and *E. coli*. Nevertheless, the data presented in this section can be a useful first tool to investigate the role of phosphorylation in dendritic cell maturation.

Uniprot ID	Name	Ratio	Sequence
<i>E. coli</i> vs <i>B. vulgatus</i>			
A2APM2	CD44	<i>B. vulgatus</i> only	S(0.995)QEMVHLVNKEPS(0.003)ET(0.001)PDQCMTADETR
A6X8Z5	Cdc42 GTPase	<i>B. vulgatus</i> only	DDSPSSLGS(1)PEEEQPK
B2RXC2	Inositol 1,4,5-trisphosphate 3-kinase B	<i>B. vulgatus</i> only	AALS(1)PGS(0.044)VFS(0.956)PGR
Q9JIX8	Acin1, Apoptotic chromatin condensation inducer in the nucleus	<i>B. vulgatus</i> only	S(0.015)LS(0.984)PLS(0.43)GT(0.285)T(0.285)DT(0.001)K
P15066	Transcription factor junD	<i>B. vulgatus</i> only	LAS(1)PELER
P97496	SWI/SNF complex subunit SMARCC1	<i>B. vulgatus</i> only	RKPS(1)PS(1)PPPTATESR
Q6PDG5	SWI/SNF complex subunit SMARCC2	<i>B. vulgatus</i> only	S(1)DGDPIVDPEK
Q61165	Sodium/hydrogen exchanger 1, Slc9a1	<i>B. vulgatus</i> only	IGS(1)DPLAYEPK
Q8BUR4	Dock1, Dedicator of cytokinesis protein 1	<i>B. vulgatus</i> only	S(1)QVINVIGNER
Q8C078	Camkk2	<i>B. vulgatus</i> only	S(1)FGNPFEGSR
P97377	Cdk2	<i>B. vulgatus</i> only	IGEGT(1)Y(1)GVVYK (Thr 14/Tyr15)
P98078	Dab2	2.903	S(0.884)S(0.116)PNPFVGS(1)PPK
Q6A068	Cell division cycle 5-like protein	1.767	GGLNT(0.999)PLHES(0.001)DFS(0.026)GVT(0.974)PQR
<i>E. coli</i> vs. PBS			
A2APM2	CD44	PBS only	S(0.995)QEMVHLVNKEPS(0.003)ET(0.001)PDQCMTADETR
Q60875	Rho guanine nucleotide exchange factor 2	PBS only	LS(1)PPHS(1)PR
Q61165	Sodium/hydrogen exchanger 1, Slc9a1	PBS only	IGS(1)DPLAYEPK
A2AIV8	Caspase recruitment domain-containing protein 9	PBS only	QQQLDMLILS(0.012)S(0.044)DLEDS(0.153)S(0.791)PR
E9PU87	Serine/threonine-protein kinase SIK3	PBS only	GPS(0.001)PLVT(0.002)MT(0.002)PAVPAVT(0.127)PVDEES(0.934)S(0.934)DGEPDQEAQVR
Q9JIX8	Acin1,	PBS only	S(0.015)LS(0.984)PLS(0.43)GT(0.285)T(0.285)DT(0.001)K
P13405	Retinoblastoma-associated protein	PBS only	IPGGNIYIS(1)PLKS(0.999)PY(0.001)K
P49138	MAP kinase-activated protein kinase 2	PBS only	MLS(0.544)GS(0.544)PGQT(0.912)PPAPFPS(1)PPPPAPAQPPPPFPQFHVK
P70671	Interferon regulatory factor 3	PBS only	DEGS(0.001)S(0.001)DLAIVS(0.029)DPS(0.029)QQLPS(0.94)PNVNNFLNPAPQENPLK
P97310	DNA replication licensing factor MCM2	PBS only	RGLLYDS(1)S(1)EEDEERPAR
Q66JS6	Eukaryotic translation initiation factor 3 subunit J-B	PBS only	AAAAAAAAAAGDS(0.999)DS(0.998)WDADT(0.001)FS(0.001)MEDPVRK
Q60591	Nuclear factor of activated T-cells, cytoplasmic 2	PBS only	S(0.496)LS(0.496)PGLLYG(0.007)QQPS(0.002)LLAAPLGLADAHR
Q9CZW5	Mitochondrial import receptor subunit TOM70	PBS only	AS(0.763)PALGS(0.233)GHHDGS(0.002)GDS(0.002)LEMSSLDL
P97492	Regulator of G-protein signaling 14	3.353	S(0.854)LGS(0.808)GES(0.179)ES(0.155)ES(0.004)RPGK
P16951	Cyclic AMP-dependent transcription factor ATF-2	4.669	NDSVIVADQT(1)PT(0.988)PT(0.012)R
Q6PDG5	SWI/SNF complex subunit SMARCC2	5.325	S(1)DGDPIVDPEK
<i>B. vulgatus</i> vs. PBS			
A2AIV8	Caspase recruitment domain-containing protein 9	PBS only	QQQLDMLILS(0.012)S(0.044)DLEDS(0.153)S(0.791)PR
P49138	MAP kinase-activated protein kinase 2	PBS only	MLS(0.544)GS(0.544)PGQT(0.912)PPAPFPS(1)PPPPAPAQPPPPFPQFHVK
A2AIV8	Caspase recruitment domain-containing protein 9	0.397	NSQELSLPQDLEEDAQLS(1)DK
P16951	Cyclic AMP-dependent transcription factor ATF-2	1.996	NDSVIVADQT(1)PT(0.988)PT(0.012)R
P25799	Nuclear factor NF-kappa-B p105 subunit	2.171	S(1)DDEES(0.997)LT(0.003)LPEK
Q8VBT6	Apolipoprotein B receptor	2.407	GQEETSGAPDLS(1)PER
Q14AX6	Cdk12	3.781	NNS(1)PAPPQAPVK
P97310	DNA replication licensing factor MCM2	3.901	RRIS(1)DPLT(0.587)S(0.072)S(0.34)PGR
P97377	Cdk2	3.174	IGEGT(1)Y(1)GVVYK
Q9JIX8	Acin1, Apoptotic chromatin condensation inducer in the nucleus	5.031	S(0.015)LS(0.984)PLS(0.43)GT(0.285)T(0.285)DT(0.001)K
P25911	Tyrosine-protein kinase Lyn	<i>B. vulgatus</i> only	DNLNDDEVDS(1)K
A6X8Z5	Cdc42 GTPase	<i>B. vulgatus</i> only	DDSPSSLGS(1)PEEEQPK
Q6PDG5	SWI/SNF complex subunit SMARCC2	<i>B. vulgatus</i> only	S(1)DGDPIVDPEK
P97492	Regulator of G-protein signaling 14	<i>B. vulgatus</i> only	S(0.854)LGS(0.808)GES(0.179)ES(0.155)ES(0.004)RPGK

Table 3 A list of selected proteins that are differentially phosphorylated among 3 pairwise comparisons of stimulated dendritic cells. Only proteins with central functions to cellular processes are included in the list, along with the Uniprot accession IDs and phosphosequences.

A Phosphorylated Amino Acids



B Inferred Kinase Activity

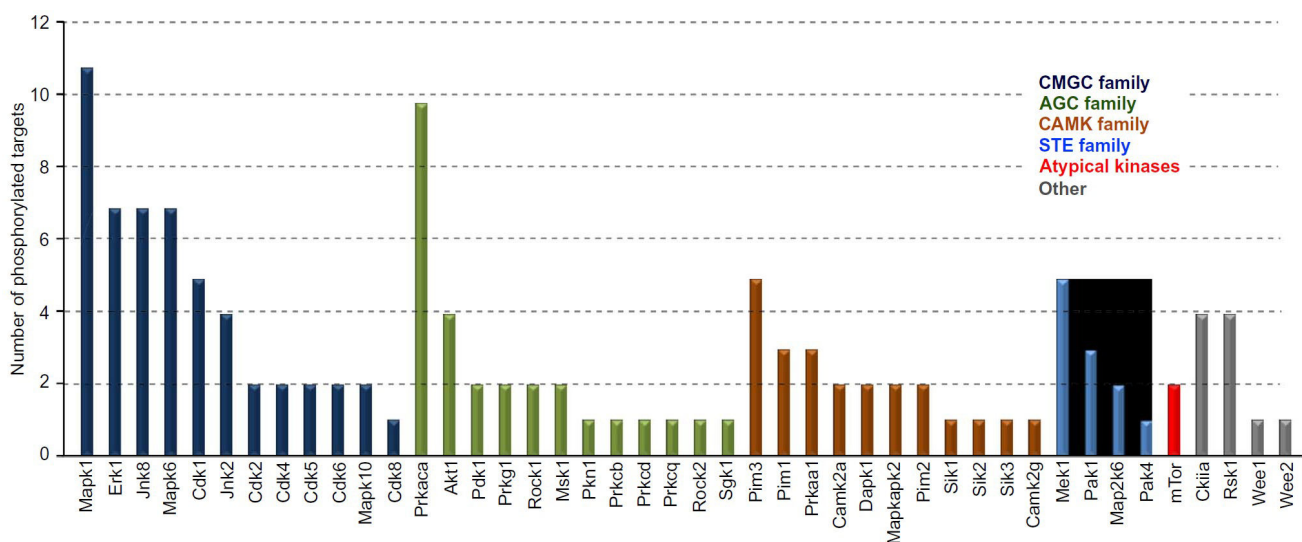


Fig. 4. a) Distribution of phosphorylated amino acid residues. **b)** List of kinases and the number of target phosphosites that are found in the experimental dataset for each kinase listed. Kinases are grouped into 5 major families, with the kinase with highest number of phosphorylated targets shown first.

Pathway name	# Phosphopeptides detected by MassSpec	# Proteins in reactome database	MS/database ratio	p value
Apoptotic cleavage of cellular proteins	4	38	0.00444392	9.73E - 04
Mitotic prophase	5	75	0.0087709	0.00171496
Apoptotic execution phase	4	47	0.00549643	0.00210655
Depolymerisation of the nuclear lamina	2	10	0.00116945	0.00591492
Nuclear envelope breakdown	3	45	0.00526254	0.01488664
Hyaluronan uptake and degradation	2	18	0.00210502	0.0180745
Apoptosis	4	91	0.01064203	0.0203461
Breakdown of the nuclear lamina	2	3	3.51E - 04	5.61E - 04
Activation of CaMK IV	1	2	2.34E - 04	0.02243458
Hyaluronan metabolism	2	22	0.0025728	0.02622534
Condensation of prophase chromosomes	2	22	0.0025728	0.02622534
Cyclin A/B1 associated events during G2/M transition	2	23	0.00268974	0.0284562
Programmed cell death	4	102	0.01192843	0.02926745

Table 4 Reactome pathway analysis with phosphorylated peptides. All 118 peptides that were differentially phosphorylated in *B. vulgatus* vs. *E. coli* stimulated DCs were used as the input, and the resulting pathways enriched in phosphorylated peptides are indicated in the list. p-value indicates the results of multiple hypothesis testing performed by the Reactome software, and significance threshold is defined at $p < 0.05$.

3.5. Results summary and discussion

In this study we have performed label-free shotgun proteomic and phosphoproteomic analysis of murine dendritic cells to study their immune response against *B. vulgatus* and *E. coli* stimulation. Based on our mass spectrometry results, we have generated lists of differentially expressed or differentially phosphorylated peptides. We have used the convenient 2D display functionalities of the Voronoi treemaps to show all the differentially expressed proteins and the cellular processes they take part in. We have observed that the majority of the proteins have functions assigned to metabolism, transcription/translation and immune response. Proteins with immune and inflammation related functions showed a general trend of being expressed at a lower level in the *B. vulgatus* stimulated sample compared to the *E. coli* stimulated sample, and showed increased expression of several anti-inflammatory factors. *E. coli* stimulated dendritic cells, on the other hand, showed increased expression or induction of factors such as iNOS, COX2 and CCL5, which have pro-inflammatory effects. Of those factors, iNOS is a regulator of cytokine production and Th1 response, and its activity is increased in ulcerative colitis and Crohn's disease (Bogdan, 2001; Boughton-Smith et al., 1993; Niedbala et al., 1999; Rachmilewitz et al., 1995). Inhibition of iNOS expression results in reduction of inflammation and disease severity in DSS models of colitis in mice and experimental colitis in rats (Camuesco et al., 2004; Sakthivel & Guruvayoorappan, 2013). COX2 is another factor that is induced under inflammatory conditions, and is a well known target for non-steroidal anti-inflammatory drugs (Hawkey, 1999; Seibert & Masferrer, 1994; Wang & Dubois, 2010). Similar to iNOS, COX2 expression was also observed to be increased in the intestinal epithelial cells of the IBD patients (El Miedany et al., 2006; Singer et al., 1998). CCL5 is a macrophage and T-cell recruiter to the inflammatory sites, and colonic biopsies of IBD patients have increased CCL5 mRNA expression, moreover, blocking the CCL5 functions resulted in reduced disease severity and neutrophil recruitment in a DSS mouse model of colitis (Yu et al., 2016). The subsequent pathway analysis we have performed suggested that IRF pathway, dendritic cell maturation pathway and TLR signaling pathways were involved in creating the observed DC maturation phenotypes, and additional pathways such as PPAR signaling, LXR/RXR pathway, and TREM1 signaling pathways were enriched in differentially expressed proteins. PPARs are ligand inducible transcription factors which control several important inflammatory mediators,

and several of their targets i.e. $\text{I}\kappa\text{B}\kappa\beta$, STAT5A, IL1 α , IL1 β are shown to be down-regulated upon *B. vulgatus* stimulation according to our mass spectrometry data. The LXR/RXR pathway exerts its immune modulatory functions by inhibiting iNOS, COX2 and IL-6. Our data suggests regulation in LXR pathway as pro-inflammatory LXR targets IL1 α , IL1 β , iNOS and MMP9 levels are reduced in *B. vulgatus* treated samples compared to *E. coli* stimulated samples. Overall, our pathway analysis points to a regulatory effect *B. vulgatus* on signaling pathways that control inflammation and thereby a reduction of pro-inflammatory gene expression. The following upstream regulator analysis we performed identified 37 factors that were predicted to be affected by the bacterial treatment, which have various key regulatory functions in a multitude of cellular processes. Compared to *E. coli* treatment, 29 of upstream regulators are shown to be inhibited upon treatment with *B. vulgatus* and 8 upstream regulators are shown to be activated. Among these factors are several regulators with well defined immune factors. IRF3, TLR4, TICAM1, IFN- γ , and MyD88 are examples for these factors, and they were predicted to be in an inactive state after *B. vulgatus* stimulation, which is in line with the silent, inflammation suppressive dendritic cell phenotype. In addition to these however, there were several upstream regulators that were predicted to be in an active state upon *B. vulgatus* stimulation, such as PTGER4, ABCA1, SOCS1, and LXR α , all of which have downstream targets with key importance. Among these factors, we considered ABCA1 as a particularly interesting regulator. Its major functions are transporting cellular cholesterol and phospholipids to cell periphery and thereby controlling the rate of HDL (high-density lipoprotein) formation (Oram & Yokoyama, 1996; Yokoyama, 1998). These transport functions of ABCA1 and their regulation have wide ranging consequences in the context of immunity and inflammation. A study by Thompson et al. showed that ABCA1 actively participates in LPS efflux from macrophages, as the administration of an activator of ABCA1 expression resulted in increased efflux of LPS and cholesterol from macrophages (Thompson et al., 2010). Increased LPS efflux is important for LPS tolerance, as removal of LPS from the cell results in limitation of LPS tolerance to shorter time intervals. Increased HDL formation, which is regulated by ABCA1, has also been shown to reduce LPS endotoxicity by binding and sequestering LPS and reducing TNF- α release, and in ABCA1 $^{-/-}$ murine macrophages, LPS challenge results in increased mRNA levels in major pro-inflammatory factors such as MCP-1, IL-1 β , TNF- α , IL-6, IL-12, iNOS and COX2, compared to wild-type macrophages

(Levine et al., 1993). The transport functions of ABCA1 have branching and multifaceted effects on inflammatory response against LPS, and can be an important dampening factor to prevent overwhelming inflammation. As our upstream regulator analysis predicted differential activation of ABCA1 by *B. vulgatus*, ABCA1 may be one of the main mediators of the inflammation suppressing effects of *B. vulgatus*. Needless to say, this is a corollary to a bioinformatical analysis, and thus needs to be confirmed by further experiments.

Taken together, our shotgun proteomics experiment identified differentially expressed and differentially phosphorylated proteins between dendritic cells stimulated with the symbiont *B. vulgatus* and pathobiont *E. coli*. Among these are cytokines, transcription factors, cellular adhesion molecules, and cell surface markers that are integral to immune regulation. Our pathway analysis showed involvement of major immune signaling pathways during dendritic cell maturation, and implicated several pathways such as PPAR signaling, LXR/RXR activation and glucocorticoid signaling pathways that are not studied in detail in an inflammation and DC maturation context. Our upstream regulator analysis identified 37 major factors that were differentially regulated between the two stimulations; among those are PTGER4, ABCA1, SOCS1, LXR α and DUSP1 which are promising candidates to investigate further. Our phosphoproteome analysis showed differential phosphorylation in 118 phosphosites including those belonging to epigenetic factors, transcription factors and major cell cycle regulators. Our results will enable researchers to investigate the differences in dendritic cell proteomes in detail, both from a general cellular processes level and from a detailed pathway/single protein level. As proteome experiments are comprehensive, any single regulatory protein or pathway can be investigated further to advance our knowledge in dendritic cell maturation and its roles in inflammatory diseases.

ACKNOWLEDGEMENTS

I would like to thank in particular to Dr. Julia Frick for her continuous support and guidance during my entire PhD. Without her extraordinary qualities as a group leader and a colleague, her kindness and support, and willingness to provide freedom and encouragement, this work would not be possible.

I would like to thank Prof. Nadine Ziemert for her generous support as a supervisor during my PhD process, and sharing her expertise and knowledge on the subject.

I would like to thank Prof. Boris Macek, Prof. Sven Nahnsen and the members of their teams for their invaluable contributions as collaboration partners.

I would like to thank Dr. Kerstin Gronbach for promptly training and guiding me in the complicated matter of animal handling and experimentation, without hesitating to spend many hours with me.

I would like to thank our technical assistants Andrea Schäfer and Annika Bender for their countless assistances and support for the experiments.

I would also like to thank Dr. Alexander Steimle for teaching me several important protocols, for his intellectual input and his ideas and help regarding the experiments.

I would like to thank Dr. Sarah Menz for sharing her expertise, help and ideas in every instance over the years we worked together.

I would like to thank all the remaining members of AG Frick for creating a cordial, healthy and supportive working environment, not to mention the pleasant memories and experiences I have gathered so far.

I would like to thank Prof. Sven Nahnsen, and Prof. Dr. Alexander Weber for offering supervision as reviewers and members of the defence committee.

Bibliography

- Akira, S., Takeda, K., & Kaisho, T. (2001). Toll-like receptors: Critical proteins linking innate and acquired immunity. *Nature Immunology*. <https://doi.org/10.1038/90609>
- Allocca, M., Jovani, M., Fiorino, G., Schreiber, S., & Danese, S. (2013). Anti-IL-6 Treatment for Inflammatory Bowel Diseases: Next Cytokine, Next Target. *Current Drug Targets*. <https://doi.org/10.2174/13894501113146660224>
- Atreya, R., & Neurath, M. F. (2005). Involvement of IL-6 in the Pathogenesis of Inflammatory Bowel Disease and Colon Cancer. *Clinical Reviews in Allergy & Immunology*. <https://doi.org/10.1385/CRIAI:28:3:187>
- Baek, S. J. (2002). Dual Function of Nonsteroidal Anti-Inflammatory Drugs (NSAIDs): Inhibition of Cyclooxygenase and Induction of NSAID-Activated Gene. *Journal of Pharmacology and Experimental Therapeutics*. <https://doi.org/10.1124/jpet.301.3.1126>
- Bernardo, D., Vallejo-Díez, S., Mann, E. R., Al-Hassi, H. O., Martínez-Abad, B., Montalvillo, E., ... Knight, S. C. (2012). IL-6 promotes immune responses in human ulcerative colitis and induces a skin-homing phenotype in the dendritic cells and T cells they stimulate. *European Journal of Immunology*. <https://doi.org/10.1002/eji.201142327>
- Bettelli, E., Carrier, Y., Gao, W., Korn, T., Strom, T. B., Oukka, M., ... Kuchroo, V. K. (2006). Reciprocal developmental pathways for the generation of pathogenic effector TH17 and regulatory T cells. *Nature*. <https://doi.org/10.1038/nature04753>
- Biancone, L., Tosti, C., De Nigris, F., Fantini, M., & Pallone, F. (2003). Selective cyclooxygenase-2 inhibitors and relapse of inflammatory bowel disease [7]. *Gastroenterology*. [https://doi.org/10.1016/S0016-5085\(03\)00983-1](https://doi.org/10.1016/S0016-5085(03)00983-1)
- Bogdan, C. (2001). Nitric oxide and the immune response. *Nature Immunology*. <https://doi.org/10.1038/ni1001-907>
- Boughton-Smith, N. K., Evans, S. M., Whittle, B. J. R., Moncada, S., Hawkey, C. J., Cole, A. T., & Balsitis, M. (1993). Nitric oxide synthase activity in ulcerative colitis and Crohn's disease. *The Lancet*. [https://doi.org/10.1016/0140-6736\(93\)91476-3](https://doi.org/10.1016/0140-6736(93)91476-3)
- Braegger, C., Nicholls, S., & Murch, S. (1992). Tumour necrosis factor alpha in stool as a marker of intestinal inflammation. *The Lancet*. [https://doi.org/10.1016/0140-6736\(92\)90999-J](https://doi.org/10.1016/0140-6736(92)90999-J)
- Bron, P. A., Van Baarlen, P., & Kleerebezem, M. (2012). Emerging molecular insights into the interaction between probiotics and the host intestinal mucosa. *Nature Reviews Microbiology*. <https://doi.org/10.1038/nrmicro2690>
- Camuesco, D., Comalada, M., Rodríguez-Cabezas, M. E., Nieto, A., Lorente, M. D., Concha, A., ... Gálvez, J. (2004). The intestinal anti-inflammatory effect of quercitrin is associated with an inhibition in iNOS expression. *British Journal of Pharmacology*. <https://doi.org/10.1038/sj.bjp.0705941>

- Chan, S. H., Perussia, B., Gupta, J. W., Kobayashi, M., Pospíšil, M., Young, H. a, ... Trinchieri, G. (1991). Induction of interferon gamma production by natural killer cell stimulatory factor: characterization of the responder cells and synergy with other inducers. *The Journal of Experimental Medicine*. <https://doi.org/10.1084/jem.173.4.869>
- Chinen, T., Komai, K., Muto, G., Morita, R., Inoue, N., Yoshida, H., ... Yoshimura, A. (2011). Prostaglandin E2 and SOCS1 have a role in intestinal immune tolerance. *Nature Communications*. <https://doi.org/10.1038/ncomms1181>
- Coleman, J. W. W. (2001). Nitric oxide in immunity and inflammation. *International Immunopharmacology*. [https://doi.org/10.1016/S1567-5769\(01\)00086-8](https://doi.org/10.1016/S1567-5769(01)00086-8)
- Dalod, M., Chelbi, R., Malissen, B., & Lawrence, T. (2014). Dendritic cell maturation: Functional specialization through signaling specificity and transcriptional programming. *EMBO Journal*. <https://doi.org/10.1002/emboj.201488027>
- de Saint-Vis, B., Fugier-Vivier, I., Massacrier, C., Gaillard, C., Vanbervliet, B., Aït-Yahia, S., ... Caux, C. (1998). The cytokine profile expressed by human dendritic cells is dependent on cell subtype and mode of activation. *Journal of Immunology (Baltimore, Md. : 1950)*. <https://doi.org/10.4049/jimmunol.166.7.4312>
- Dianda, L., Hanby, A., Wright, N., Sebesteny, A., Hayday, A., & Owen, M. J. (1997). T cell receptor-alpha beta-deficient mice fail to develop colitis in the absence of a microbial environment. *The American Journal of Pathology*.
- Du, X., & Low, M. G. (2001). Down-regulation of glycosylphosphatidylinositol-specific phospholipase D induced by lipopolysaccharide and oxidative stress in the murine monocyte- macrophage cell line RAW 264.7. *Infection and Immunity*. <https://doi.org/10.1128/IAI.69.5.3214-3223.2001>
- Dudek, A. M., Martin, S., Garg, A. D., & Agostinis, P. (2013). Immature, semi-mature, and fully mature dendritic cells: Toward a DC-cancer cells interface that augments anticancer immunity. *Frontiers in Immunology*. <https://doi.org/10.3389/fimmu.2013.00438>
- Duerr, R. H., Taylor, K. D., Brant, S. R., Rioux, J. D., Silverberg, M. S., Daly, M. J., ... Cho, J. H. (2006). A genome-wide association study identifies IL23R as an inflammatory bowel disease gene. *Science (New York, N.Y.)*. <https://doi.org/10.1126/science.1135245>
- El Miedany, Y., Youssef, S., Ahmed, I., & El Gaafary, M. (2006). The gastrointestinal safety and effect on disease activity of etoricoxib, a selective cox-2 inhibitor in inflammatory bowel diseases. *The American Journal of Gastroenterology*. <https://doi.org/10.1111/j.1572-0241.2006.00384.x>
- Fabregat, A., Jupe, S., Matthews, L., Sidiropoulos, K., Gillespie, M., Garapati, P., ... D'Eustachio, P. (2018). The Reactome Pathway Knowledgebase. *Nucleic Acids Research*. <https://doi.org/10.1093/nar/gkx1132>

- Frank, D. N., Robertson, C. E., Hamm, C. M., Kpadeh, Z., Zhang, T., Chen, H., ... Li, E. (2011). Disease phenotype and genotype are associated with shifts in intestinal-associated microbiota in inflammatory bowel diseases. *Inflammatory Bowel Diseases*. <https://doi.org/10.1002/ibd.21339>
- Franke, A., Balschun, T., Karlsen, T. H., Sventoraityte, J., Nikolaus, S., Mayr, G., ... Schreiber, S. (2008). Sequence variants in IL10, ARPC2 and multiple other loci contribute to ulcerative colitis susceptibility. *Nature Genetics*. <https://doi.org/10.1038/ng.221>
- Frick, J. S., Zahir, N., Müller, M., Kahl, F., Bechtold, O., Lutz, M. B., ... Autenrieth, I. B. (2006). Colitogenic and non-colitogenic commensal bacteria differentially trigger DC maturation and Th cell polarization: An important role for IL-6. *European Journal of Immunology*. <https://doi.org/10.1002/eji.200635840>
- Fujimoto, M., & Naka, T. (2003). Regulation of cytokine signaling by SOCS family molecules. *Trends in Immunology*. <https://doi.org/10.1016/j.it.2003.10.008>
- Gabay, C. (2006). Interleukin-6 and chronic inflammation. *Arthritis Research and Therapy*. <https://doi.org/10.1186/ar1917>
- Gronbach, K., Flade, I., Holst, O., Lindner, B., Ruscheweyh, H. J., Wittmann, A., ... Frick, J. S. (2014). Endotoxicity of lipopolysaccharide as a determinant of T-cell-mediated colitis induction in mice. *Gastroenterology*. <https://doi.org/10.1053/j.gastro.2013.11.033>
- Guslandi, M., Mezzi, G., Sorghi, M., & Testoni, P. A. (2000). *Saccharomyces boulardii* in maintenance treatment of Crohn's disease. *Dig Dis Sci*.
- Hawkey, C. (1999). COX-2 inhibitors. *The Lancet*. [https://doi.org/10.1016/S0140-6736\(98\)12154-2](https://doi.org/10.1016/S0140-6736(98)12154-2)
- Horino, J., Fujimoto, M., Terabe, F., Serada, S., Takahashi, T., Soma, Y., ... Naka, T. (2008). Suppressor of cytokine signaling-1 ameliorates dextran sulfate sodium-induced colitis in mice. *International Immunology*. <https://doi.org/10.1093/intimm/dxn033>
- Hornbeck, P. V., Zhang, B., Murray, B., Kornhauser, J. M., Latham, V., & Skrzypek, E. (2015). PhosphoSitePlus, 2014: Mutations, PTMs and recalibrations. *Nucleic Acids Research*. <https://doi.org/10.1093/nar/gku1267>
- Hsieh, C. S., Macatonia, S. E., Tripp, C. S., Wolf, S. F., O'Garra, A., & Murphy, K. M. (1993). Development of TH1 CD4+T cells through IL-12 produced by Listeria-induced macrophages. *Science*. <https://doi.org/10.1126/science.8097338>
- Jarrossay, D., Napolitani, G., Colonna, M., Sallusto, F., & Lanzavecchia, A. (2001). Specialization and complementarity in microbial molecule recognition by human myeloid and plasmacytoid dendritic cells. *European Journal of Immunology*. [https://doi.org/10.1002/1521-4141\(200111\)31:11<3388::AID-IMMU3388>3.0.CO;2-Q](https://doi.org/10.1002/1521-4141(200111)31:11<3388::AID-IMMU3388>3.0.CO;2-Q)
- Jensen, S. S., & Gad, M. (2010). Differential induction of inflammatory cytokines by dendritic cells treated with novel TLR-agonist and cytokine based cocktails: Targeting dendritic cells in autoimmunity. *Journal of Inflammation*. <https://doi.org/10.1186/1476-9255-7-37>

- Joseph, S. B., Bradley, M. N., Castrillo, A., Bruhn, K. W., Mak, P. A., Pei, L., ... Tontonoz, P. (2004). LXR-dependent gene expression is important for macrophage survival and the innate immune response. *Cell*. <https://doi.org/10.1016/j.cell.2004.09.032>
- Joseph, S. B., Castrillo, A., Laffitte, B. A., Mangelsdorf, D. J., & Tontonoz, P. (2003). Reciprocal regulation of inflammation and lipid metabolism by liver X receptors. *Nature Medicine*. <https://doi.org/10.1038/nm820>
- Kadowaki, N., Ho, S., Antonenko, S., de Waal Malefyt, R., Kastelein, R. A., Bazan, F., & Liu, Y.-J. (2001). Subsets of Human Dendritic Cell Precursors Express Different Toll-like Receptors and Respond to Different Microbial Antigens. *The Journal of Experimental Medicine*. <https://doi.org/10.1084/jem.194.6.863>
- Kam, P. C. A., & See, A. U. L. (2000). Cyclo-oxygenase isoenzymes: Physiological and pharmacological role. *Anaesthesia*. <https://doi.org/10.1046/j.1365-2044.2000.01271.x>
- Kawai, T., & Akira, S. (2010). The role of pattern-recognition receptors in innate immunity: Update on toll-like receptors. *Nature Immunology*. <https://doi.org/10.1038/ni.1863>
- Keubler, L. M., Buettner, M., Häger, C., & Bleich, A. (2015). A multihit model: Colitis lessons from the interleukin-10-deficient mouse. *Inflammatory Bowel Diseases*. <https://doi.org/10.1097/MIB.0000000000000468>
- Kinjo, I., Hanada, T., Inagaki-Ohara, K., Mori, H., Aki, D., Ohishi, M., ... Yoshimura, A. (2002). SOCS1/JAB is a negative regulator of LPS-induced macrophage activation. *Immunity*. [https://doi.org/10.1016/S1074-7613\(02\)00446-6](https://doi.org/10.1016/S1074-7613(02)00446-6)
- Kishimoto, T., Akira, S., Narazaki, M., & Taga, T. (1995). Interleukin-6 Family of Cytokines and gp130. *Blood*. <https://doi.org/7632928>
- Kontoyiannis, D., Pasparakis, M., Pizarro, T. T., Cominelli, F., & Kollias, G. (1999). Impaired on/off regulation of TNF biosynthesis in mice lacking TNF AU- rich elements: Implications for joint and gut-associated immunopathologies. *Immunity*. [https://doi.org/10.1016/S1074-7613\(00\)80038-2](https://doi.org/10.1016/S1074-7613(00)80038-2)
- Korn, T., Bettelli, E., Oukka, M., & Kuchroo, V. K. (2009). IL-17 and Th17 Cells. *Annual Review of Immunology*. <https://doi.org/10.1146/annurev.immunol.021908.132710>
- Krämer, A., Green, J., Pollard, J., & Tugendreich, S. (2014). Causal analysis approaches in ingenuity pathway analysis. *Bioinformatics*. <https://doi.org/10.1093/bioinformatics/btt703>
- Lanzavecchia, A. (1990). Receptor-mediated antigen uptake and its effect on antigen presentation to class II-restricted T lymphocytes. *Annual Review of Immunology*. <https://doi.org/10.1146/annurev.iy.08.040190.004013>
- Levine, D. M., Parker, T. S., Donnelly, T. M., Walsh, A., & Rubin, A. L. (1993). In vivo protection against endotoxin by plasma high density lipoprotein. *Proceedings of the National Academy of Sciences of the United States of America*. <https://doi.org/10.1073/pnas.90.24.12040>
- Li, B., Alli, R., Vogel, P., & Geiger, T. L. (2014). IL-10 modulates DSS-induced colitis through a macrophage-ROS-NO axis. *Mucosal Immunology*. <https://doi.org/10.1038/mi.2013.103>

- Lutz, M. B., & Schuler, G. (2002). Immature, semi-mature and fully mature dendritic cells: Which signals induce tolerance or immunity? *Trends in Immunology*. [https://doi.org/10.1016/S1471-4906\(02\)02281-0](https://doi.org/10.1016/S1471-4906(02)02281-0)
- Malchow, H. A. (1997). Crohn's disease and Escherichia coli: A new approach in therapy to maintain remission of colonic crohn's disease? *Journal of Clinical Gastroenterology*. <https://doi.org/10.1097/00004836-199712000-00021>
- Manetti, R., Parronchi, P., Giudizi, M. G., Piccinni, M. P., Maggi, E., Trinchieri, G., & Romagnani, S. (1993). Natural killer cell stimulatory factor (interleukin 12 [IL-12]) induces T helper type 1 (Th1)-specific immune responses and inhibits the development of IL-4-producing Th cells. *The Journal of Experimental Medicine*. <https://doi.org/10.1084/jem.177.4.1199>
- Mannon, P. J., Fuss, I. J., Mayer, L., Elson, C. O., Sandborn, W. J., Present, D., ... Strober, W. (2004). Anti-Interleukin-12 Antibody for Active Crohn's Disease. *New England Journal of Medicine*. <https://doi.org/10.1056/NEJMoa033402>
- McCartney, S. A., Mitchell, J. A., Fairclough, P. D., Farthing, M. J., & Warner, T. D. (1999). Selective COX-2 inhibitors and human inflammatory bowel disease. *Alimentary Pharmacology & Therapeutics*. <https://doi.org/10.1046/j.1365-2036.1999.00585.x>
- Mellman, I., & Steinman, R. M. (2001). Dendritic cells: Specialized and regulated antigen processing machines. *Cell*. [https://doi.org/10.1016/S0092-8674\(01\)00449-4](https://doi.org/10.1016/S0092-8674(01)00449-4)
- Mocellin, S., Panelli, M. C., Wang, E., Nagorsen, D., & Marincola, F. M. (2003). The dual role of IL-10. *Trends in Immunology*. [https://doi.org/10.1016/S1471-4906\(02\)00009-1](https://doi.org/10.1016/S1471-4906(02)00009-1)
- Morgan, X. C., Tickle, T. L., Sokol, H., Gevers, D., Devaney, K. L., Ward, D. V., ... Huttenhower, C. (2012). Dysfunction of the intestinal microbiome in inflammatory bowel disease and treatment. *Genome Biology*. <https://doi.org/10.1186/gb-2012-13-9-r79>
- Mostecky, J., Showalter, B. M., & Rothman, P. B. (2005). Early growth response-1 regulates lipopolysaccharide-induced suppressor of cytokine signaling-1 transcription. *Journal of Biological Chemistry*. <https://doi.org/10.1074/jbc.M408938200>
- Mudter, J., & Neurath, M. F. (2007). IL-6 signaling in inflammatory bowel disease: Pathophysiological role and clinical relevance. *Inflammatory Bowel Diseases*. <https://doi.org/10.1002/ibd.20148>
- Mueller, C. (2002). Tumour necrosis factor in mouse models of chronic intestinal inflammation. *Immunology*. <https://doi.org/10.1046/j.1365-2567.2002.01329.x>
- Neurath, M. F., Fuss, I., Pasparakis, M., Alexopoulou, L., Haralambous, S., Meyer zum Büschenfelde, K. H., ... Kollias, G. (1997). Predominant pathogenic role of tumor necrosis factor in experimental colitis in mice. *European Journal of Immunology*. <https://doi.org/10.1002/eji.1830270722>
- Niedbala, W., Wei, X. Q., Piedrafita, D., Xu, D., & Liew, F. Y. (1999). Effects of nitric oxide on the induction and differentiation of Th1 cells. *Eur J Immunol*. [https://doi.org/10.1002/\(SICI\)1521-4141\(199908\)29:08<2498::AID-IMMU2498>3.0.CO;2-M](https://doi.org/10.1002/(SICI)1521-4141(199908)29:08<2498::AID-IMMU2498>3.0.CO;2-M)

- Niess, J. H., Brand, S., Gu, X., Landsman, L., Jung, S., McCormick, B. A., ... Reinecker, H. C. (2005). CX3CR1-mediated dendritic cell access to the intestinal lumen and bacterial clearance. *Science*. <https://doi.org/10.1126/science.1102901>
- Ohl, L., Mohaupt, M., Czeloth, N., Hintzen, G., Kiafard, Z., Zwirner, J., ... Förster, R. (2004). CCR7 governs skin dendritic cell migration under inflammatory and steady-state conditions. *Immunity*. <https://doi.org/10.1016/j.immuni.2004.06.014>
- Okada, M., Kitahara, M., Kishimoto, S., Matsuda, T., Hirano, T., & Kishimoto, T. (1988). IL-6/BSF-2 functions as a killer helper factor in the in vitro induction of cytotoxic T cells. *Journal of Immunology (Baltimore, Md. : 1950)*. [https://doi.org/10.1016/0192-0561\(88\)90486-9](https://doi.org/10.1016/0192-0561(88)90486-9)
- Oram, J. F., & Yokoyama, S. (1996). Apolipoprotein-mediated removal of cellular cholesterol and phospholipids. *Journal of Lipid Research*.
- Ott, S. J., Musfeldt, M., Wenderoth, D. F., Hampe, J., Brant, O., Fölsch, U. R., ... Schreiber, S. (2004). Reduction in diversity of the colonic mucosa associated bacterial microflora in patients with active inflammatory bowel disease. *Gut*. <https://doi.org/10.1136/gut.2003.025403>
- Otto, A., Bernhardt, J., Meyer, H., Schaffer, M., Herbst, F. A., Siebourg, J., ... Becher, D. (2010). Systems-wide temporal proteomic profiling in glucose-starved *Bacillus subtilis*. *Nature Communications*. <https://doi.org/10.1038/ncomms1137>
- Ouyang, W., Rutz, S., Crellin, N. K., Valdez, P. A., & Hymowitz, S. G. (2011). Regulation and Functions of the IL-10 Family of Cytokines in Inflammation and Disease. *Annual Review of Immunology*. <https://doi.org/10.1146/annurev-immunol-031210-101312>
- Probst, H. C., Lagnel, J., Kollias, G., & Van Den Broek, M. (2003). Inducible transgenic mice reveal resting dendritic cells as potent inducers of CD8+ T cell tolerance. *Immunity*. [https://doi.org/10.1016/S1074-7613\(03\)00120-1](https://doi.org/10.1016/S1074-7613(03)00120-1)
- Rachmilewitz, D., Stamler, J. S., Bachwich, D., Karmeli, F., Ackerman, Z., & Podolsky, D. K. (1995). Enhanced colonic nitric oxide generation and nitric oxide synthase activity in ulcerative colitis and Crohn's disease. *Gut*. <https://doi.org/10.1136/gut.36.5.718>
- Rao, K. M. (2015). Molecular mechanisms regulating iNOS expression in various cell types. *Journal of Toxicology and Environmental Health. Part B, Critical Reviews*. <https://doi.org/10.1080/109374000281131>
- Reimund, J. M., Wittersheim, C., Dumont, S., Muller, C. D., Baumann, R., Poindron, P., & Duclos, B. (1996). Mucosal inflammatory cytokine production by intestinal biopsies in patients with ulcerative colitis and Crohn's disease. *Journal of Clinical Immunology*. <https://doi.org/10.1007/BF01540912>
- Rutgeerts, P., Hiele, M., Geboes, K., Peeters, M., Penninckx, F., Aerts, R., & Kerremans, R. (1995). Controlled trial of metronidazole treatment for prevention of crohn's recurrence after ileal resection. *Gastroenterology*. [https://doi.org/10.1016/0016-5085\(95\)90121-3](https://doi.org/10.1016/0016-5085(95)90121-3)
- Sabat, R., Grütz, G., Warszawska, K., Kirsch, S., Witte, E., Wolk, K., & Geginat, J. (2010). Biology of interleukin-10. *Cytokine and Growth Factor Reviews*. <https://doi.org/10.1016/j.cytogfr.2010.09.002>

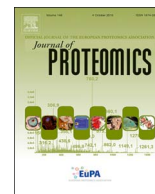
- Sadlack, B., Merz, H., Schorle, H., Schimpl, A., Feller, A. C., & Horak, I. (1993). Ulcerative colitis-like disease in mice with a disrupted interleukin-2 gene. *Cell*. [https://doi.org/10.1016/0092-8674\(93\)80067-O](https://doi.org/10.1016/0092-8674(93)80067-O)
- Sakthivel, K. M., & Guruvayoorappan, C. (2013). Amentoflavone inhibits iNOS, COX-2 expression and modulates cytokine profile, NF- κ B signal transduction pathways in rats with ulcerative colitis. *International Immunopharmacology*. <https://doi.org/10.1016/j.intimp.2013.09.022>
- Sallusto, B. F., & Lanzavecchia, A. (1994). Dendritic cell use macropinocytosis and the mannose receptor to concentrate macromolecules in the major histocompatibility complex class II compartment: downregulation by cytokines and bacterial products. *Journal of Experimental Medicine*.
- Schmitz, J., Owyang, A., Oldham, E., Song, Y., Murphy, E., McClanahan, T. K., ... Kastelein, R. A. (2005). IL-33, an interleukin-1-like cytokine that signals via the IL-1 receptor-related protein ST2 and induces T helper type 2-associated cytokines. *Immunity*. <https://doi.org/10.1016/j.immuni.2005.09.015>
- Schröder, N. W., Opitz, B., Lamping, N., Michelsen, K. S., Zähringer, U., Göbel, U. B., & Schumann, R. R. (2000). Involvement of lipopolysaccharide binding protein, CD14, and Toll-like receptors in the initiation of innate immune responses by *Treponema glycolipids*. *J. Immunol.* <https://doi.org/10.4049/jimmunol.165.5.2683>
- Schultz, M., Tonkonogy, S. L., Sellon, R. K., Veltkamp, C., Godfrey, V. L., Kwon, J., ... Sartor, R. B. (1999). IL-2-deficient mice raised under germfree conditions develop delayed mild focal intestinal inflammation. *American Journal of Physiology - Gastrointestinal and Liver Physiology*.
- Seibert, K., & Masferrer, J. L. (1994). Role of inducible cyclooxygenase (COX-2) in inflammation. *Receptor*.
- Sellon, R. K., Tonkonogy, S., Schultz, M., Dieleman, L. A., Grenther, W., Balish, E., ... Sartor, R. B. (1998). Resident enteric bacteria are necessary for development of spontaneous colitis and immune system activation in interleukin-10-deficient mice. *Infection and Immunity*.
- Siewe, L., Bollati-Fogolin, M., Wickenhauser, C., Krieg, T., Müller, W., & Roers, A. (2006). Interleukin-10 derived from macrophages and/or neutrophils regulates the inflammatory response to LPS but not the response to CpG DNA. *European Journal of Immunology*. <https://doi.org/10.1002/eji.200636012>
- Singer, I. I., Kawka, D. W., Schloemann, S., Tessner, T., Riehl, T., & Stenson, W. F. (1998). Cyclooxygenase 2 is induced in colonic epithelial cells in inflammatory bowel disease. *Gastroenterology*. [https://doi.org/10.1016/S0016-5085\(98\)70196-9](https://doi.org/10.1016/S0016-5085(98)70196-9)
- Sjoelund, V., Smelkinson, M., & Nita-Lazar, A. (2014). Phosphoproteome profiling of the macrophage response to different toll-like receptor ligands identifies differences in global phosphorylation dynamics. *Journal of Proteome Research*. <https://doi.org/10.1021/pr5002466>

- Spörri, R., & Reis e Sousa, C. (2005). Inflammatory mediators are insufficient for full dendritic cell activation and promote expansion of CD4+ T cell populations lacking helper function. *Nature Immunology*. <https://doi.org/10.1038/ni1162>
- Starr, R., Metcalf, D., Elefanty, A. G., Brysha, M., Willson, T. A., Nicola, N. A., ... Alexander, W. S. (1998). Liver degeneration and lymphoid deficiencies in mice lacking suppressor of cytokine signaling-1. *Proceedings of the National Academy of Sciences*. <https://doi.org/10.1073/pnas.95.24.14395>
- Steinman, R. M. (1988). Cytokines amplify the function of accessory cells. *Immunology Letters*. [https://doi.org/10.1016/0165-2478\(88\)90028-4](https://doi.org/10.1016/0165-2478(88)90028-4)
- Sturlan, S., Oberhuber, G., Beinhauer, B. G., Tichy, B., Kappel, S., Wang, J., & Rogy, M. A. (2001). Interleukin-10-deficient mice and inflammatory bowel disease associated cancer development. *Carcinogenesis*. <https://doi.org/10.1093/carcin/22.4.665>
- Takeda, K., Clausen, B. E., Kaisho, T., Tsujimura, T., Terada, N., Förster, I., & Akira, S. (1999). Enhanced Th1 activity and development of chronic enterocolitis in mice devoid of stat3 in macrophages and neutrophils. *Immunity*. [https://doi.org/10.1016/S1074-7613\(00\)80005-9](https://doi.org/10.1016/S1074-7613(00)80005-9)
- Takeuchi, O., Hoshino, K., Kawai, T., Sanjo, H., Takada, H., Ogawa, T., ... Akira, S. (1999). Differential roles of TLR2 and TLR4 in recognition of gram-negative and gram-positive bacterial cell wall components. *Immunity*. [https://doi.org/10.1016/S1074-7613\(00\)80119-3](https://doi.org/10.1016/S1074-7613(00)80119-3)
- Tanaka, T., Narazaki, M., & Kishimoto, T. (2014). Il-6 in inflammation, Immunity, And disease. *Cold Spring Harbor Perspectives in Biology*. <https://doi.org/10.1101/cshperspect.a016295>
- Tang, C., Liu, Y., Kessler, P. S., Vaughan, A. M., & Oram, J. F. (2009). The macrophage cholesterol exporter ABCA1 functions as an anti-inflammatory receptor. *Journal of Biological Chemistry*. <https://doi.org/10.1074/jbc.M109.047472>
- Taurog, J. D., Richardson, J. A., Croft, J. T., Simmons, W. A., Zhou, M., Fernández-Sueiro, J. L., ... Hammer, R. E. (1994). The germfree state prevents development of gut and joint inflammatory disease in HLA-B27 transgenic rats. *The Journal of Experimental Medicine*. <https://doi.org/10.1084/jem.180.6.2359>
- Thompson, P. A., Gauthier, K. C., Varley, A. W., & Kitchens, R. L. (2010). ABCA1 promotes the efflux of bacterial LPS from macrophages and accelerates recovery from LPS-induced tolerance. *Journal of Lipid Research*. <https://doi.org/10.1194/jlr.M007435>
- Trembleau, S., Penna, G., Bosi, E., Mortara, A., Gately, M. K., & Adorini, L. (1995). Interleukin 12 administration induces T helper type 1 cells and accelerates autoimmune diabetes in NOD mice. *Journal of Experimental Medicine*. <https://doi.org/10.1084/jem.181.2.817>
- Trombetta, E. S., Ebersold, M., Garrett, W., Pypaert, M., Mellman, I., Germain, R. N., ... Malefyt, R. de W. (2003). Activation of lysosomal function during dendritic cell maturation. *Science (New York, N.Y.)*. <https://doi.org/10.1126/science.1080106>

- Turunen, U. M., Farkkila, M. A., Hakala, K., Seppala, K., Sivonen, A., Ogren, M., ... Miettinen, T. A. (1998). Long-term treatment of ulcerative colitis with ciprofloxacin: A prospective, double-blind, placebo-controlled study. *Gastroenterology*. [https://doi.org/10.1016/S0016-5085\(98\)70076-9](https://doi.org/10.1016/S0016-5085(98)70076-9)
- Waidmann, M., Bechtold, O., Frick, J. S., Lehr, H. A., Schubert, S., Dobrindt, U., ... Autenrieth, I. B. (2003). *Bacteroides vulgatus* protects against *Escherichia coli*-induced colitis in gnotobiotic interleukin-2-deficient mice. *Gastroenterology*. [https://doi.org/10.1016/S0016-5085\(03\)00672-3](https://doi.org/10.1016/S0016-5085(03)00672-3)
- Wang, D., & Dubois, R. N. (2010). The role of COX-2 in intestinal inflammation and colorectal cancer. *Oncogene*. <https://doi.org/10.1038/onc.2009.421>
- Wills-Karp, M., Nathan, A., Page, K., & Karp, C. L. (2010). New insights into innate immune mechanisms underlying allergenicity. *Mucosal Immunology*. <https://doi.org/10.1038/mi.2009.138>
- Wittmann, A., Bron, P. A., Swam, I. I. Van, & Kleerebezem, M. (2015). TLR Signaling-induced CD103-expressing Cells Protect Against Intestinal Inflammation, (January). <https://doi.org/10.15496/publikation-6339>
- Yokoyama, S. (1998). Apolipoprotein-mediated cellular cholesterol efflux. *Biochimica et Biophysica Acta - Lipids and Lipid Metabolism*. [https://doi.org/10.1016/S0005-2760\(98\)00032-0](https://doi.org/10.1016/S0005-2760(98)00032-0)
- Yu, C., Zhang, S., Wang, Y., Zhang, S., Luo, L., & Thorlacius, H. (2016). Platelet-Derived CCL5 Regulates CXC Chemokine Formation and Neutrophil Recruitment in Acute Experimental Colitis. *Journal of Cellular Physiology*. <https://doi.org/10.1002/jcp.25081>

Contents lists available at [ScienceDirect](https://www.sciencedirect.com)

Journal of Proteomics

journal homepage: www.elsevier.com/locate/jprot

Proteome and phosphoproteome analysis of commensally induced dendritic cell maturation states

Ali Giray Korkmaz^{a,*}, Todor Popov^a, Loulou Peisl^a, Marius Cosmin Codrea^b, Sven Nahnsen^b, Alexander Steimle^a, Ana Velic^c, Boris Macek^c, Martin von Bergen^d, Joerg Bernhardt^e, Julia-Stefanie Frick^a

^a Institute of Medical Microbiology and Hygiene, University of Tübingen, Germany

^b Quantitative Biology Center, University of Tübingen, Germany

^c Proteome Center, University of Tübingen, Germany

^d Helmholtz Centre for Environmental Research - UFZ, Leipzig, Germany

^e Ernst-Moritz-Arndt Universität Greifswald, Institute for Microbiology, Germany

ARTICLE INFO

Keywords:

Commensals

B. vulgatus

Dendritic cells

Inflammation

Shotgun proteomics

Expression analysis

ABSTRACT

Dendritic cells (DCs) can shape the immune system towards an inflammatory or tolerant state depending on the bacterial antigens and the environment they encounter. In this study we provide a proteomic catalogue of differentially expressed proteins between distinct DC maturation states, brought about by bacteria that differ in their endotoxicity. To achieve this, we have performed proteomics and phosphoproteomics on murine DC cultures. Symbiont and pathobiont bacteria were used to direct dendritic cells into a semi-mature and fully-mature state, respectively. The comparison of semi-mature and fully-mature DCs revealed differential expression in 103 proteins and differential phosphorylation in 118 phosphosites, including major regulatory factors of central immune processes. Our analyses predict that these differences are mediated by upstream elements such as SOCS1, IRF3, ABCA1, TLR4, and PTGER4. Our analyses indicate that the symbiont bacterial strain affects DC proteome in a distinct way, by downregulating inflammatory proteins and activating anti-inflammatory upstream regulators.

Biological significance

In this study we have investigated the responses of immune cells to distinct bacterial stimuli. We have used the symbiont bacterial strain *B. vulgatus* and the pathobiont *E. coli* strain to stimulate cultured primary dendritic cells and performed a shotgun proteome analysis to investigate the protein expression and phosphorylation level differences on a genome level. We have observed expression and phosphorylation level differences in key immune regulators, transcription factors and signal transducers. Moreover, our subsequent bioinformatics analysis indicated regulation at several signaling pathways such as PPAR signaling, LXR/RXR activation and glucocorticoid signaling pathways, which are not studied in detail in an inflammation and DC maturation context. Our phosphoproteome analysis showed differential phosphorylation in 118 phosphosites including those belonging to epigenetic regulators, transcription factors and major cell cycle regulators. We anticipate that our study will facilitate further investigation of immune cell proteomes under different inflammatory and non-inflammatory conditions.

1. Introduction

The human gut microbiota is composed of approximately 100 trillion bacteria that belong to over 1000 species. Humans and their gut microbial ecosystem have coevolved to exist in homeostasis, and the bacteria residing in the gut provide numerous benefits to the human host such as aiding digestion, supporting gut development, and

preventing pathogenic bacteria to colonize the gut. Two important and prevalent species of gut microbiota are the gram negative bacteria *E. coli* and *B. vulgatus*, which have notable differences in terms of their interaction with the host and their effects on gut homeostasis. Waidmann et al. have shown that monocolonization of germ free IL2^{-/-} mice with *E. coli* leads to colitis whereas monocolonization with *B. vulgatus* does not. Moreover, co-colonization with *B. vulgatus* protects

* Corresponding author.

E-mail address: giray.korkmaz@med.uni-tuebingen.de (A.G. Korkmaz).

<https://doi.org/10.1016/j.jprot.2017.11.008>

Received 17 February 2017; Received in revised form 18 September 2017; Accepted 14 November 2017

1874-3919/ © 2017 Published by Elsevier B.V.

mice from inflammatory bowel disease (IBD) inducing effects of *E. coli* [1]. This suggests that the two bacteria species have significant differences in regulating the immune responses of the host; however, their effects on the immune cells and regulation of immunological pathways are unknown.

Dendritic cells are potent regulators of immune responses and exist in different maturation states. DC maturation states have been previously shown to be influential in eliciting tolerance and protecting from disease [2,3]. Our group has previously shown that DCs isolated from colitic mice show increased expression of cell surface activation markers and proinflammatory cytokines, whereas DCs isolated from protected mice show a semi-mature phenotype. This maturation state difference of DCs have also been shown *in vitro*, where *E. coli* stimulation of immature DCs leads to high levels of proinflammatory cytokine secretion. On the other hand, stimulation of BMDCs with *B. vulgatus* leads to low levels of proinflammatory cytokine secretion and renders them unresponsive to further stimulus [4,5]. These findings prompted us to investigate the differential immune responses mounted against these bacteria, and we performed a label free quantitative proteome analysis to catalogue the differences in protein expression patterns between two different maturation states.

Our proteomics experiments revealed relative abundance differences in 301 proteins between different dendritic cell maturation states (any protein that exhibit a relative abundance difference among the 3 pairwise comparisons of *E. coli* vs. PBS, *B. vulgatus* vs. PBS, *B. vulgatus* vs. *E. coli* stimulations is included). These 301 differentially expressed proteins were then used as the experimental data set for further bioinformatics downstream analysis. Functional grouping and pathway analysis revealed differences in major immune regulatory pathways and processes such as IRF signaling, TLR signaling and leukocyte activation pathways. Besides these pathways which are directly tied to central immune functions, pathways such as PPAR signaling, LXR/RXR activation and JAK/Stat signaling were observed to be taking part in creating the distinct maturation phenotypes. Our further analyses were targeted to major upstream regulators and revealed 37 proteins that were differentially activated between *B. vulgatus* and *E. coli* stimulated DCs. Among these are factors such as PTGER4, ABCA1, DUSP1 and SOCS1 that regulate inflammatory processes. Taken together, we created a proteome catalogue of different dendritic cell maturation states, and investigated the cellular processes mediating their phenotypical differences. We anticipate that our results will contribute to dissecting the dendritic cell maturation process in further detail, and thereby improve our understanding of immune regulation in inflammatory diseases.

2. Materials and methods

2.1. Bacterial strains

Bacteria used for stimulating mouse dendritic cells were *Escherichia coli* and *Bacteroides vulgatus* [1]. The *E. coli* strain was cultured in Luria-Bertani (LB) medium at 37 °C under aerobic conditions, the *B. vulgatus* strain was cultured in Brain-Heart-Infusion (BHI) medium at 37 °C under anaerobic conditions. Bacterial concentration was determined by photometry at OD₆₀₀.

2.2. Murine bone marrow dendritic cell culture

The mice used are 6–10 weeks old female C57BL/6NCrI, purchased from Charles River Laboratories and kept under specific pathogen-free conditions for two weeks before bone marrow isolation. Necessary animal experimentation permission was granted by the local authority on animal experimentation (Regierungspräsidium Tübingen, Anzeige 01.12.11). All proteome and phosphoproteome analyses were done in two biological replicates, each biological replicate consisting of cells pooled from 8 mice. The animals were sacrificed by euthanasia

followed by cervical dislocation. Bone marrows of femur and tibia were aspirated, and the resulting cells were cultured in VLE-RPMI-medium (Biochrom, FG1415) supplemented with 10% heat inactivated fetal calf serum (Sigma, F7524), 1% non-essential amino acids (Biochrom, K0293), 100 Units/mL Penicillin, 100 µg/mL Streptomycin, 50 µmol/l 2-Mercaptoethanol and 0.5 ng/mL GM-CSF produced in house using the murine myeloma cell line P3X63. A detailed protocol for obtaining and culturing BMDCs was described before [6], and used with the modification of shortening the culture time to 7 days instead of 10. After 7 days of culture, the resulting population was analyzed by flow cytometry for the presence of DCs, harvested and stimulated with the bacterial strains *E. coli* and *B. vulgatus* at an MOI1 for 16 h under cell culture conditions. At the end of the stimulation, dendritic cell activation/maturation was analyzed by flow cytometry (cellular fraction) and ELISA (culture supernatant).

2.3. Flow cytometry analysis

After stimulation with bacterial strains for 16 h, cells were harvested and stained with fluorophore conjugated primary antibodies CD11c-APC (BD, 550261), MHC class II-FITC(BD, 553623), CD40-FITC(553723). Stained cells were measured by LSRFortessa (BD Biosciences) and analyzed with FlowJo software (Version 7.6, Tree Star Inc.).

2.4. ELISA

Enzyme linked immunosorbent assays have been performed on cell culture supernatants of DCs stimulated as indicated above. Cytokine concentrations in supernatants have been determined using ELISA kits for IL-6 (BD, 555240), IL-1β (BD, 559603), TNF-α (BD, 555268), and IL12p40 (BD, 555165). ELISAs were performed as described in manufacturer's protocols.

2.5. Protein digestion

For the analysis of phosphoproteome two milligrams of the protein extracts derived from the DC culture upon bacterial stimulation were digested in solution with trypsin as described previously [7,8]. For proteome analysis immunoprecipitated proteins of 20 µg of sample were loaded on a 10% SDS-PAGE gel. After short gel run and brief Coomassie staining each gel piece was cut into small pieces. Destaining was performed by washing three times with 10 mM ammonium bicarbonate (ABC) and acetonitrile (ACN) (1:1, v/v). This was followed by protein reduction with 10 mM dithiothreitol (DTT) in 20 mM ABC for 45 min at 56 °C, and alkylation with 55 mM iodoacetamide (IAA) in 20 mM ABC for 30 min at room temperature in the dark. The gel pieces were then washed twice for 20 min in destaining solution followed by dehydration with can in a vacuum centrifuge. The residual liquid was removed and gel pieces were rehydrated at room temperature by adding 13 ng/µl sequencing grade trypsin in 20 mM ABC. Digestion of proteins was performed at 37 °C overnight. The resulting peptides were extracted in three subsequent incubation steps: 1) with 30% ACN/3% TFA; 2) with 80% ACN/0.5% acetic acid; and 3) with 100% ACN. Supernatants were combined, ACN was evaporated in a vacuum centrifuge and peptides were desalted using C18 StageTips.

2.6. Phosphopeptide enrichment

Phosphopeptide enrichment and phosphoproteome analysis was done as described previously [9], with minor modifications: about 95% of the peptides were separated by strong cation exchange (SCX) chromatography with a gradient of 0 to 35% SCX solvent B resulting in eleven fractions that were subjected to phosphopeptide enrichment by TiO₂ beads. Fractions containing a high amount of peptides were subjected to TiO₂ enrichment multiple times. Elution from the beads

was performed three times with 100 μ l of 40% ammonia hydroxide solution in 60% acetonitrile (pH > 10.5). Enrichment of phosphopeptides from the SCX flow-through was done in five cycles, which were then pooled and measured in triplicates.

2.7. Mass spectrometry

LC-MS/MS analyses were performed on an EasyLC nano-HPLC (Proxeon Biosystems) coupled to an LTQ Orbitrap XL or an LTQ Orbitrap Elite mass spectrometer (Thermo Scientific) as described previously [10]. The peptide mixtures were injected onto the column in HPLC solvent A (0.5% acetic acid) at a flow rate of 500 nL/min and subsequently eluted with a 230 min gradient of 5%–33% HPLC solvent B (80% ACN in 0.5% acetic acid). During peptide elution the flow rate was kept constant at 200 nL/min. Mass tolerance for precursor ions and fragment ions were 20 ppm. For proteome analysis, 15 most intense precursor ions were sequentially fragmented in each scan cycle (Orbitrap Elite). The phosphoproteome analysis was exclusively done on the Orbitrap XL, with five most intense precursor ions fragmented by multistage activation of neutral loss ions at -98 , -49 , and -32.6 Th relative to the precursor ion [11]. In all measurements, sequenced precursor masses were excluded from further selection for 90 s. The target values for the LTQ were 5000 charges (MS/MS) and 106 charges (MS); the maximum allowed fill times were 1000 ms. Lock-mass option was used for real-time recalibration of MS spectra [12]. The experiments were performed in three technical replicates for each biological replicate.

2.8. Experimental design and statistical rationale

Label-free proteome and phosphoproteome experiments were run with two biological replicates each, consisting of cells pooled from a total of 8 mice for each biological replicate. Each biological replicate was then divided into 3 technical replicates and handled separately under the exact conditions and run with the same parameters. Mass spectrometry performed on unstimulated cells (denoted as PBS sample) was used as the control group, whereas *B. vulgatus* and *E. coli* stimulated cells served as experimental subsets. The data was searched against UniProt mouse database (version February 2014, comprising 51,373 sequences). In order to estimate the false discovery rate (FDR) of peptide and protein identifications, the reversed sequences were appended to the original FASTA entries. In addition, the known contaminants from the common Repository of Adventitious Proteins (<http://www.thegpm.org/crap>) were excluded. The following modifications were used: fixed - Carbamidomethyl(C) and variable -Acetyl(N-term); Oxidation(M); Phospho (STY). The identifications scoring and FDR were calculated as described in Cox et al. [13]. The raw mass spectrometry data was processed with MaxQuant version 1.5.0.25 [14]. The data was searched against UniProt mouse database (version February 2014) with the following modifications: fixed - Carbamidomethyl(C) and variable -Acetyl(N-term); Oxidation(M); Phospho (STY). In the absence of isoform-specific peptides, the protein isoforms were grouped together and regarded as equally represented. The protein and peptides intensities were quantile normalized in R [15]. The differential expression analysis of the proteins and peptide modifications was performed with linear mixed models R (nlme) [16,17]. The difference in protein expression arising from bacterial stimulation and stimulation duration was calculated, also taking into account the variations between biological and technical replicates. Mathematically, the differential expression analysis of the proteins and peptide modifications is represented as a linear mixed model, that models the response Y (see formula below) as a function of the factors stimulation and time and the random effect which is technical replicates nested within biological replicates. The model used is as follows: $Y = \beta_0 + \beta_1 X_1 + \beta_2 X_2 + \beta_3 X_1 X_2 + \varepsilon(\gamma_b/\gamma_t)$, where Y is the response variable, β_0 is the intercept, β_1 , β_2 , β_3 are slope coefficients, and $\varepsilon(\gamma_b/\gamma_t)$

γ_t) is the random effect contribution of technical replicates γ_t nested within biological replicates γ_b . Post-hoc analysis was performed with Tukey's "Honest Significant Difference" method to get the actual pairwise differences among PBS control, *B. vulgatus* and *E. coli* stimulated DCs [15]. This standard procedure accounts for multiple comparisons (the three conditions) and reports adjusted p -values. Correction for multiple hypothesis testing (in our case, multiple proteins) was done as described by Storey et al. at a false discovery rate $FDR < 0.05$ (indicated as q -value) [18,19]. In total we have identified 4922 proteins of which 2142 were quantified in at least one of the treatments in at least 4 out of the 6 replicates. For example, in order to be quantified to determine it is differentially expressed or not, a protein needs to be detected in 4 technical replicates out of 6 in any treatment group. Any protein that doesn't have a consistent detection pattern is deemed unreliable and left out for further quantitation. For the phosphoproteome part of our study, quantification of individual phosphopeptides was done by measuring peptide intensities, as provided by MaxQuant. The validity and accuracy of this approach was previously reported [20]. During the analysis, the proteins exhibiting a similar expression pattern were excluded from the list of differentially phosphorylated proteins. This can be regarded as a "normalization effect" to account for significant changes that were caused by the overall protein concentration levels. For example, a protein that has an increase in phosphorylation level as well as a significantly increased expression level was excluded. The mass spectrometry proteomics data have been deposited to the ProteomeXchange Consortium via the PRIDE [21] partner repository with the dataset identifier PXD003738.

2.9. Voronoi treemaps

For global gene expression visualization we applied Voronoi tree-maps as introduced previously [22] [23]. The presented treemaps subdivide the 2D plane into subsections according the hierarchical data structure of gene functional assignments. For the top level the total area is subdivided into main categories, afterwards the main categories into subcategories and the subcategories into cells representing the differentially expressed proteins. As proteins are involved in multiple processes, one protein is often represented several times in respective processes/subprocesses. A color scheme has been used to depict expression differences; orange color denotes increased expression whereas blue color denotes decreased expression according to the indicated comparison. Color scale is adjusted by \log_2 ratios, brighter colors indicating stronger expression differences.

2.10. Protein functional pathway analysis

Functional annotation of 301 differentially expressed proteins was carried out using Gene Ontology(GO) based software on DAVID website (the Database for Annotation, Visualization and Integrated Discovery, v6.7, NCBI). Network analysis, causal networks analysis and upstream regulator analysis were done using Ingenuity Pathway Analysis (IPA®, QIAGEN Redwood City, www.qiagen.com/ingenuity) [24].

2.11. Western blotting

Protein lysates were prepared from murine bone marrow derived dendritic cells isolated and cultured as described above. Cultured BMDCs were challenged with *B. vulgatus* or *E. coli* for 16 h prior to lysis or remained unchallenged for 16 h to serve as the control group. BMDCs cultured from each mouse were treated separately; there was no pooling of the biological samples. Lysis buffer consisted of 50 mM Tris-HCl, 150 mM NaCl, 0.5% Nonidet P40, 0.4 mM DTT, protease inhibitor mixture (Pierce, #88665), 1 mM sodium orthovanadate, 5 mM sodium fluoride, 5 mM β -glycerophosphate, and 1 mM EDTA. iNOS (CST, #2982), RIG-1 (CST, #4200), COX2 (CST, #4842) and β -actin (13E5, CST, #4970) monoclonal antibodies were purchased from Cell

Signaling Technology. Equal amounts of tissue lysate (30 μ g) were run in SDS-PAGE gels and transferred semi-dry to a nitrocellulose membrane (Applichem, A52), followed by blocking for 1 h in blocking buffer (LI-COR, P/N 927). Membranes were then incubated overnight at 4 $^{\circ}$ C with the primary antibody and for 2 h with the secondary antibody in room temperature, the chemiluminescent signal was detected by LI-COR Odyssey and quantified with Image Studio Lite Version 5.2.

3. Results

3.1. Dendritic cells of different maturation states differ in their expression of cytokines and cell surface activation markers

Immune regulatory cytokine release is one of the important functions of dendritic cells which bridge them with other effector cells of the immune system. As expected, cytokine secretion profiles of dendritic cells are distinct for different effector/maturation states, as shown by previous work [2,25,26]. In the context of inflammatory bowel disease (IBD), our group has reported distinct cytokine release patterns of DCs in mice colonized with *B. vulgatus* and *E. coli* [27]. In this study we aimed to replicate this condition *in vitro*, by stimulating DCs with *B. vulgatus* which gives rise to semi-mature dendritic cells, and by stimulating with *E. coli* which gives rise to mature dendritic cells. After stimulation for 16 h or 16 h + 24 h (restimulation with *E. coli*), ELISA for IL-6, TNF α , IL-1 β and IL-12p40 was performed on cell culture supernatants. Steady state DCs secrete negligible levels of proinflammatory cytokines whereas *E. coli* stimulated cells secrete highest levels of cytokines. Proinflammatory cytokine secretion is at intermediate levels in *B. vulgatus* stimulated cells, indicating their limited response to this symbiotic bacterial strain. Challenging these cells again with *E. coli*

results in a different expression pattern of proinflammatory cytokine and cell surface activation markers than restimulating the PBS controls and *E. coli* stimulated cells, depicting their unique state in the maturation/activation spectrum (Fig. 1). This distinct response to different bacterial strains is dependent on intact TLR2 and TLR4 signaling, as TLR2/TLR4 double knockout mice show no significant difference on cytokine secretion (Suppl. Fig. 1a).

Upon encountering antigens dendritic cells upregulate surface activation markers MHC-II, which is a major antigen presenting molecule and CD40, an important costimulatory molecule. As dendritic cell activation is an integral part of dendritic cell function, we assessed the surface expression of MHC-II and CD40 in *B. vulgatus* and *E. coli* stimulated cells. The percentage of MHC-II positive cells showed an intermediate increase upon *B. vulgatus* stimulation (47%), and a higher increase was observed in *E. coli* stimulated cells (70%). CD40 expression followed a similar pattern, increasing slightly in *B. vulgatus* challenged cells (25%), and considerably in *E. coli* challenged cells (87%). This difference in cell surface activation marker expression disappears when TLR2 $^{-/-}$ TLR4 $^{-/-}$ double knockout mice is used (Suppl. Fig. 1b), indicating that the difference in DC activation status between *B. vulgatus* and *E. coli* stimulated cells depends on intact TLR2/TLR4 signaling, similar to the case of proinflammatory cytokine secretion.

3.2. General patterns of difference in proteome between DC maturation states

As dendritic cell function is closely tied to dendritic cell maturation status, expression level differences in proteins involved in major cellular processes are to be expected. Therefore, in this section we aimed to provide a general look on affected cellular processes as a starting

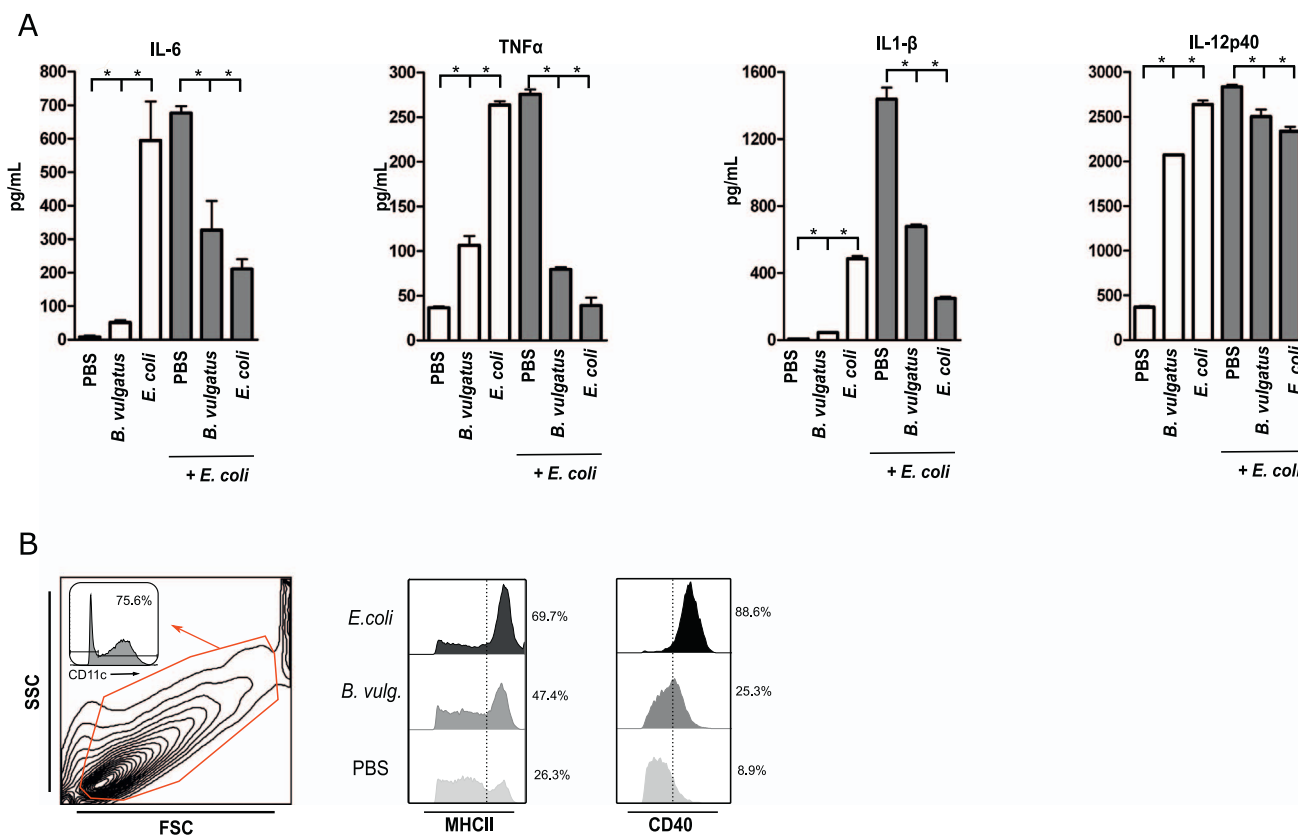
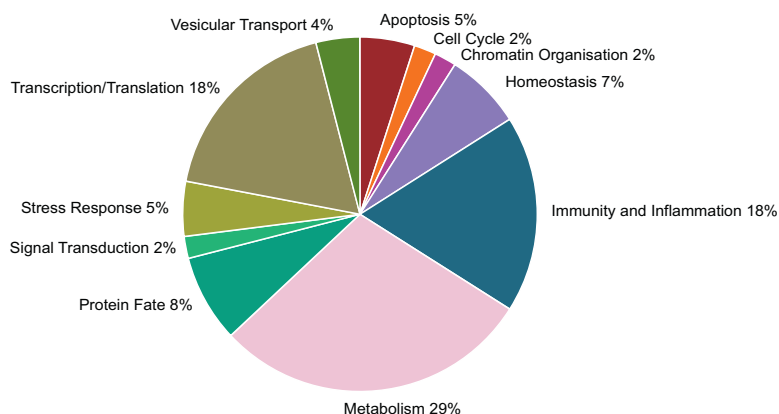


Fig. 1. a) Cytokine secretion profiles of cultured bone marrow derived dendritic cells, isolated from wild type C57BL/6 mice. Stimulation is done 7 days of dendritic cell culture, by incubating with live bacteria for 16 h for the first stimulation, and 24 h for the additional *E. coli* stimulation. ELISA is performed with cell culture supernatants for all cases. * $p < 0.05$. b) Flow cytometric analysis of cell surface markers. Viable cell population is gated on FSC/SSC axis, which was gated again depending on CD11c expression. CD11c $^{+}$ population was used for the assessment of MHC-II and CD40 expression. Results are representative of 3 independent experiments.

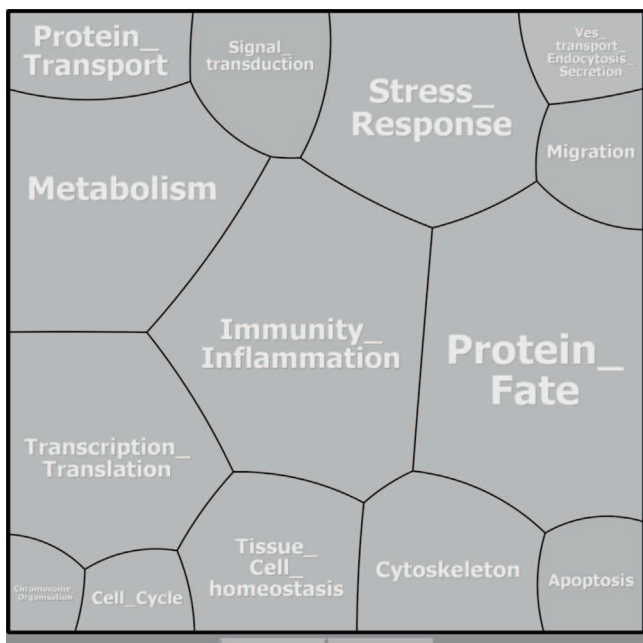
point for analysis of our shotgun proteomics results. We uploaded a total of 301 proteins that were regulated among three pairwise comparisons (i.e. *B. vulgatus* vs. *E. coli*, *B. vulgatus* vs. PBS and *E. coli* vs. PBS at 16 h) to DAVID website and functionally annotated them to clusters. These clusters were then organized into 14 major cellular processes and a general distribution of those proteins to functions can be seen in Fig. 2a. To provide another level of detail, the clusters shown in Fig. 2b has been further divided into subprocesses according to Gene Ontology terms, using software provided via DAVID website (Fig. 2f). We chose to visualize our data on major cellular processes, subprocesses of those,

and single proteins belonging to these subprocesses, by using Voronoi tessellations. This method enables the visualization of detailed, multi-level data on a 2D scale, and expression levels can be represented in various intensities of color [28]. In Fig. 2, the data is represented in different possible levels of detail; Fig. 2b shows only the major processes, and Fig. 2f shows subprocesses as polygons clustered together within a bigger polygon. Fig. 2c,d,e provide the highest level of detail, by representing proteins in single cells within the smaller polygons that depict subprocesses, which in turn belong to major cellular processes visualized in the biggest polygons. As one protein can have functions

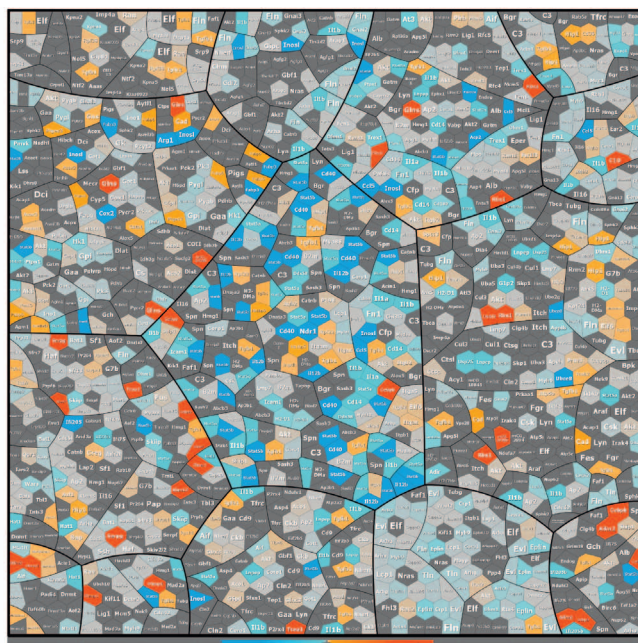
A



B



C



*B. vulgatus*16h vs *E.coli* 16h

Fig. 2. Visual summary of differential protein expression between dendritic cell maturation states. a) Functional classification of all regulated proteins. Protein IDs were uploaded to DAVID website and annotated to major cellular processes according to Gene Ontology database. b) Voronoi treemap layout for representing major cellular processes. This layout is used for all Voronoi treemaps in our study. c,d,e) Expression differences of single proteins belonging to all 3 pairwise comparisons. The clusters from (b) are represented as biggest polygons and single proteins are represented as single cells. f,g) Magnification of the immunity/inflammation cluster. At this level of detail subprocesses belonging to the cluster are shown as smaller polygons. Colors represent expression level differences. Orange: increased expression, Blue: decreased expression, Light grey: no change, Dark grey: protein not detected. Color intensity is adjusted to the expression level difference on log₂ scale, brighter colors indicating a higher expression level difference. (For interpretation of the references to color in this figure legend, the reader is referred to the web version of this article.)

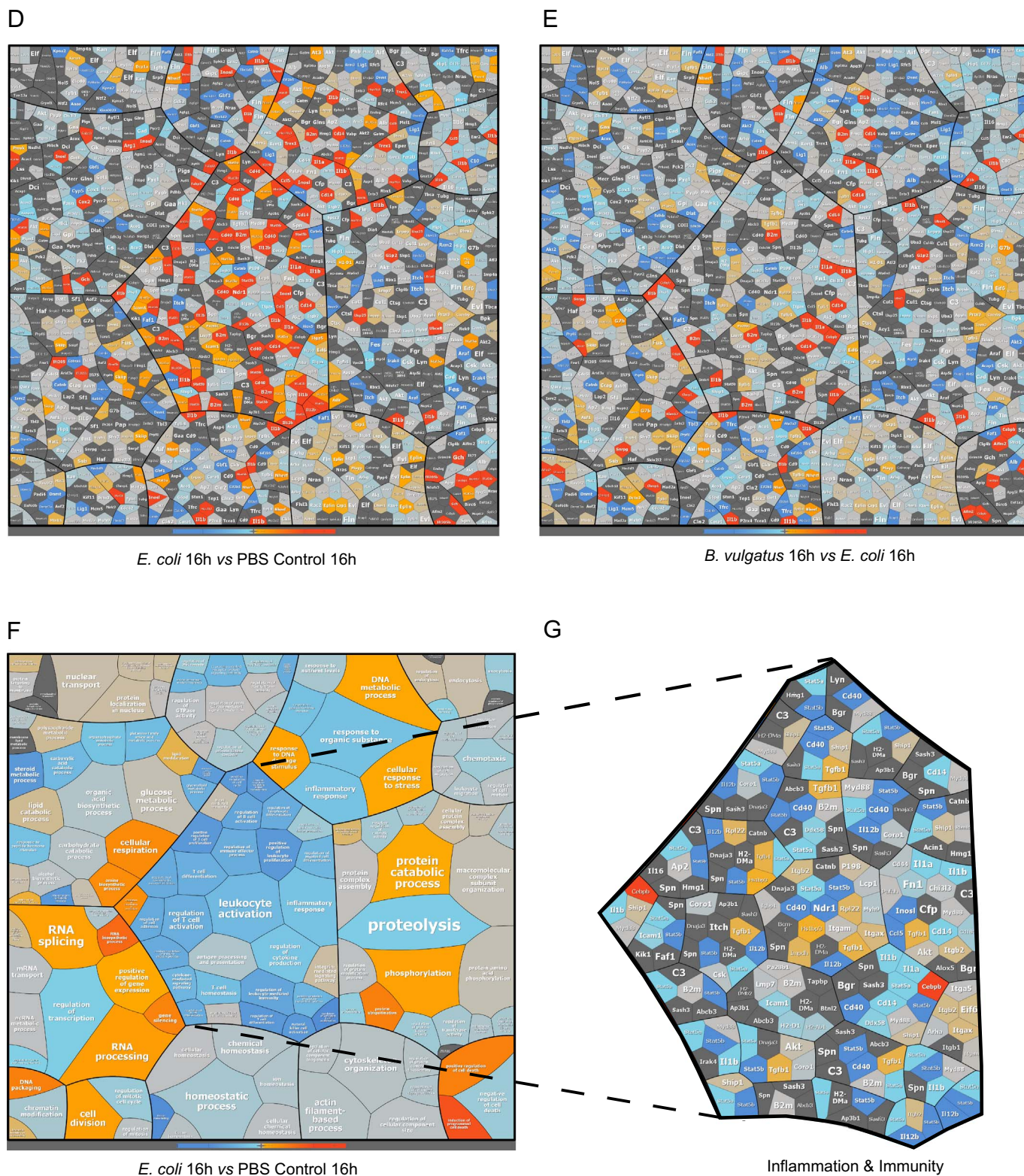


Fig. 2. (continued)

related to several processes, such proteins are represented by more than one cell. By efficiently visualizing data in 2D, Voronoi treemaps enables the comparison of expression level differences and patterns between immature, semi-mature and fully mature DCs in different levels of detail, depending on the interests of the researcher.

As expected, upon stimulation with bacteria, a dynamic regulation is seen between different dendritic cell maturation states. A total of 151

proteins are regulated during semi-maturation (53 up- and 98 down-regulated), 181 proteins are regulated during full-maturation (96 up- and 85 down-regulated), and 103 proteins (33 up- and 70 down-regulated) between semi-mature and fully mature DCs. 183 proteins were detected only in PBS 16 h controls, 52 proteins were detected only in *B. vulgatus* 16 h sample, and 61 proteins were detected only in *E. coli* 16 h sample. On a more specific scale, almost all subprocesses in the

immunity cluster show pronounced upregulation upon *E. coli* stimulation. This is in contrast with when semi-mature (*B. vulgatus* stimulated) DCs are compared to fully mature (*E. coli* stimulated) DCs, where the subprocesses belonging to immunity cluster have lower expression levels in semi-mature dendritic cells. Immunity cluster is of special importance, since this cluster harbors proteins with potent immunoregulatory effects such as IL-1 α , IL1- β , iNOS, COX2, CCL5 and RIG1 all of which have lower expression levels compared to *E. coli* stimulated sample. On the other hand, TGF β 1, which has potent anti-inflammatory effects, is upregulated upon *B. vulgatus* stimulation. This suggests that *B. vulgatus* exerts a different effect on DCs compared to *E. coli* on the level of immune regulation, and in particular downregulates major proinflammatory factors. This differential effect may be the major determinant underlying phenotypical and functional differences observed between semi-mature and fully mature DCs.

3.3. Upregulation of key inflammatory mediators in *E. coli* stimulated DCs

In this section we have focused on several inflammatory mediators that are shown to be differentially expressed between *B. vulgatus* and *E. coli* stimulated DCs. Effects of these proteins are decisive in directing the immune response towards an inflammatory state. According to our mass spectrometry data, IL1- β , iNOS, COX2 and RIG1, have no detectable or lower levels of expression in *B. vulgatus* stimulated dendritic cells. We aimed for reproducing the mass spectrometry data by ELISAs and Western Blots targeting these proteins. ELISA for IL1- β showed very low amounts of protein in the *B. vulgatus* stimulated sample (45 pg/mL), and a higher amount in the *E. coli* stimulated sample (485 pg/mL) (Fig. 1a, values are the averages of 4 biological replicates). The expression of iNOS, which is inducible under inflammatory conditions, can only be seen in the *E. coli* stimulated sample. Similarly, the expression of the inducible cyclooxygenase COX2 can also only be detected after *E. coli* stimulation. RIG1, which shows a gradual increase in expression among PBS/*B. vulgatus*/*E. coli* stimulation in mass spectrometry data (1/2.1/3.76), gives a similar ratio in Western Blots (1/1.9/2.53) (Fig. 5). Taken together, our data shows that for these inflammatory regulators, there is a lack of expression in *B. vulgatus* stimulated cells and the results of the mass spectrometry analysis is reproducible.

3.4. Canonical pathway and upstream regulator analysis of distinct dendritic cell maturation states

In the previous section we aimed to catalogue the differences in protein expression, provided hints to their functions, and made it accessible to any interested researcher to have a detailed look at expression level differences of proteins of interest. In this section we provide more detailed information about the canonical pathways in which the differentially regulated proteins take part and thereby bring about the differences between immature, semi-mature and fully mature DCs. For this purpose we used Ingenuity Pathway Analysis (IPA), which assesses the effect of signaling pathways in creating the differences between any given comparisons, depending on the enrichment values of regulated proteins in a pathway. The input data set we used for the analysis is the total of 301 differentially regulated proteins resulting from all pair-wise comparisons. Enrichment score is defined as $-\log_{10}(\text{p-value})$, and the threshold is set at 1.5. The resulting top 20 pathways belonging to the analysis between semi-mature and fully mature DCs are reported in Table 1. As expected, signaling pathways such as IRF signaling, DC maturation pathway, TREM1 and TLR signaling pathways are reported to be involved as these are central to the immune functions of the dendritic cells. Moreover, PPAR signaling, LXR/RXR activation, JAK/Stat signaling and glucocorticoid receptor signaling is also included in the report. These pathways can also be investigated further in the context of immune regulation by dendritic cells, since they harbor important factors such as STAT5a, PTGS2, iNOS, CEBPB and several

interleukins and cytokines. Our data contains the relative abundance values of these proteins as well and thus, can be used to further investigate the effects of these pathways in immune response.

We next performed an IPA upstream regulator analysis to determine the factors that play a major role in creating the observed expression differences between *B. vulgatus* and *E. coli* stimulated dendritic cells. Upstream regulator analysis is a functionality of the IPA, and is based on a hand-curated literature-based information database Ingenuity[®] Knowledge Base on upstream transcriptional regulators and their effects on downstream targets [29]. The algorithm assesses the number of targets and expression levels of each target that is present in the experimenter's dataset, and then compares them with the expected activation state according to the knowledge database. The result is a list of upstream regulators with a z-score indicating their level of activation/inhibition, and an overlap *p*-value assessing the consistency and statistical significance of the match (only the upstream regulators with a *p*-value < 0.01 are considered for our analysis). Our IPA upstream regulator analysis results for the comparison of semi-mature vs. fully mature DCs are shown in Fig. 3 and in further detail in Table 2. In line with the observed downregulation of proteins involved in the immunity cluster of *B. vulgatus* stimulated DCs, the upstream immune regulators and proinflammatory signals are predicted by the software to be downregulated. Such proteins include IRF3, TLR4, TLR2 and IFN γ which are potent activators of immune responses against pathogens. Interestingly, several other factors that have not been studied in an immunity/inflammation or dendritic cell maturation context such as MAVS, SAMS1, DOCK8 and TBK1 were also downregulated. Despite a general trend of downregulation in upstream regulators, *B. vulgatus* stimulated DCs also showed predicted activation of several factors. We considered the activated factors to be of special interest, since they may provide an answer to the protective and anti-inflammatory properties of *B. vulgatus* exposure observed *in vitro* and *in vivo*. These proteins include SOCS1, which is an important and well-studied negative regulator of cytokine production. Conditional suppression of SOCS1 in colonic T-cells of DSS treated mice increases colitis severity [30], and SOCS1^{-/-} Rag2^{-/-} mice develop spontaneous colitis [31]. PTGER4 (prostaglandin E receptor 4), an anti-inflammatory regulator; ABCA1, a lipid transported with inflammation suppression function [32]; and NR1H3 (liver x receptor α), a transcription factor with inhibitory effects on proinflammatory cytokine expression [33,34] (for more information see discussion). The molecular targets of these upstream regulators are shown in Table 3, and were all detected in our mass spectrometry experiment. Taken together, our data suggests that *B. vulgatus* stimulation exerts its anti-inflammatory effects by inhibiting major proinflammatory factors and activating anti-inflammatory regulators.

3.5. Quantitative phosphoproteome analysis of DC maturation states

The differential expression of various proteins and the patterns arising from expression analysis provide a valuable insight into the workings of dendritic cells; however, comparison of protein abundance in a sample is only one part of the whole picture. An additional important source of information is the post-translational regulation of protein activity by phosphorylation, which was the focus of our phosphoproteome experiments. Similarly to the proteome expression analysis experiment, we stimulated murine BMDCs with *B. vulgatus*, *E. coli*, and PBS, and collected the protein from the cellular fraction. As phosphorylation is a highly dynamic process and occurs much faster than changes in expression levels [35], we limited bacterial stimulation to 30 min contrary to 16 h stimulation we have done for total proteome analysis. After stimulation and sample collection, the phosphopeptides in the samples were enriched using strong cation exchange (SCX) and TiO₂ chromatography and analyzed with an Orbitrap XL. In total we identified 919 phosphosites on 544 peptides, of which 118 sites were differentially phosphorylated between semi-mature and fully mature dendritic cells. Also, there are 283 phosphoevents that are unique to

Table 1

Canonical pathway analysis using IPA. Top 20 signaling pathways determined by ingenuity pathway analysis of the *B. vulgatus* vs. *E. coli* comparison at 16 h are shown. The pathway with the highest enrichment score is shown at the top position, the higher the enrichment score, the more proteins that are detected by mass spectrometry are associated with the pathway compared to the background database (mouse proteome).

Affected pathways	Enrichment Score	Proteins detected by mass spectrometry
Activation of IRF by cytosolic PRRs	5.81	DHX58,IFIH1,IKKBK,CD40,PPIB,DDX58,STAT2,PIN1,IRF3,IFIT2,ISG15
Dendritic cell maturation	4.12	B2M,AKT2,IL1A,ICAM1,HLA-A,MYD88,HLA-DQB1,IKKBK,AKT1,CD40,HLA-DMA,IL12B,FSCN1,HLA-DMB,IL1B,STAT2,PIK3CD,HLA-DRB5
TREM1 signaling	4.04	ITGB1,STAT5A,AKT2,ICAM1,AKT1,MPO,CD40,MYD88,ITGA5,IL1B,STAT5B,ITGAX
Communication between innate and adaptive immune cells	3.91	B2M,IL1A,CD40,HLA-A,IL12B,IL1B,CCL5,HLA-DRB5
Toll-like receptor signaling	3.91	IKKBK,IL1A,MYD88,IL12B,CD14,IL1B,IRAK4,TRAF1
Role of PRRs in recognition of bacteria and viruses	3.79	OAS1,IL1A,C3,MYD88,CCL5,IRF3,OAS3,IFIH1,CLEC7A,IL12B,TGFB1,DDX58,IL1B,CLEC6A,PIK3C,PRKCB
Retinoic acid mediated apoptosis signaling	3.55	ZC3HAV1,DAP3,PARP3,PARP9,PARP14
PPAR signaling	3.50	IKKBK,STAT5A,IL1A,NRAS,IL1B,PTGS2,STAT5B
Glucocorticoid receptor signaling	3.44	PRKACB,STAT5A,AKT2,NRAS,ICAM1,HSPA1B,SMARCD2,CEBPB,CCL5,PTGES3,PRKAG1,IKKBK,GTf2B,AKT1,POLR2A,POLR2C,PCK2,POLR2E,TGFB1,PRKAA1,IL1B,PIK3CD,PTGS2,NOS2,STAT5B
LXR/RXR activation	3.24	IL1A,ECHS1,C3,CD36,IRF3,ALB,LYZ,FASN,IL1B,CD14,ACACA,PTGS2,NOS2,HADH,MMP9
CD40 signaling	2.95	IKKBK,ICAM1,CD40,PTGS1,PIK3CD,PTGS2,MAPKAPK2,TRAF1
LPS/IL-1 mediated inhibition of RXR Function	2.82	ALDH4A1,IL1A,CPT1A,MYD88,ACOX1,GSTO1,ALDH9A1,IL4I1,ALDH1L1,ALDH3A2,ALDH1A2,CPT2,FABP4,CD14,IL1B,ALDH3B1,ALDH18A1,FABP5,FABP3,ACOX3
JAK/Stat signaling	2.73	STAT5A,AKT2,AKT1,NRAS,PTPN1,STAT2,PIK3CD,CEBPB,STAT5B
Agranulocyte adhesion and diapedesis	2.61	ITGB1,IL1A,MYH9,ICAM1,FN1,MYH14,ITGA5,CCL5,GLG1,GNAI2,ITGB2,GNAI3,IL1B,CCL6,MMP9
MAPK signaling	2.51	NRAS,ZC3HAV1,PIK3CD,PARP3,RPS6KA1,PARP9,PARP14
Death receptor signaling	2.45	ACIN1,IKKBK,ZC3HAV1,PARP3,PARP9,PARP14

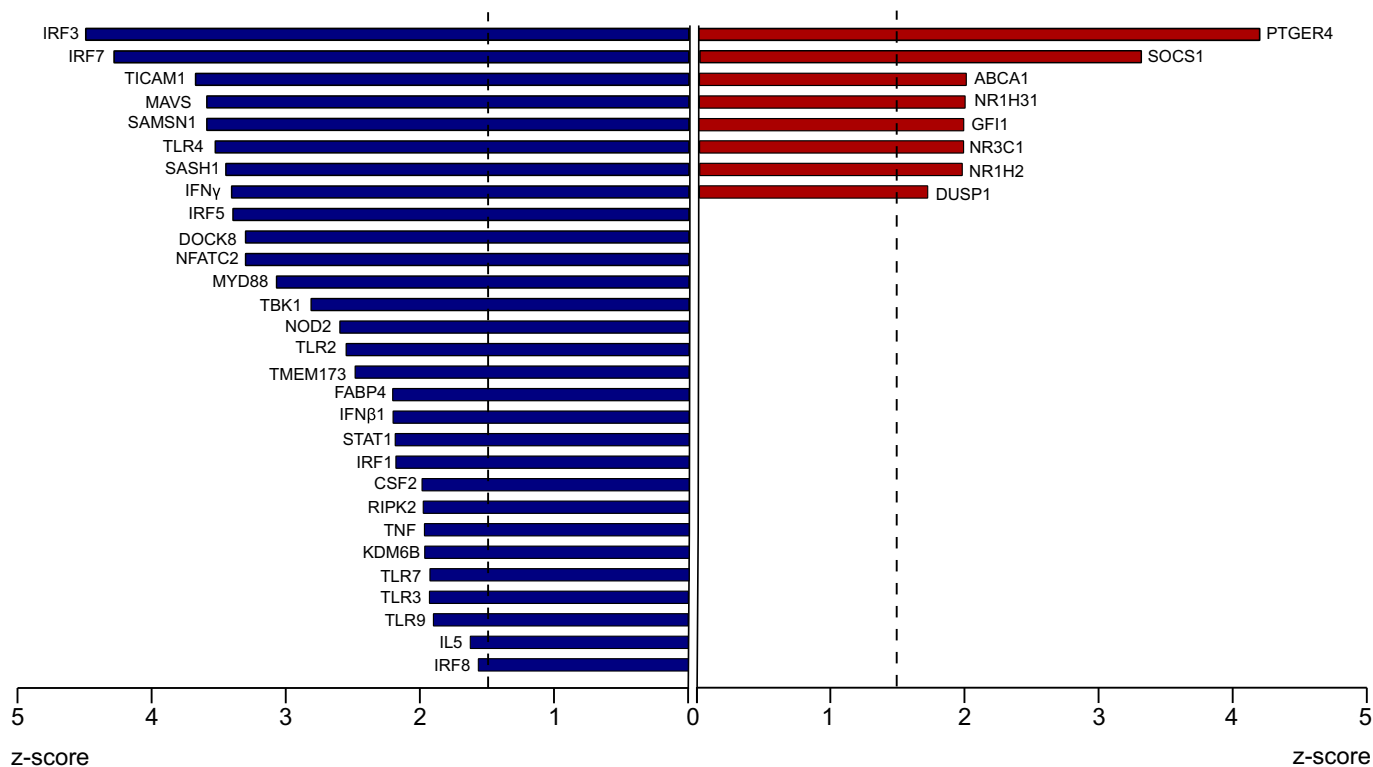


Fig. 3. Upstream regulator prediction. IPA upstream regulator analysis was performed to predict key regulatory molecules that underlie the expression pattern differences observed between semi-mature and fully mature DCs. The activation z-score is used to determine the activation states of upstream factors and molecules with z-score > 1.5 are considered to be activated (red bars), whereas molecules with z-score < 1.5 are considered to be inactivated (blue bars). All listed upstream regulators have an overlap of p-value < 0.01. The overlap p-value uses Fisher's Exact Test to assess the statistical significance of the overlap between the dataset genes and the genes that are regulated by the upstream regulator. (For interpretation of the references to color in this figure legend, the reader is referred to the web version of this article.)

PBS control at 16 h, 120 phosphoevents that are unique to *B. vulgatus* 16 h stimulation sample, and 18 phosphoevents that are unique to *E. coli* 16 h stimulation sample. The phospho amino acid distribution for all phosphoevents is shown in Fig. 4a, with the pThr:pSer:pTyr ratio of 121:9:1.

To determine which kinases take part in the phosphorylation of the 465 differentially regulated phosphosites (all 3 pairwise comparisons are considered and total number of regulated phosphosites combined), we have performed a kinase inference analysis. We have used the kinase-substrate database available at PhosphositePlus [36], and

Table 2

List of upstream regulators and their targets that were detected as being differentially regulated between *B. vulgatus* and *E. coli* treated cells at 16 h. The activation z-score is used to determine the activation states of upstream factors, with positive values indicating activation and negative values indicating inhibition. All indicated upstream regulators have an overlap p-value < 0.01. The overlap p-value uses Fisher's Exact Test to assess the statistical significance of the overlap between the dataset genes and the genes that are regulated by the upstream regulator.

Upstream regulator	Molecule type	z-Score	Target proteins detected by mass spectrometry
Activated			
			CD40,CMPK2,DDX58,GBP2,GBP4,IFI16,IFI47,IFIT1B,IFIT2,IGTP,IL12B,IL41,ISG20,NOS2,PARP14,
PTGER4	G-protein coupled receptor	4.194	PTGS2,RNF213,TOR3A
SOCS1	Other	3.302	DDX58,GBP5,IFI16,IFI47,IFIT1B,IFIT2,IFIT3,IL1B,ISG15,NOS2,OAS1,PTGS2
ABCA1	Transporter	1.998	IL12B,IL1B,NOS2,PTGS2
NR1H3	Ligand-dependent nuclear receptor	1.99	CCL5,IL1B,NOS2,PTGS2
GF11	Transcription regulator	1.982	CD40,ICAM1,IL1A,IL1B
NR3C1	Ligand-dependent nuclear receptor	1.977	CCL5,GBP2,GLUL,IFIT1B,IFIT2,IL12B,IL1A,IL1B,ISG15,OASL
NR1H2	Ligand-dependent nuclear receptor	1.966	CCL5,IL1B,NOS2,PTGS2
DUSP1	phosphatase	1.71	CD40,IL1A,IL1B,PTGS2
Inhibited			
IRF3	Transcription regulator	- 4.509	CCL5,CMPK2,DDX58,DHX58,GBP5,IFI16,IFI47,IFIT1B,IFIT2,IFIT3,IGTP,ISG15,ISG20,NT5C3A, OAS1,OASL,PARP14,SLFN1,STAT2,TREX1,UBE2L6
IRF7	Transcription regulator	- 4.298	CMPK2,DDX58,DHX58,GBP5,IFI16,IFI47,IFIT2,IFIT3,IGTP,ISG15,ISG20,NT5C3A,OAS1,OASL, PARP14,SLFN1,STAT2,TREX1,UBE2L6
TICAM1	Other	- 3.69	CCL5,CD40,CFB,CMPK2,ICAM1,IFI16,IFI47,IFIT1B,IFIT2,IFIT3,IGTP,IL12B,IL1A,IL1B,ISG15,ISG20, NES,OASL,PTGS2,SLC7A2
MAVS	Other	- 3.606	CCL5,CMPK2,DDX58,DHX58,IFIT2,IFIT3,ISG15,ISG20,NT5C3A,OAS1,OASL,STAT2,UBE2L6
SAMSN1	Other	- 3.606	CD40,CMPK2,IFIT1B,IFIT2,IFIT3,IL12B,ISG15,ISG20,OASL,PTGS2,STAT2,STAT5A,USP25
TLR4	Transmembrane receptor	- 3.543	CCL5,CD40,CFB,CMPK2,ICAM1,IFI16,IFI47,IFIT1B,IFIT2,IFIT3,IGTP,IL12B,IL1A,IL1B,ISG15,ISG20, PTGS2,STAT2,STAT5A,TRAF1,USP25
SASH1	OTHER	- 3.464	CD40,CMPK2,IFIT1B,IFIT2,IFIT3,IL12B,ISG15,ISG20,OASL,PTGS2,STAT2,USP25
IFNG	cytokine	- 3.421	ARG1,CCL5,CD40,GBP2,GBP4,GBP5,ICAM1,IL12B,IL1A,IL1B,NOS2,PTGS2,SLFN1
IRF5	Transcription regulator	- 3.411	CMPK2,DDX58,DHX58,IFIT2,IFIT3,ISG15,ISG20,NT5C3A,OAS1,OASL,STAT2,UBE2L6
DOCK8	Other	- 3.317	CD40,CMPK2,IFIT1B,IFIT2,IFIT3,IL12B,ISG15,ISG20,PTGS2,STAT2,USP25
NFATC2	Transcription regulator	- 3.317	CD40,CMPK2,IFIT1B,IFIT2,IFIT3,ISG15,ISG20,OASL,PTGS2,STAT2,USP25
MYD88	Other	- 3.086	ARG1,CCL5,CD40,CMPK2,ICAM1,IFIT1B,IFIT2,IL12B,IL1A,IL1B,ISG15,NES,NOS2,OASL, PTGS2,SLC7A2
TBK1	Kinase	- 2.828	CD40,CMPK2,IFIT1B,IFIT2,IL12B,IL1A,ISG20,PTGS2
NOD2	Other	- 2.613	CD40,ICAM1,IL12B,IL1A,IL1B,NOS2,TRAF1
TLR2	Transmembrane receptor	- 2.566	ARG1,CCL5,CD40,IL12B,IL1B,NOS2,PTGS2
TMEM173	Other	- 2.499	CCL5,GBP5,IFI16,IL1B,NOS2,OASL
FABP4	Transporter	- 2.219	IL12B,IL1A,IL1B,NOS2,PTGS2
IFNB1	Cytokine	- 2.216	CCL5,CD40,CMPK2,GBP2,GBP4,GBP5,IFI16,IFI47,IFIT1B,IFIT2,IFIT3,IGTP,IL12B,NOS2,NT5C3A,STAT2
STAT1	Transcription regulator	- 2.2	CCL5,CD40,GBP2,ICAM1,IFIT1B,ISG15,NOS2,OASL
IRF1	Transcription regulator	- 2.195	CCL5,CD40,GBP2,IL12B,NOS2,PTGS2
CSF2	Cytokine	- 2	CD40,IL12B,IL1B,NOS2
RIPK2	Kinase	- 1.991	CD40,ICAM1,NOS2,TRAF1
TNF	Cytokine	- 1.982	CD40,GBP2,NOS2,PTGS2
KDM6B	Other	- 1.98	CCL5,CD40,IGTP,IL12B,OASL
TLR7	Transmembrane receptor	- 1.941	CD40,IL12B,ISG15,STAT2
TLR3	Transmembrane receptor	- 1.939	CCL5,CD40,IL12B,IL1B
TLR9	Transmembrane receptor	- 1.908	CD40,IFIT1B,IL12B,STAT2
IL5	Cytokine	- 1.633	GBP2,GBP4,NDRG1,NOS2,P4HA1,UCHL3
IRF8	Transcription regulator	- 1.573	CCL5,CD40,ICAM1,IL12B,ISG15

searched for the phosphorylated sequences detected in our experiments. Matching the substrates found with their respective kinases, we have generated a list of kinases that are responsible for the differential phosphorylation events in our experiments. As can be seen from Fig. 4b, the majority (80/126) of detected and database-defined phosphorylations are carried out by CMGC and AGC family of kinases, with Mapk1 and Prkaca phosphorylating the highest number of targets. It appears that MAP kinases and cyclin dependent kinases have an active role in shaping the bacteria treated DC phosphoproteome, in addition, AKT1 and mTOR are active and have respectively 4 and 2 phosphorylated targets in our dataset.

After inferring the active kinases upon bacterial stimulation, we searched for differentially phosphorylated proteins that have central functions in various cellular processes such as immunity, cell division, chromatin modifications and major cellular signaling pathways. A list of such differentially regulated proteins can be seen in Table 3 for all 3 pairwise comparisons. We have observed that upon stimulation with bacteria for 30 min the pivotal cell cycle regulator protein CDK2 is phosphorylated exclusively in *B. vulgatus* stimulated sample at residues T14 and Y15, which are reported to inactivate the protein. Along with

CDK2, phosphorylation of CDC42 GTPase and DOCK1 protein at indicated residues are exclusive to the *B. vulgatus* stimulated sample. Two important members of the epigenetic regulator SWI/SNF complex, SMARCC1 and SMARCC2, are also only phosphorylated in the *B. vulgatus* sample, indicating a possible involvement of epigenetic factors during bacterial challenge. Other proteins with important roles include: ACIN1, a potent apoptosis effector; inositol kinase B, which is a major signal transduction relay protein found in the plasma membrane; and the transcription factor junD. Taken together, stimulating the dendritic cells with *B. vulgatus* or *E. coli* results in differential phosphorylation of pivotal cell cycle proteins, chromatin regulators and transcription factors.

In addition, we performed a reactome analysis on differentially phosphorylated proteins to determine the pathways that are statistically overrepresented in dendritic cells stimulated with symbiont and pathobiont bacteria. Reactome is an open-source, manually curated and peer-reviewed database of biological reactions and pathways [37]. We used the 118 differentially phosphorylated peptides in *B. vulgatus* vs. *E. coli* stimulation comparison as input, and results are presented in Table 4. Reactome analysis showed that, differentially phosphorylated

Table 3

A list of selected proteins that are differentially phosphorylated among 3 pairwise comparison of stimulated dendritic cells. Only proteins with central functions to cellular processes are included in the list, along with the Uniprot accession IDs and phosphosequences.

Uniprot ID	Name	Ratio	Sequence
<i>E. coli</i> vs <i>B. vulgatus</i>			
A2APM2	CD44	<i>B. vulgatus</i> only	S(0.995)QEMVHLVNEKPS(0.003)ET(0.001)PDQCMTADETR
A6X8Z5	Cdc42 GTPase	<i>B. vulgatus</i> only	DDSPSSLGS(1)PEEEQPK
B2RXC2	Inositol 1,4,5-trisphosphate 3-kinase B	<i>B. vulgatus</i> only	AALS(1)PGS(0.044)VFS(0.956)PGR
Q9JIX8	Acin1, Apoptotic chromatin condensation inducer in the nucleus	<i>B. vulgatus</i> only	S(0.015)LS(0.984)PLS(0.43)GT(0.285)T(0.285)DT(0.001)K
P15066	Transcription factor junD	<i>B. vulgatus</i> only	LAS(1)PELER
P97496	SWI/SNF complex subunit SMARCC1	<i>B. vulgatus</i> only	RKPS(1)PS(1)PPPTATESR
Q6PDG5	SWI/SNF complex subunit SMARCC2	<i>B. vulgatus</i> only	S(1)DGDPIVDPEK
Q61165	Sodium/hydrogen exchanger 1, Slc9a1	<i>B. vulgatus</i> only	IGS(1)DPLAYEPK
Q8BUR4	Dock1, Dedicator of cytokinesis protein 1	<i>B. vulgatus</i> only	S(1)QVINVIGNER
Q8C078	Camkk2	<i>B. vulgatus</i> only	S(1)FGNPFEGSR
P97377	Cdk2	<i>B. vulgatus</i> only	IGEGT(1)Y(1)GVVYK (Thr 14/Tyr15)
P98078	Dab2	2.903	S(0.884)S(0.116)PNPFVGS(1)PPK
Q6A068	Cell division cycle 5-like protein	1.767	GGLNT(0.999)PLHES(0.001)DFS(0.026)GVT(0.974)PQR
<i>E. coli</i> vs. PBS			
A2APM2	CD44	PBS only	S(0.995)QEMVHLVNEKPS(0.003)ET(0.001)PDQCMTADETR
Q60875	Rho guanine nucleotide exchange factor 2	PBS only	LS(1)PPHS(1)PR
Q61165	Sodium/hydrogen exchanger 1, Slc9a1	PBS only	IGS(1)DPLAYEPK
A2AIV8	Caspase recruitment domain-containing protein 9	PBS only	QQQLDMLLILS(0.012)S(0.044)DLEDS(0.153)S(0.791)PR
E9PU87	Serine/threonine-protein kinase SIK3	PBS only	GPS(0.001)PLVT(0.002)MT(0.002)PAVPAVT(0.127)PVDEES(0.934)S(0.934)DGEPDQEAVQR
Q9JIX8	Acin1,	PBS only	S(0.015)LS(0.984)PLS(0.43)GT(0.285)T(0.285)DT(0.001)K
P13405	Retinoblastoma-associated protein	PBS only	IPGGNIYIS(1)PLKS(0.999)PY(0.001)K
P49138	MAP kinase-activated protein kinase 2	PBS only	MLS(0.544)GS(0.544)PGQT(0.912)PPAPFPS(1)PPPPAPAQPPPPFPQFHVK
P70671	Interferon regulatory factor 3	PBS only	DEGS(0.001)S(0.001)DLAIVS(0.029)DPS(0.029)QQLPS(0.94)PNVNNFLNPAPQENPLK
P97310	DNA replication licensing factor MCM2	PBS only	RGLLYDS(1)S(1)EEDEERPAR
Q66JS6	Eukaryotic translation initiation factor 3 subunit J-B	PBS only	AAAAAAAAAAGDS(0.999)DS(0.998)WDADT(0.001)FS(0.001)MEDPVRK
Q60591	Nuclear factor of activated T-cells, cytoplasmic 2	PBS only	S(0.496)LS(0.496)PGLLYG(0.007)QQPS(0.002)LLAAPLGLADHR
Q9CZW5	Mitochondrial import receptor subunit TOM70	PBS only	AS(0.763)PALGS(0.233)GHHDGS(0.002)GDS(0.002)LEMSSLDR
P97492	Regulator of G-protein signaling 14	3.353	S(0.854)LGS(0.808)GES(0.179)ES(0.155)ES(0.004)RPGK
P16951	Cyclic AMP-dependent transcription factor ATF-2	4.669	NDSVIVADQT(1)PT(0.988)PT(0.012)R
Q6PDG5	SWI/SNF complex subunit SMARCC2	5.325	S(1)DGDPIVDPEK
<i>B. vulgatus</i> vs. PBS			
A2AIV8	Caspase recruitment domain-containing protein 9	PBS only	QQQLDMLLILS(0.012)S(0.044)DLEDS(0.153)S(0.791)PR
P49138	MAP kinase-activated protein kinase 2	PBS only	MLS(0.544)GS(0.544)PGQT(0.912)PPAPFPS(1)PPPPAPAQPPPPFPQFHVK
A2AIV8	Caspase recruitment domain-containing protein 9	0.397	NSQELSLPQDLEEDAQLS(1)DK
P16951	Cyclic AMP-dependent transcription factor ATF-2	1.996	NDSVIVADQT(1)PT(0.988)PT(0.012)R
P25799	Nuclear factor NF-kappa-B p105 subunit	2.171	S(1)DDEES(0.997)LT(0.003)LPEK
Q8VBT6	Apolipoprotein B receptor	2.407	GQEETSGAPDLS(1)PER
Q14AX6	Cdk12	3.781	NNS(1)PAPPQAPVK
P97310	DNA replication licensing factor MCM2	3.901	RRIS(1)DPLT(0.587)S(0.072)S(0.34)PGR
P97377	Cdk2	3.174	IGEGT(1)Y(1)GVVYK
Q9JIX8	Acin1, Apoptotic chromatin condensation inducer in the nucleus	5.031	S(0.015)LS(0.984)PLS(0.43)GT(0.285)T(0.285)DT(0.001)K
P25911	Tyrosine-protein kinase Lyn	<i>B. vulgatus</i> only	DNLNDDEVDS(1)K
A6X8Z5	Cdc42 GTPase	<i>B. vulgatus</i> only	DDSPSSLGS(1)PEEEQPK
Q6PDG5	SWI/SNF complex subunit SMARCC2	<i>B. vulgatus</i> only	S(1)DGDPIVDPEK
P97492	Regulator of G-protein signaling 14	<i>B. vulgatus</i> only	S(0.854)LGS(0.808)GES(0.179)ES(0.155)ES(0.004)RPGK

proteins are predominantly enriched in pathways concerning cell division, mTOR pathway, stress response pathways and signaling pathways such as PI3K pathway. Considering the importance of the pathways enriched in differentially phosphorylated proteins, it can be stated that *B. vulgatus* and *E. coli* are able to affect various pathways that are not limited to only immunological functions, but also take part in diverse cellular processes such as cell cycle, cell growth and apoptosis. Further analysis and confirmation should be carried out in order to determine whether the predicted regulation is also a biological reality and whether the observed phosphorylation of the members of these pathways can contribute to the pathogenicity difference of *B. vulgatus* and *E. coli* and the resulting differences in dendritic cell phenotypes.

4. Discussion

In this study we used label-free shotgun proteomics on dendritic cells as a platform to study immune cell responses to symbiotic and

pathobiont bacteria. The flexible nature of dendritic cell response to bacterial challenge was observed on a proteome level by the number of differentially regulated proteins. Compared to unstimulated immature DCs, upon stimulation with the commensal *B. vulgatus* 151 proteins, and upon stimulation with pathogenic *E. coli* 181 proteins were differentially regulated. Moreover, a comparison between *B. vulgatus* stimulated semi-mature DCs and *E. coli* stimulated fully mature DCs revealed differential expression in 103 proteins. The gene ontology based functional annotation and clustering of the differentially expressed proteins showed that functions related to metabolism, transcription/translation and immune response constituted the major fraction of functions. Concerning any further analysis, our paper focuses on the distinction between *B. vulgatus* and *E. coli* stimulated DCs, as we aimed to investigate the differences in the proteome of immune cells responding to symbiotic and pathobiont bacteria. We have also analyzed the data concerning PBS vs. *B. vulgatus* and PBS vs. *E. coli* and the resulting data is available as supplementary material for interested readers

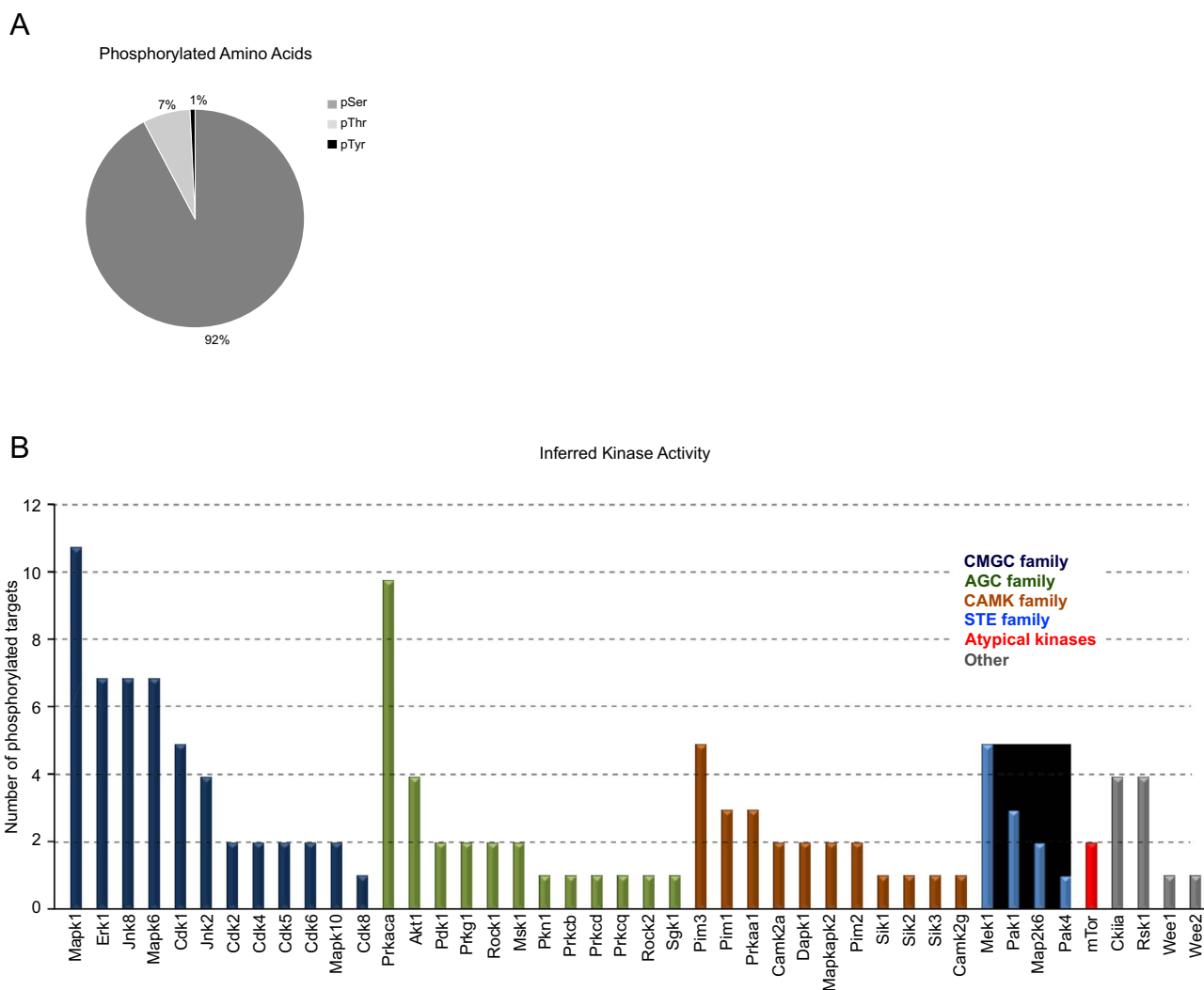


Fig. 4. a) Distribution of phosphorylated amino acid residues. b) List of kinases and the number of target phosphosites that are found in the experimental dataset for each kinase listed. Kinases are grouped into 5 major families, with the kinase with highest number of phosphorylated targets shown first.

(supplementary excel files 1 and 2).

Voronoi treemaps enabled us to display functional clusters of the differentially expressed proteins, together with their expression value. As indicated by the prevalence of blue color, proteins with immunity/inflammation related functions are downregulated in the *B. vulgatus* stimulated sample. This led us to the conclusion that symbiotic bacteria, in our case *B. vulgatus*, can direct the immune cells to a more repressed state in terms of proinflammatory regulators and thereby prevent a fulminant response to bacterial stimulus. The opposite effect can be seen in *E. coli* stimulated dendritic cells, in which a strong upregulation of immune functions is observed, compared to PBS controls. A closer investigation of upregulated immune functions in *E. coli* indicates iNOS, COX2, and CCL5 as potent immune regulators. iNOS, the inducible nitric oxide synthase, regulates cytokine production and Th1 response and has been shown to have increased activity in ulcerative colitis and Crohn's disease [38–41]. Inhibition of iNOS expression results in reduction of inflammation and disease severity in DSS models of colitis in mice and experimental colitis in rats [42,43]. The inducible cyclooxygenase COX2 is also expressed under inflammatory conditions and is an attractive target for non-steroidal anti-inflammatory drugs (NSAIDs) [44–46]. Increased expression of COX2 has been observed in intestinal epithelial cells of IBD patients, and COX2 inhibitors have anti-inflammatory effects in IBD patients [47,48]. The chemokine CCL5 is involved in recruiting macrophages, basophils and T-cells to

inflammatory sites. Increased CCL5 mRNA expression has been reported in colonic biopsies of IBD patients, and immunoneutralization of CCL5 reduced disease activity and neutrophil recruitment in a DSS mouse model of colitis [49].

The pathway analysis we performed using IPA tools shows that IRF signaling pathway, dendritic cell maturation pathways, and TLR signaling pathway are among the pathways with the highest relevance to the observed maturation difference. This is in line with the current literature which covers the involvement of these pathways in immune responses upon bacterial challenge. In addition to these, we have also detected signaling pathways such as PPAR signaling, LXR/RXR pathway, and TREM1 signaling pathways. PPARs are ligand inducible transcription factors which control several important inflammatory mediators that are detected in our proteome experiment such as IL1 α , STAT5a, I κ B κ . PPAR γ expression is reported to be downregulated in patients with active ulcerative colitis [50], and the loss of PPAR γ abolishes the protective effect of probiotic bacteria in mice with DSS colitis [51]. In our data, several important proinflammatory PPAR targets such as I κ B κ , STAT5A, IL1 α , IL1 β are shown to be downregulated upon *B. vulgatus* stimulation, supporting IPA prediction of PPAR pathway involvement and suppression of proinflammatory factors. Polymorphisms in PPAR γ and LXR have been associated with the risk of developing colitis [52]. Joseph et al. showed for the first time that LXRs are potent immune modulators, exerting their effect by

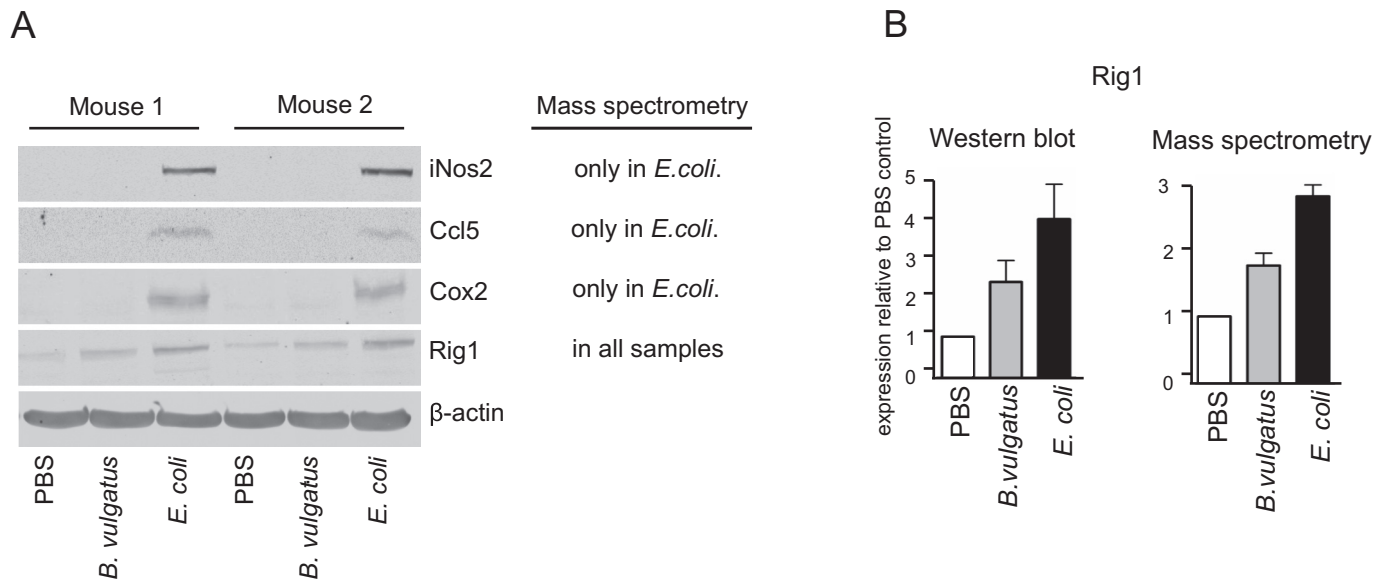


Fig. 5. a) Expression levels of several selected proteins of interest were determined by Western blots done with whole-cell extracts prepared from BMDCs derived from two C57BL/6 mice, unstimulated (PBS) and stimulated for 16 h with *B. vulgatus* or *E. coli*. β-actin was included as a loading control. Results are representative of 2 independent experiments. b) Comparison of expression levels of RIG-1 protein by Western blot and mass spectrometry data. Expression level in the PBS control is taken as baseline expression and set to 1. All band intensities in the Western blot graph are normalized to β-actin.

inhibiting iNOS, COX2 and IL-6. LXRs protective effect was further exemplified by inducing colitis in LXR deficient mice which had decreased survival and increase in disease markers compared to wild-type controls [53]. In line with these findings, our data shows regulation in LXR pathway as proinflammatory LXR targets IL1α, IL1β, iNOS and MMP9 are downregulated in *B. vulgatus* treated samples. TREM1 is a cell surface receptor that strongly amplifies proinflammatory immune responses of leukocytes [54]. Increased TREM1 expression was reported in inflammatory bowel disease patients and expression levels correlated with disease activity [55]. As in the signaling pathways we mentioned above, we also have reduced expression of TREM1 proinflammatory targets in *B. vulgatus* stimulated DCs. The general pattern emerging from the pathway analysis is that, *B. vulgatus* regulates signaling pathways that control inflammation and reduces the expression of proinflammatory genes or increases the expression of anti-inflammatory proteins, thereby having an overall protective effect against a strong inflammatory response.

The upstream regulator analysis report of Ingenuity® Pathway Analysis contains 37 major regulatory proteins which exert their effects

on a plethora of processes and functions (Fig. 3). Compared with *E. coli* stimulated DCs, 29 of upstream regulators are shown to be inhibited upon stimulation with *B. vulgatus* and 8 upstream regulators are shown to be activated. The majority of the upstream regulators included in the report have well defined immune regulatory functions. As we hypothesized that *B. vulgatus* stimulation results in a more silent, inflammation suppressive immune cell phenotype, the inhibition of major upstream regulators such as IRF3, TLR4, TICAM1, IFNγ, MyD88 is to be expected. However, *B. vulgatus* stimulation results not only in the inhibition of proinflammatory regulators, but also in upregulation of several key factors such as PTGER4, ABCA1, SOCS1, and LXRα. All these upstream regulators have downstream targets of key immunological importance. PTGER4 (Prostaglandin E receptor 4) is a G-protein coupled receptor for prostaglandin E2. A novel locus modulating PTGER4 levels have been discovered to be associated with Crohn's disease [56], which has been replicated by additional independent genome-wide association studies [57,58]. Additional studies showed that PTGER4 knockout mice succumb to severe colitis after DSS administration [59], whereas administration of PTGER4 agonists offers

Table 4

Reactome pathway analysis with phosphorylated peptides. All 118 peptides that were differentially phosphorylated in *B. vulgatus* vs. *E. coli* stimulated DCs were used as the input, and the resulting pathways enriched in phosphorylated peptides are indicated in the list. p-value indicates the results of multiple hypothesis testing performed by the reactome software, and significance threshold is defined at < 0.

Pathway name	# Phosphopeptides detected by MassSpec	# Proteins in reactome database	MS/database ratio	p value
Apoptotic cleavage of cellular proteins	4	38	0.00444392	9.73E - 04
Mitotic prophase	5	75	0.0087709	0.00171496
Apoptotic execution phase	4	47	0.00549643	0.00210655
Depolymerisation of the nuclear lamina	2	10	0.00116945	0.00591492
Nuclear envelope breakdown	3	45	0.00526254	0.01488664
Hyaluronan uptake and degradation	2	18	0.00210502	0.0180745
Apoptosis	4	91	0.01064203	0.0203461
Breakdown of the nuclear lamina	2	3	3.51E - 04	5.61E - 04
Activation of CaMK IV	1	2	2.34E - 04	0.02243458
Hyaluronan metabolism	2	22	0.0025728	0.02622534
Condensation of prophase chromosomes	2	22	0.0025728	0.02622534
Cyclin A/B1 associated events during G2/M transition	2	23	0.00268974	0.0284562
Programmed cell death	4	102	0.01192843	0.02926745

protection from DSS colitis [60]. Taken together, these studies indicate a positive effect of PTGER4 activation on inflammatory bowel disease outcome, which is in line with our finding that PTGER4 is activated upon stimulation by the symbiont *B. vulgatus* when compared with the pathobiont *E. coli*.

SOCS1 (suppressor of cytokine signaling 1) is another factor that is predicted to be activated by *B. vulgatus* stimulation. SOCS1 has suppressive functions on cytokine signaling and its targets include IFN α , IFN γ , IL6, IL12 and TNF α [61]. SOCS1 knockout mice die within 3 weeks as a result of severe systemic inflammation [62], whereas SOCS1^{-/-} Rag2^{-/-} mice develop spontaneous colitis [31]. SOCS1 is a crucial factor for endotoxin tolerance as SOCS1^{-/-} macrophages are unable to turn off proinflammatory cytokine expression under tolerance inducing conditions and overexpression of SOCS1 in macrophages inhibits LPS signaling by reducing TNF α expression and suppressing TLR4- $\text{I}\kappa\text{B}$ pathway [63].

ABCA1 (ATP-binding cassette transporter 1) transports cellular cholesterol and phospholipids to membrane bound apoA-I, thereby controlling the rate of HDL formation [64,65]. Transport functions of ABCA1 and its regulation have wide ranging consequences in the context of immunity and inflammation. A study by Thompson et al. showed that ABCA1 actively participates in LPS efflux from macrophages. Administration of T0901317, a nonsteroidal activator of ABCA1 expression, resulted in increased efflux of LPS and cholesterol from macrophages, an effect not observed in ABCA1^{-/-} cells. Increased LPS efflux is important for LPS tolerance, as removal of LPS from the cell results in limitation of LPS tolerance to shorter time intervals. This phenomenon is also observed in ABCA1^{-/-} macrophages showed delayed recovery from LPS tolerance and did not respond to inflammatory cytokine inducing stimuli [66]. Increased HDL formation, which is regulated by ABCA1, has also been shown to reduce LPS endotoxicity by binding and sequestering LPS and reducing TNF- α release. In ABCA1^{-/-} murine macrophages, LPS challenge results in increased mRNA levels in major proinflammatory factors such as MCP-1, IL-1 β , TNF- α , IL-6, IL-12, iNOS and COX2, compared to wild-type macrophages [67]. Intraperitoneal injection of LPS to ABCA1^{-/-} mice also elevated plasma levels of IL-1 β and IL-12p40, providing further evidence to the LPS hypersensitivity observed *in vitro*. Taken together, the transport functions of ABCA1 have branching and multifaceted effects on inflammatory response against LPS, and can be an important dampening factor to prevent overwhelming inflammation. Our analysis predicts differential activation of ABCA1 pathway upon stimulation with *B. vulgatus*, which is in line with the anti-inflammatory role of *B. vulgatus* in IBD and anti-inflammatory effects of ABCA1 activation as discussed above.

The phosphoproteomics analysis yielded 465 differentially regulated phosphosites on 301 peptides. Among these proteins whose phosphorylation were absent in the indicated sites in *E. coli* stimulated DCS are cell cycle related kinases such as CDK2 and CDC42, transcription factors junD and NFAT-2, cytokine expression regulator IRF3 and epigenetic factors such as SMARCC1 and SMARCC2. Considering the functions of these proteins and the cellular pathways they take part in (Table 3), it is possible that stimulation with symbiont and pathobiont bacteria affects many other cellular processes than only immune related functions. Several phosphoevents we have detected are well described in literature. For example, *B. vulgatus* stimulated DCs harbor cell inactivating phosphorylation at position Tyr14/Thr15 of CDK2 [68], which was absent in *E. coli* stimulated dendritic cells. Similarly, ATF-2 phosphorylation at residues Thr69/Thr71 was only detected in *B. vulgatus* stimulated sample, and these phosphorylation events have been shown to lead to the transcriptional activation of ATF-2 [69], and may increase intrinsic histone acyltransferase activity of ATF-2 [70]. Targets of ATF-2 include cytokines, cell cycle regulators, transcription factors, and apoptosis regulators [71]. Well defined and functionally assessable phosphorylation events such as those belonging to CDK2 and ATF-2 can provide interesting leads for further investigation, and information on the regulation of phosphoproteome helps to obtain a more

comprehensive picture of the effects of symbiont and pathobiont bacteria on dendritic cell maturation and immunity.

Taken together, our shotgun proteomics experiment identified differentially expressed and differentially phosphorylated proteins between dendritic cells stimulated with the symbiont *B. vulgatus* and pathobiont *E. coli*. Among these are cytokines, transcription factors, cellular adhesion molecules, and cell surface markers that are integral to immune regulation. Our pathway analysis showed involvement of major immune signaling pathways during dendritic cell maturation, and implicated several pathways such as PPAR signaling, LXR/RXR activation and glucocorticoid signaling pathways that are not studied in detail in an inflammation and DC maturation context. Our upstream regulator analysis identified 37 major factors that were differentially regulated between the two stimulations; among those are PTGER4, ABCA1, SOCS1, LXR α and DUSP1 which are promising candidates to investigate further. Our phosphoproteome analysis showed differential phosphorylation in 118 phosphosites including those belonging to epigenetic factors, transcription factors and major cell cycle regulators. Our results will enable researchers to investigate the differences in dendritic cell proteomes in detail, both from a general cellular processes level and from a detailed pathway/single protein level. As proteome experiments are comprehensive, any single regulatory protein or pathway can be investigated further to advance our knowledge in dendritic cell maturation and its roles in inflammatory diseases.

Supplementary data to this article can be found online at <https://doi.org/10.1016/j.jprot.2017.11.008>.

Grant support

Work by J.S.F was supported by the DFG (DFG FR 2087/6-1, DFG FR 2087/8-1, CRC685, SPP1656) the DFG research training group 1708, the Bundesministerium für Bildung und Forschung (BMBF) (TTU 06.803) and the German Center for Infection Research (DZIF). Work by M.C. Codrea and S. Nahnsen was supported by the DFG (Quantitative Biology Center (QBiC) GZ: KO2313/6-1).

Conflict of interest

The authors declare no conflict of interest.

Transparency document

The Transparency document associated with this article can be found, in online version.

Acknowledgements

We thank Izabela Sierzputowska, Andrea Schaefer, Annika Bender and Silke Wahl for their valuable assistance in experiments; Nico Jehmlich, Alexander Steimle, Jan Maerz, Florent Jouy for valuable discussions, and Liam Whiteley for critical reading of the manuscript.

References

- [1] M. Waidmann, et al., *Bacteroides vulgatus* protects against *Escherichia coli*-induced colitis in gnotobiotic interleukin-2-deficient mice, *Gastroenterology* 125 (1) (2003) 162–177.
- [2] M. Menges, et al., Repetitive injections of dendritic cells matured with tumor necrosis factor alpha induce antigen-specific protection of mice from autoimmunity, *J. Exp. Med.* 195 (1) (2002) 15–21.
- [3] M.B. Lutz, Therapeutic potential of semi-mature dendritic cells for tolerance induction, *Front. Immunol.* 3 (2012) 123.
- [4] J.S. Frick, et al., Colitogenic and non-colitogenic commensal bacteria differentially trigger DC maturation and Th cell polarization: an important role for IL-6, *Eur. J. Immunol.* 36 (6) (2006) 1537–1547.
- [5] M. Muller, et al., Intestinal colonization of IL-2 deficient mice with non-colitogenic *B. vulgatus* prevents DC maturation and T-cell polarization, *PLoS One* 3 (6) (2008) e2376.
- [6] M.B. Lutz, et al., An advanced culture method for generating large quantities of

- highly pure dendritic cells from mouse bone marrow, *J. Immunol. Methods* 223 (1) (1999) 77–92.
- [7] B. Macek, et al., The serine/threonine/tyrosine phosphoproteome of the model bacterium *Bacillus Subtilis*, *Molecular & Cellular Proteomics: MCP* 6 (4) (2007) 697–707.
- [8] H.K.S. Leiros, et al., Trypsin specificity as elucidated by LIE calculations, X-ray structures, and association constant measurements, *Protein Sci.* 13 (4) (2004) 1056–1070.
- [9] J.V. Olsen, B. Macek, High accuracy mass spectrometry in large-scale analysis of protein phosphorylation, *Methods Mol. Biol.* 492 (2009) 131–142.
- [10] A. Koch, K. Krug, S. Pengelley, B. Macek, S. Hauf, Mitotic substrates of the kinase aurora with roles in chromatin regulation identified through quantitative phosphoproteomics of fission yeast, *Sci. Signal.* 4 (179) (2011) (rs6).
- [11] M.J. Schroeder, J. Shabanowitz, J.C. Schwartz, D.F. Hunt, J.J. Coon, A neutral loss activation method for improved phosphopeptide sequence analysis by quadrupole ion trap mass spectrometry, *Anal. Chem.* 76 (13) (2004) 3590–3598.
- [12] J.V. Olsen, et al., Parts per million mass accuracy on an Orbitrap mass spectrometer via lock mass injection into a C-trap, *Molecular & Cellular Proteomics: MCP* 4 (12) (2005) 2010–2021.
- [13] J. Cox, et al., Andromeda: a peptide search engine integrated into the MaxQuant environment, *J. Proteome Res.* 10 (4) (2011) 1794–1805.
- [14] J. Cox, M. Mann, MaxQuant enables high peptide identification rates, individualized p.p.b.-range mass accuracies and proteome-wide protein quantification, *Nat. Biotechnol.* 26 (12) (2008) 1367–1372.
- [15] Team R-C, R: A Language and Environment for Statistical Computing, (2015).
- [16] J.C.B.D. Pinheiro, *Mixed-effects Models in S and S-PLUS*, Springer, 2000.
- [17] J.B.D. Pinheiro, S. DebRoy, D. Sarkar, R Core Team, nlme: Linear and Nonlinear Mixed Effects Models. R Package Version 3.1, 118 (2014).
- [18] J.D. Storey, A direct approach to false discovery rates, *J Roy Stat Soc B* 64 (2002) 479–498.
- [19] Y. Benjamini, Y. Hochberg, Controlling the false discovery rate - a practical and powerful approach to multiple testing, *J Roy Stat Soc B Met* 57 (1) (1995) 289–300.
- [20] K. Sharma, et al., Ultradeep human phosphoproteome reveals a distinct regulatory nature of Tyr and Ser/Thr-based signaling, *Cell Rep.* 8 (5) (2014) 1583–1594.
- [21] J.A. Vizcaino, et al., 2016 update of the PRIDE database and its related tools, *Nucleic Acids Res.* 44 (D1) (2016) D447–D456.
- [22] M. Balzer, Voronoi treemaps, IEEE Symposium on Information Visualization (InfoVis 2005), 2005.
- [23] J. Bernhardt, Visualizing gene expression data via Voronoi treemaps, Sixth International Symposium on Voronoi Diagrams, 2009, pp. 233–241.
- [24] Anonymous (2014).
- [25] H.R. Christensen, H. Frokiaer, J.J. Pestka, Lactobacilli differentially modulate expression of cytokines and maturation surface markers in murine dendritic cells, *J. Immunol.* 168 (1) (2002) 171–178.
- [26] M.B. Lutz, G. Schuler, Immature, semi-mature and fully mature dendritic cells: which signals induce tolerance or immunity? *Trends Immunol.* 23 (9) (2002) 445–449.
- [27] K. Gronbach, et al., Endotoxicity of lipopolysaccharide as a determinant of T-cell-mediated colitis induction in mice, *Gastroenterology* 146 (3) (2014) 765–775.
- [28] A. Otto, et al., Systems-wide temporal proteomic profiling in glucose-starved *Bacillus Subtilis*, *Nat. Commun.* 1 (9) (2010) 137.
- [29] A. Kramer, J. Green, J. Pollard Jr., S. Tugendreich, Causal analysis approaches in ingenuity pathway analysis, *Bioinformatics* 30 (4) (2014) 523–530.
- [30] J. Horino, et al., Suppressor of cytokine signaling-1 ameliorates dextran sulfate sodium-induced colitis in mice, *Int. Immunol.* 20 (6) (2008) 753–762.
- [31] T. Chinen, et al., Prostaglandin E2 and SOCS1 have a role in intestinal immune tolerance, *Nat. Commun.* 2 (2011) 190.
- [32] C. Tang, Y. Liu, P.S. Kessler, A.M. Vaughan, J.F. Oram, The macrophage cholesterol exporter ABCA1 functions as an anti-inflammatory receptor, *J. Biol. Chem.* 284 (47) (2009) 32336–32343.
- [33] S.B. Joseph, et al., LXR-dependent gene expression is important for macrophage survival and the innate immune response, *Cell* 119 (2) (2004) 299–309.
- [34] S.B. Joseph, A. Castrillo, B.A. Laffitte, D.J. Mangelsdorf, P. Tontonoz, Reciprocal regulation of inflammation and lipid metabolism by liver X receptors, *Nat. Med.* 9 (2) (2003) 213–219.
- [35] V. Sjoelund, M. Smelkinson, A. Nita-Lazar, Phosphoproteome profiling of the macrophage response to different toll-like receptor ligands identifies differences in global phosphorylation dynamics, *J. Proteome Res.* 13 (11) (2014) 5185–5197.
- [36] Anonymous
- [37] D. Croft, et al., The reactome pathway knowledgebase, *Nucleic Acids Res.* 42 (2014) D472–477 database issue.
- [38] C. Bogdan, Nitric oxide and the immune response, *Nat. Immunol.* 2 (10) (2001) 907–916.
- [39] W. Niedbala, X.Q. Wei, D. Piedrafita, D. Xu, F.Y. Liew, Effects of nitric oxide on the induction and differentiation of Th1 cells, *Eur. J. Immunol.* 29 (8) (1999) 2498–2505.
- [40] D. Rachmilewitz, et al., Enhanced colonic nitric oxide generation and nitric oxide synthase activity in ulcerative colitis and Crohn's disease, *Gut* 36 (5) (1995) 718–723.
- [41] N.K. Boughton-Smith, et al., Nitric oxide synthase activity in ulcerative colitis and Crohn's disease, *Lancet* 342 (8867) (1993) 338–340.
- [42] D. Camuesco, et al., The intestinal anti-inflammatory effect of quercitrin is associated with an inhibition in iNOS expression, *Br. J. Pharmacol.* 143 (7) (2004) 908–918.
- [43] K.M. Sakthivel, C. Gurusvayoorappan, Amentoflavone inhibits iNOS, COX-2 expression and modulates cytokine profile, NF-kappaB signal transduction pathways in rats with ulcerative colitis, *Int. Immunopharmacol.* 17 (3) (2013) 907–916.
- [44] D. Wang, R.N. Dubois, The role of COX-2 in intestinal inflammation and colorectal cancer, *Oncogene* 29 (6) (2010) 781–788.
- [45] K. Seibert, J.L. Masferrer, Role of inducible cyclooxygenase (COX-2) in inflammation, *Receptor* 4 (1) (1994) 17–23.
- [46] C.J. Hawkey, COX-2 inhibitors, *Lancet* 353 (9149) (1999) 307–314.
- [47] I.I. Singer, et al., Cyclooxygenase 2 is induced in colonic epithelial cells in inflammatory bowel disease, *Gastroenterology* 115 (2) (1998) 297–306.
- [48] Y. El Miedany, S. Youssef, I. Ahmed, M. El Gaafary, The gastrointestinal safety and effect on disease activity of etoricoxib, a selective cox-2 inhibitor in inflammatory bowel diseases, *Am. J. Gastroenterol.* 101 (2) (2006) 311–317.
- [49] C. Yu, et al., Platelet-derived CCL5 regulates CXC chemokine formation and neutrophil recruitment in acute experimental colitis, *J. Cell. Physiol.* 231 (2) (2016) 370–376.
- [50] X. Dou, J. Xiao, Z. Jin, P. Zheng, Peroxisome proliferator-activated receptor-gamma is downregulated in ulcerative colitis and is involved in experimental colitis-associated neoplasia, *Oncol. Lett.* 10 (3) (2015) 1259–1266.
- [51] J. Bassaganya-Riera, et al., Probiotic bacteria produce conjugated linoleic acid locally in the gut that targets macrophage PPAR gamma to suppress colitis, *PLoS One* 7 (2) (2012) e31238.
- [52] V. Andersen, et al., Polymorphisms in NF-kappa B, PXR, LXR, PPAR gamma and risk of inflammatory bowel disease, *World J. Gastroenterol.* 17 (2) (2011) 197–206.
- [53] T. Jakobsson, et al., The oxysterol receptor LXRβ protects against DSS-and TNBS-induced colitis in mice, *Mucosal Immunol.* 7 (6) (2014) 1416–1428.
- [54] A. Bouchon, F. Facchetti, M.A. Weigand, M. Colonna, TREM-1 amplifies inflammation and is a crucial mediator of septic shock, *Nature* 410 (6832) (2001) 1103–1107.
- [55] M. Schenk, A. Bouchon, F. Seibold, C. Mueller, TREM-1—expressing intestinal macrophages crucially amplify chronic inflammation in experimental colitis and inflammatory bowel diseases, *J. Clin. Invest.* 117 (10) (2007) 3097–3106.
- [56] C. Libioulle, et al., Novel Crohn disease locus identified by genome-wide association maps to a gene desert on 5p13.1 and modulates expression of PTGER4, *PLoS Genet.* 3 (4) (2007) (e58).
- [57] D.P. McGovern, et al., Genome-wide association identifies multiple ulcerative colitis susceptibility loci, *Nat. Genet.* 42 (4) (2010) 332–337.
- [58] M. Prager, J. Büttner, C. Büning, PTGER4 modulating variants in Crohn's disease, *Int. J. Color. Dis.* 29 (8) (2014) 909–915.
- [59] K. Kabashima, et al., The prostaglandin receptor EP4 suppresses colitis, mucosal damage and CD4 cell activation in the gut, *J. Clin. Invest.* 109 (7) (2002) 883–893.
- [60] G.-L. Jiang, et al., The prevention of colitis by E Prostanoid receptor 4 agonist through enhancement of epithelium survival and regeneration, *J. Pharmacol. Exp. Ther.* 320 (1) (2007) 22–28.
- [61] M. Fujimoto, T. Naka, Regulation of cytokine signaling by SOCS family molecules, *Trends Immunol.* 24 (12) (2003) 659–666.
- [62] R. Starr, et al., Liver degeneration and lymphoid deficiencies in mice lacking suppressor of cytokine signaling-1, *Proc. Natl. Acad. Sci.* 95 (24) (1998) 14395–14399.
- [63] I. Kinjo, et al., SOCS1/JAB is a negative regulator of LPS-induced macrophage activation, *Immunity* 17 (5) (2002) 583–591.
- [64] J. Oram, S. Yokoyama, Apolipoprotein-mediated removal of cellular cholesterol and phospholipids, *J. Lipid Res.* 37 (12) (1996) 2473–2491.
- [65] S. Yokoyama, Apolipoprotein-mediated cellular cholesterol efflux, *Biochimica et Biophysica Acta (BBA)-Lipids and Lipid Metabolism* 1392 (1) (1998) 1–15.
- [66] P.A. Thompson, K.C. Gauthier, A.W. Varley, R.L. Kitchens, ABCA1 promotes the efflux of bacterial LPS from macrophages and accelerates recovery from LPS-induced tolerance, *J. Lipid Res.* 51 (9) (2010) 2672–2685.
- [67] D.M. Levine, T.S. Parker, T.M. Donnelly, A. Walsh, A.L. Rubin, In vivo protection against endotoxin by plasma high density lipoprotein, *Proc. Natl. Acad. Sci.* 90 (24) (1993) 12040–12044.
- [68] Y. Gu, J. Rosenblatt, D.O. Morgan, Cell cycle regulation of CDK2 activity by phosphorylation of Thr160 and Tyr15, *EMBO J.* 11 (11) (1992) 3995–4005.
- [69] D.M. Ouwens, et al., Growth factors can activate ATF2 via a two-step mechanism: phosphorylation of Thr71 through the Ras-MEK-ERK pathway and of Thr69 through RalGDS-Src-p38, *EMBO J.* 21 (14) (2002) 3782–3793.
- [70] H. Kawasaki, et al., ATF-2 has intrinsic histone acetyltransferase activity which is modulated by phosphorylation, *Nature* 405 (6783) (2000) 195–200.
- [71] P. Lopez-Bergami, E. Lau, Z. Ronai, Emerging roles of ATF2 and the dynamic AP1 network in cancer, *Nat. Rev. Cancer* 10 (1) (2010) 65–76.

TLR Signaling-induced CD103-expressing Cells Protect Against Intestinal Inflammation

Alexandra Wittmann, PhD,^{*,†} Peter A. Bron, PhD,^{‡,§} Iris I. van Swam,^{‡,§} Michiel Kleerebezem, PhD,^{‡,§,||} Patrick Adam, MD,[¶] Kerstin Gronbach, PhD,^{*} Sarah Menz, Dipl. Troph.,^{*} Isabell Flade, MSc,^{*} Annika Bender,^{*} Andrea Schäfer,^{*} Ali Giray Korkmaz, MS,^{*} Raphael Parusel, MSc,^{*} Ingo B. Autenrieth, MD,^{*} and Julia-Stefanie Frick, MD^{*}

Background: Toll-like receptor (TLR) expression in patients with inflammatory bowel disease is increased when compared with healthy controls. However, the impact of TLR signaling during inflammatory bowel disease is not fully understood.

Methods: In this study, we used a murine model of acute phase inflammation in bone marrow chimeric mice to investigate in which cell type TLR2/4 signal induction is important in preventing intestinal inflammation and how intestinal dendritic cells are influenced. Mice were either fed with wild-type bacteria, able to initiate the TLR2/4 signaling cascade, or with mutant strains with impaired signal induction capacity.

Results: The induction of the TLR2/4 signal cascade in epithelial cells resulted in inflammation in bone marrow chimeric mice, whereas induction in hematopoietic cells had an opposed function. Furthermore, feeding of wild-type bacteria prevented disease; however, differing signal induction of bacteria had no effect on lamina propria dendritic cell activation. In contrast, functional TLR2/4 signals resulted in increased frequencies of CD103-expressing lamina propria and mesenteric lymph node dendritic cells, which were able to ameliorate disease.

Conclusions: The TLR-mediated amelioration of disease, the increase in CD103-expressing cells, and the beneficial function of TLR signal induction in hematopoietic cells indicate that the increased expression of TLRs in patients with inflammatory bowel disease might result in counterregulation of the host and serve in preventing disease.

(*Inflamm Bowel Dis* 2015;21:507–519)

Key Words: DSS, intestinal Toll-like receptors, bone marrow chimeric mice, lamina propria dendritic cells

The intestine is the immunologically most active organ in the body, permanently challenged by great loads of antigens. To maintain intestinal homeostasis, it is essential for this organ to mount a balanced immune response to fight intruders but not to overreact towards commensal and nutritional antigens. In inflammatory bowel

disease (IBD), this balance is impaired. For the establishment of systemic and mucosal tolerance, antigen-presenting dendritic cells (DCs) are crucial. DCs either sample actively by extending dendrites towards the lumen without disrupting tight junctions^{1,2} or DCs receive antigens, which have been transcytosed by other cell types, such as microfold cells^{3,4} or goblet cells.⁵ After antigen uptake, DCs migrate to the mesenteric lymph nodes (MLNs) and present sampled antigens to naive T cells.³ Upon antigen uptake through phagocytosis^{6,7} or macropinocytosis,⁸ DCs undergo a maturation process resulting in increased surface expression of peptide bound MHC class II complexes⁹ and costimulatory molecules CD80, CD86, and CD40.¹⁰ Moreover, maturation induces CCR7 expression on DCs.³ The state of DC activation is important in maintaining intestinal homeostasis because an increased DC activation has been associated with intestinal inflammation.¹¹ Pattern recognition receptors such as Toll-like receptors (TLR) identify bacteria, recognizing conserved microbial-associated molecular patterns, e.g., bacterial lipoteichoic acids and lipoproteins (TLR2) or bacterial lipopolysaccharide (LPS) (TLR4).^{12,13} Patients with IBD exhibit an increased expression of TLR4 on intestinal epithelial cells¹⁴ and an enhanced TLR2 and TLR4 surface expression on intestinal macrophages¹⁵ and myeloid colonic DCs.¹⁶ However, these observations do not help us in answering the question of whether

Supplemental digital content is available for this article. Direct URL citations appear in the printed text and are provided in the HTML and PDF versions of this article on the journal's Web site (www.ibdjournal.org).

Received for publication October 21, 2014; Accepted October 21, 2014.

From the ^{*}Interfaculty Institute for Microbiology and Infection Medicine, Department for Medical Microbiology and Hygiene, University of Tübingen, Tübingen, Germany; [†]Institute of Food Research, Norwich Research Park, Norwich, United Kingdom; [‡]NIZO Food Research, Ede, the Netherlands; [§]TI Food and Nutrition, Wageningen, the Netherlands; ^{||}Host Microbe Interactomics Group, Wageningen University, Wageningen, the Netherlands; and [¶]Institute of Pathology, University of Tübingen, Tübingen, Germany.

Supported by the German Research Foundation (DFG FR 2087/6–1, DFG FR 2087/8–1, CRC 685, SPP1656) the DFG research training group (Graduiertenkolleg) 1708, the Federal Ministry of Education and Research (BMBF) and the German Centre for Infection Research (DZIF).

The authors have no conflicts of interest to disclose.

Reprints: Julia-Stefanie Frick, MD, Interfaculty Institute for Microbiology and Infection Medicine Tübingen, Elfriede-Aulhorn-Straße 6, 72076 Tübingen, Germany (e-mail: Julia-Stefanie.Frick@med.uni-tuebingen.de).

Copyright © 2015 Crohn's & Colitis Foundation of America, Inc.

DOI 10.1097/MIB.0000000000000292

Published online 2 February 2015.

increased expression of TLRs is the reason for disease development or a counterregulation of the host's immunity.

Receptor-mediated protection is demonstrated by the fact that *tlr2*- and *tlr4*-deficient mice are more susceptible to dextran sulfate sodium salt (DSS) than wild-type (WT) mice.¹⁷ DSS models acute intestinal inflammation¹⁸ resembling human IBD demonstrated by the fact that human therapeutic agents¹⁹ ameliorate disease. Therefore, DSS offers the possibility of elucidating TLR signal induction during acute inflammation. In addition, differing expressions of TLRs in varying cell types might be of importance. The fact that DCs express higher levels of TLRs in IBD implies an important function of DCs in disease development. Indeed, DCs can ambivalently influence intestinal inflammation since depletion of DCs during DSS colitis has resulted in exacerbation²⁰ and attenuation of intestinal inflammation.²¹ The aim of this study was to identify the cell type responsible for the TLR-mediated protection against DSS-induced disease. Moreover, the impact on the intestinal immune response and in particular on DC composition, activation state, and TLR2 and TLR4 expression on DCs was investigated by using bone marrow chimeric mice (BMCM) and bacterial mutant strains with impaired TLR2/4 signal induction capacity. The *Lactobacillus plantarum* Δ *dltX-D* mutant strain (LP-Mut) lacks D-alanylation of teichoic acids, which leads to a weaker induction of the TLR2 pathway,^{22,23} and the genetically modified *Escherichia coli* JM83 Δ *htrB htrB_{Pg}* mutant strain (EC-Mut) features an altered lipid A structure as compared with the *E. coli* JM83 (EC) WT strain, which results in a reduced TLR4 signal induction. This is demonstrated by a significantly reduced IL-8 secretion of Mono-Mac-6 cells after stimulation with EC-Mut LPS when compared with cells stimulated with EC LPS.²⁴ For the recognition of LPS, the phosphorylation and acylation pattern of the lipid A are of importance.²⁵

MATERIALS AND METHODS

Animals

C57Bl/6 Ola Hsd mice were purchased from Harlan and maintained in individually ventilated cages. B6.SJL-*Ptprca^a Pepcb^b*/BoyCrl (CD45.1) (Charles River), B6.129-Tlr2^{tm1Kir}/J (TLR2 KO), and B6.B10ScN-Tlr4^{lps-del}/JthJ (TLR4 KO) mice (The Jackson Laboratory) were bred and maintained under specific pathogen-free conditions. Animal experiments were reviewed and approved by an appropriate institutional review committee (Genehmigung H5/10 and H9/11 Regierungspräsidium Tübingen).

Generation of BMCM

C57Bl/6, CD45.1, TLR2 KO, and TLR4 KO mice were lethally irradiated (9.5 Gy male, 9 Gy female) and after 6 hours 1×10^7 freshly isolated bone marrow cells were intravenously injected. BMCM were maintained in individually ventilated cages, were given drinking water containing cotrimoxazole (260 μ g/mL) for 14 days and, after additional 28 days, were used for experiments.

DSS Colitis

Acute phase colitis was induced in C57Bl/6 Ola Hsd mice by administration of 2.5% (wt/vol) DSS salt (MDBiosystems) contained in drinking water or 2.5% DSS and 1×10^{10} bacteria per milliliter contained in drinking water for 6 days. BMCM received 3.5% DSS containing drinking water for 7 days. Onset of intestinal inflammation was monitored by daily control of the body weight and the disease activity index (DAI). Immediately after mice were killed by carbon dioxide asphyxiation colon length was determined.

Bacteria

The *E. coli* JM83 Δ *htrB htrB_{Pg}* mutant strain (EC-Mut) carries in comparison with the *E. coli* JM83 (EC) WT strain a null mutation for the *htrB* gene that was complemented with a pUC18 plasmid carrying an ampicillin resistance cassette and the *htrB* gene of *Porphyromonas gingivalis* (*htrB_{Pg}*) under the control of the *lacZ* promoter.²⁴ The *L. plantarum* Δ *dltX-D*²² strain (LP-Mut) carries in comparison with the *L. plantarum* WCFS1 (LP) WT strain a genetically stable chloramphenicol resistance cassette instead of the *dltX-D* operon.²⁶

Histology

Colon sections were stained with hematoxylin and eosin (Merck) and scored in a blinded fashion as previously described.²⁷

Isolation of Lamina Propria and MLN Leukocytes

Cells were isolated as previously described.²⁸ The complete intestine was then removed, and Peyer's patches were abscised. The gut was opened longitudinally and flushed thoroughly with phosphate-buffered saline (Gibco, Darmstadt, Germany) containing fetal calf serum (1 wt/vol; Sigma, Hamburg, Germany) (PBS/FCS). Lamina propria (LP) was separated from intestinal epithelial cells by incubation in 1 mM dithiothreitol (DTT; AppliChem, Darmstadt, Germany) and 1 mM ethylenediaminetetraacetic acid containing PBS under slow rotations. The remaining intestinal tissue was washed in PBS/FCS, cut thoroughly, subsequently transferred into digestion solution (VLE RPMI 1640, Biochrom; 200 U/mL collagenase, Sigma; 5 U/mL DNase, Roche; 50 μ M β -mercaptoethanol, AppliChem; 5% FCS, Sigma; 2 mM glutamine, 2500 U/mL penicillin, 2000 μ g/mL streptomycin, GIBCO) and incubated for 60 minutes under slow rotations. LP cell suspension was centrifuged, resuspended in 40% Easycoll (Biochrom, Berlin, Germany) dilution, cautiously layered on 70% Easycoll dilution, and then centrifuged. Leukocytes were extracted from the interlayer and washed. MLNs were isolated and passed through a cell strainer with a mesh size of 100 μ m and resuspended in PBS/FCS.

Flow Cytometry

Isolated LP and MLN leukocytes were incubated in an FC Receptor Block (Fc γ III/II receptor; clone 2.4G2) before surface markers were stained. Applied antibodies were FITC-labeled anti-mouse CD3 ϵ clone 145-2C11, anti-mouse CD19 clone 1D3, anti-

mouse CD49b/Pan-NK clone DX5, APC-labeled anti-mouse CD11c clone HL3, and PE-labeled anti-mouse CD103 clone M290, biotinylated anti-mouse CD11c clone HL3, anti-mouse CD40 clone 3/23, anti-mouse CD80 clone 16 to 10A1, anti-mouse CD86 clone GL1, anti-mouse MHCII clone AF6-120.1 (BD Bioscience), anti-mouse CCR7 clone 4B12, anti-mouse TLR2 clone 6C2, anti-mouse TLR4-MD2 complex clone MTS510, anti-mouse Rat IgG_{2a} K isotype, anti-mouse Rat IgG_{2b} K isotype (eBioscience). Specimens containing biotinylated antibodies were thereafter incubated with 1 μ L of second step fluorescence conjugate (Streptavidin-PE or Streptavidin-PerCP BD Bioscience). Samples were measured on a FACSCalibur or LSRFortessa (BD Bioscience, Heidelberg, Germany) using BD CellQuest Pro or BD FACSDIVA software, respectively. Data were analyzed with FlowJo 7.6.4 (TreeStar Inc., Ashland, OR). Forward and side scatter were used to exclude dead cells, cell debris, and cell aggregates for analysis. DCs were analyzed by electronically gating on Lin⁻ (CD3 ϵ , CD19, DX5) and CD11c⁺ cells, as indicated in respective figures.

Statistics

Statistical significances were calculated with Mann-Whitney test or one-way analysis of variance and Tukey's multiple comparison test. *P* values smaller than 0.05 were considered significant.

RESULTS

Increased Surface Expression of TLR2 and TLR4 on LPDCs During DSS Colitis

The DSS model resembles acute phase colitis and offers the possibility of gaining insights into mechanisms that influence and shape the immune response under inflammatory conditions. The induction of the TLR2 or TLR4 signaling cascades was demonstrated to be protective during DSS colitis.¹⁷ To address the influence of the TLR2 or TLR4 signal induction on disease development, we first elucidated whether DSS-induced intestinal inflammation alters TLR expression on lamina propria dendritic cells (LPDCs). LPDCs of healthy untreated mice (Mock) exhibited a very weak surface expression of TLR2 (Fig. 1A) and TLR4 (Fig. 1B). In contrast, LPDCs of mice suffering from intestinal inflammation after DSS administration demonstrated a significantly increased percentage of TLR2 (Fig. 1A) and TLR4 expression (Fig. 1B) when compared with untreated mice (Mock).

Epithelial TLR2/4 Signal Induction Promotes Intestinal Inflammation

Previous studies were not able to answer the question of whether it is important to induce the TLR signaling cascade in epithelial or in hematopoietic cells. Therefore, BMCM were generated and DSS-administered. Sufficiency of bone marrow depletion and transplantation was tested by flow cytometry (see Fig., Supplemental Digital Content 1, <http://links.lww.com/IBD/>

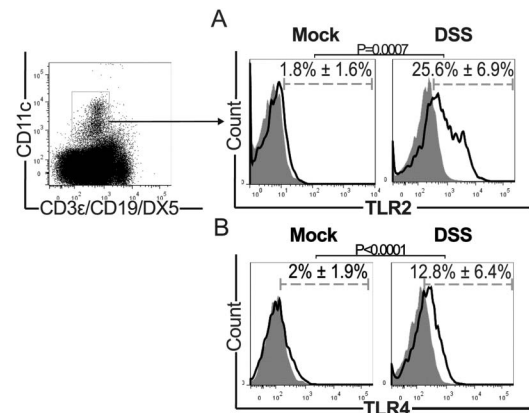
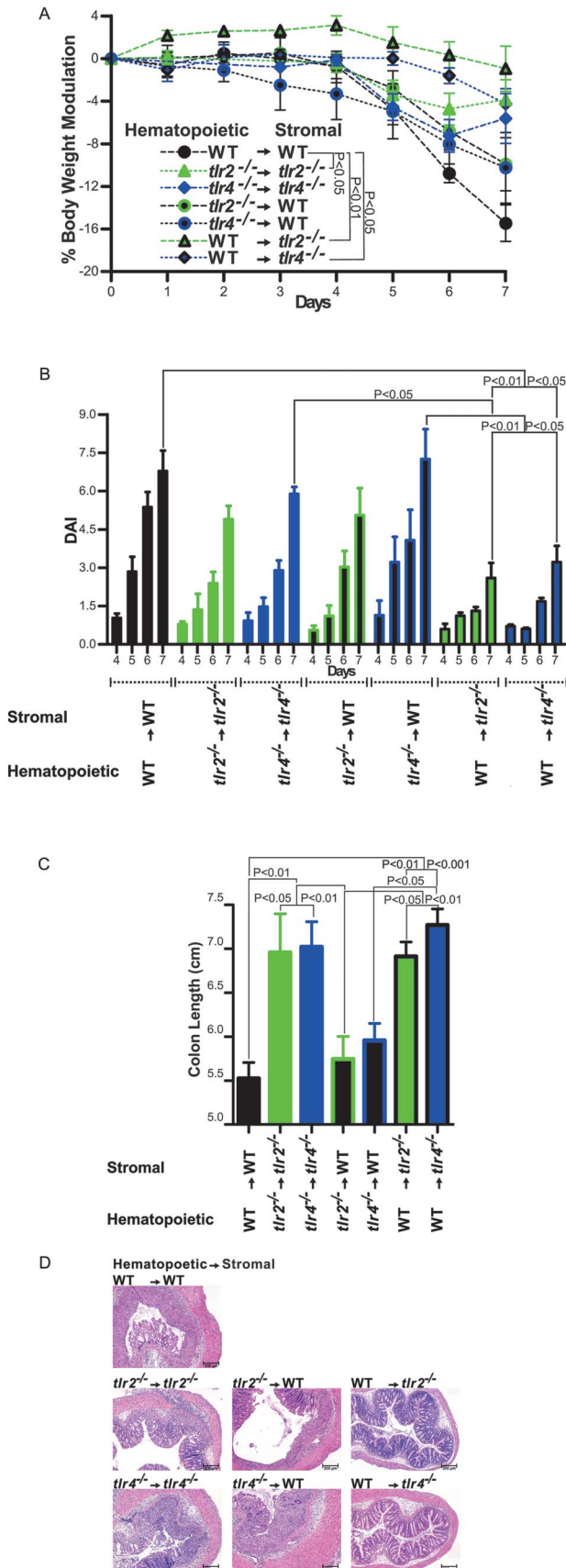


FIGURE 1. TLR expression of LPDCs. Histograms represent TLR2 (A) and TLR4 (B) (open histograms) surface expression of LPDCs of healthy mice (Mock) and DSS-administered mice with respective isotype controls (gray-filled histograms). Numbers indicate mean surface expression and SD in percentage. LPDCs were gated on CD3 ϵ , CD19, and DX5-negative and CD11c-positive cells as indicated in exemplary depicted dot plot. Significances were calculated using Mann-Whitney U test. Data represent at least 4 mice.

A749). WT mice were irradiated and received bone marrow cells of *tlr2*^{-/-} (*tlr2*^{-/-} → WT) or *tlr4*^{-/-} knockout mice (*tlr4*^{-/-} → WT) resulting in a deficiency in TLR2 or TLR4 expression on hematopoietic cells. In addition, *tlr2*^{-/-} (WT → *tlr2*^{-/-}) and *tlr4*^{-/-} knockout mice (WT → *tlr4*^{-/-}) were irradiated and transplanted with WT bone marrow cells, leading to an expression of TLR2 and TLR4 on hematopoietic cells, with intestinal epithelial cells lacking receptor expression. Irradiated (WT → WT), *tlr2*^{-/-} (*tlr2*^{-/-} → *tlr2*^{-/-}), and *tlr4*^{-/-} knockout mice (*tlr4*^{-/-} → *tlr4*^{-/-}) WT served as controls and were transplanted with genetically identical bone marrow cells. WT → WT mice exhibited a significantly higher body weight loss when compared with WT → *tlr4*^{-/-} and *tlr2*^{-/-} → *tlr2*^{-/-} mice (Fig. 2A, Table 1), whereas the body weight loss of *tlr2*^{-/-} → WT, *tlr4*^{-/-} → WT, and *tlr4*^{-/-} → *tlr4*^{-/-} lay in between (Fig. 2A, Table 1). The DAI of WT → *tlr2*^{-/-} mice was significantly reduced when compared with WT → WT, *tlr4*^{-/-} → WT, and *tlr4*^{-/-} → *tlr4*^{-/-} mice (Fig. 2B, Table 1). In addition, WT → *tlr4*^{-/-} mice exhibited a significantly decreased DAI when compared with WT → WT and *tlr4*^{-/-} → WT mice (Fig. 2B, Table 1), whereas the DAI of *tlr2*^{-/-} → *tlr2*^{-/-} and *tlr2*^{-/-} → WT mice did not significantly differ in comparison with remaining cohorts (Fig. 2B, Table 1). The colon length of WT → *tlr2*^{-/-} mice was in comparison with WT → WT and *tlr2*^{-/-} → WT mice significantly longer. Also, WT → *tlr4*^{-/-} mice were protected from a significant colon length loss when compared with WT → WT, *tlr2*^{-/-} → WT, and *tlr4*^{-/-} → WT mice (Fig. 2C, Table 1). Moreover, the colon of *tlr2*^{-/-} → *tlr2*^{-/-} and *tlr4*^{-/-} → *tlr4*^{-/-} mice was significantly longer when compared with *tlr2*^{-/-} → WT and WT → WT mice (Fig. 2C, Table 1).

As mentioned above, DSS administration results in histological changes in the intestine; therefore, BMCM mice were



analyzed for alterations in tissue structure. We observed weak changes of intestinal structure in WT → *tlr2*^{-/-} and WT → *tlr4*^{-/-} mice after DSS administration, whereas DSS administration to WT → WT, *tlr2*^{-/-} → *tlr2*^{-/-}, *tlr4*^{-/-} → *tlr4*^{-/-}, *tlr2*^{-/-} → WT, and *tlr4*^{-/-} → WT mice led to greater histological changes (Fig. 2D, Table 1).

Prevention of body weight loss, DAI, colon length loss, and histological changes in WT → *tlr2*^{-/-} and WT → *tlr4*^{-/-} mice indicate a proinflammatory function of TLR signal induction. In contrast, TLR2/4 cascade induction in hematopoietic cells seems to have an anti-inflammatory function because *tlr2*^{-/-} → *tlr2*^{-/-} and *tlr4*^{-/-} → *tlr4*^{-/-} mice also lack TLR expression on epithelial cells; however, these mice are not protected from symptoms of disease because of the additional lack of TLR signal induction on hematopoietic cells.

Attenuation of DSS Colitis by Induction of the TLR2/4 Signaling Cascade Is Associated with an Increase in CD103-expressing DCs

Next, we addressed whether the induction of the TLR2 and TLR4 signal cascade impacts the TLR expression, activation, and subset composition of LPDCs. Therefore, we first verified the differing potential of WT bacteria, initiating TLR signaling, and mutant strains, with impaired signal induction to prevent from intestinal inflammation. Before in vivo experiments were performed, mutant strains were tested in vitro. We investigated signal induction of the LP-Mut strain by stimulating HEK WT or TLR2

FIGURE 2. Epithelial TLR2/4 signal induction promotes intestinal inflammation. Graphs represent (A) modulation of initial body weight (B) disease activity index (DAI) (C) colon length, and (D) histological changes of DSS-administered irradiated WT mice transplanted with bone marrow cells of WT mice (WT → WT), black circles and black dashed line (A), black bars (B and C), DSS-administered irradiated *tlr2*^{-/-}-deficient mice transplanted with bone marrow cells of *tlr2*^{-/-}-deficient mice (*tlr2*^{-/-} → *tlr2*^{-/-}), green triangles and green dashed line (A), green bars (B and C), DSS-administered irradiated *tlr4*^{-/-}-deficient mice transplanted with bone marrow cells of *tlr4*^{-/-}-deficient mice (*tlr4*^{-/-} → *tlr4*^{-/-}), blue diamonds and blue dashed line (A), blue bars (B and C), DSS-administered irradiated WT mice transplanted with bone marrow cells of *tlr2*^{-/-}-deficient mice (*tlr2*^{-/-} → WT), black circles with green outline and black dashed line (A), black bars with green outline (B and C), DSS-administered irradiated WT mice transplanted with bone marrow cells of *tlr4*^{-/-}-deficient mice (*tlr4*^{-/-} → WT), black circles with blue outline and black dashed line (A), black bars with blue outline (B and C), DSS-administered irradiated *tlr2*^{-/-}-deficient mice transplanted with bone marrow cells of WT mice (WT → *tlr2*^{-/-}), green triangles with black outline and green dashed line (A), green bars with black outline (B and C), and DSS-administered irradiated *tlr4*^{-/-}-deficient mice transplanted with bone marrow cells of WT mice (WT → *tlr4*^{-/-}), blue diamonds with black outline and blue dashed line (A), blue bars with black outline (B and C). Significances were calculated using one-way analysis of variance and Tukey's multiple comparison test. Data represent at least 6 mice.

TABLE 1. Symptoms of DSS-induced Disease Intensity of BMCM

Genotype				
Donor → Recipient	Weight Modulation, %	DAI	Colon Length, cm	Histological Score
WT → WT	-15.5 ± 4.5 ^a	6.8 ± 2.3	5.5 ± 0.5 ^b	1.8 ± 1.0
<i>tlr2</i> ^{-/-} → <i>tlr2</i> ^{-/-}	-3.9 ± 5.0	4.9 ± 1.4	7.0 ± 1.2	1.5 ± 0.7
<i>tlr4</i> ^{-/-} → <i>tlr4</i> ^{-/-}	-5.6 ± 7.0	5.9 ± 0.8	7.0 ± 0.9	2.3 ± 0.4
<i>tlr2</i> ^{-/-} → WT	-9.9 ± 7.0	5.1 ± 3.2	5.7 ± 0.8 ^b	1.6 ± 1.2
<i>tlr4</i> ^{-/-} → WT	-10.3 ± 8.2	7.3 ± 3.1	6.0 ± 0.5 ^b	2.0 ± 0.6
WT → <i>tlr2</i> ^{-/-}	-0.9 ± 6.0	2.6 ± 1.7 ^c	6.9 ± 0.5	0.8 ± 1.0
WT → <i>tlr4</i> ^{-/-}	-5.1 ± 3.9	3.2 ± 1.7 ^c	7.3 ± 0.5	1.3 ± 0.8

Numbers indicate mean and SD of percent body weight modulation, DAI, colon length in centimeter, and histological scores of DSS-administered irradiated WT mice transplanted with bone marrow cells of WT mice (WT → WT), DSS-administered irradiated *tlr2*^{-/-}-deficient mice transplanted with bone marrow cells of *tlr2*^{-/-}-deficient mice (*tlr2*^{-/-} → *tlr2*^{-/-}), DSS-administered irradiated *tlr4*^{-/-}-deficient mice transplanted with bone marrow cells of *tlr4*^{-/-}-deficient mice (*tlr4*^{-/-} → *tlr4*^{-/-}), DSS-administered irradiated WT mice transplanted with bone marrow cells of *tlr2*^{-/-}-deficient mice (*tlr2*^{-/-} → WT), DSS-administered irradiated WT mice transplanted with bone marrow cells of *tlr4*^{-/-}-deficient mice (*tlr4*^{-/-} → WT), DSS-administered irradiated *tlr2*^{-/-}-deficient mice transplanted with bone marrow cells of WT mice (WT → *tlr2*^{-/-}), and DSS-administered irradiated *tlr4*^{-/-}-deficient mice transplanted with bone marrow cells of WT mice (WT → *tlr4*^{-/-}).

^aWT → WT versus *tlr2*^{-/-} → *tlr2*^{-/-}, WT → *tlr4*^{-/-} ($P < 0.05$), and WT → *tlr2*^{-/-} ($P < 0.01$).

^bWT → WT versus WT → *tlr2*^{-/-}, *tlr2*^{-/-} → *tlr2*^{-/-}, *tlr4*^{-/-} → *tlr4*^{-/-} ($P < 0.01$), and WT → *tlr4*^{-/-} ($P < 0.001$). *tlr2*^{-/-} → WT versus WT → *tlr2*^{-/-}, *tlr2*^{-/-} → *tlr2*^{-/-} ($P < 0.05$), WT → *tlr4*^{-/-}, and *tlr4*^{-/-} → *tlr4*^{-/-} ($P < 0.01$). *tlr4*^{-/-} → WT versus WT → *tlr4*^{-/-} ($P < 0.05$). Data represent at least 6.

^cWT → *tlr2*^{-/-} versus WT → WT, *tlr4*^{-/-} → WT ($P < 0.01$), and *tlr4*^{-/-} → *tlr4*^{-/-} ($P < 0.05$). WT → *tlr4*^{-/-} versus WT → WT and *tlr4*^{-/-} → WT ($P < 0.05$).

and TLR6 overexpressing HEK cells for 24 hours with PBS (Mock), LP, or LP-Mut with a bacteria to cell ratio of 100, by determining the IL-8 concentrations in cell culture supernatants (see Fig. A, Supplemental Digital Content 2, <http://links.lww.com/IBD/A750>, and see Table, Supplemental Digital Content 3, <http://links.lww.com/IBD/A751>). Stimulation of HEK WT cells did not induce IL-8 secretion, whereas stimulation of HEK TLR2/6 overexpressing HEK cells with LP results in a significantly increased concentration of IL-8 in cell culture supernatants when compared with PBS-stimulated (Mock) and LP-Mut-stimulated TLR2/6 overexpressing HEK cells.

Moreover, we used TLR4 surface expression of bone marrow-derived DCs (BMDCs) to elucidate the impaired capacity of EC-Mut to induce the signaling cascade because successful induction results in the internalization of the receptor.²⁹ Therefore, BMDCs were stimulated with PBS (Mock), EC, or EC-Mut with bacteria to cell ratio of 1. After 24 hours, TLR4 surface expression was determined through flow cytometry. Indeed, only BMDCs stimulated with EC exhibited a significantly decreased surface expression of TLR4 when compared with Mock cells and EC-Mut stimulated cells (see Fig. B, Supplemental Digital Content 4, <http://links.lww.com/IBD/A750>). These results demonstrate differences between the capacities of bacteria to initiate signaling. For in vivo experiments, a setup of 5 different cohorts was used. The first cohort served as a positive control for the development of intestinal inflammation and consisted of C57BL/6 mice with DSS administration only (DSS). DSS-administered and *E. coli* JM83-fed C57BL/6 mice (DSS+EC) were cohort 2, DSS-administered and *E. coli* JM83 Δ *htrB* *htrB*_{pg}-fed C57BL/6 mice (DSS+EC-Mut) were cohort 3, DSS-administered and *L. plantarum*

WCFS1-fed C57BL/6 mice (DSS+LP) were cohort 4, and cohort 5 was composed of DSS-administered and *L. plantarum* Δ *dlxX-D*-fed C57BL/6 mice (DSS+LP-Mut). Onset and development of intestinal inflammation in mice were determined by daily monitoring of the body weight development. DSS-administered and EC-fed mice lost significantly less weight when compared with DSS-administered and with DSS-administered and EC-Mut-fed mice (Fig. 3A, Table 2). DSS-administered and LP-fed mice were also protected from colitis as indicated by body weight measurements in DSS-administered, DSS-administered and LP-Mut-fed and DSS-administered and EC-Mut-fed mice (Fig. 3A, Table 2). In addition, DAI was determined daily. DSS-administered and EC-fed mice displayed a significantly decreased DAI value as compared with DSS-administered, DSS-administered and EC-Mut-fed, and DSS-administered and LP-Mut-fed mice (Fig. 3B, Table 2). Feeding of LP to mice during DSS administration led to a significant decrease of the DAI as compared with DSS-administered, DSS-administered and EC-Mut-fed, and DSS-administered and LP-Mut-fed mice (Fig. 3B, Table 2).

Strong intestinal inflammation, induced by DSS treatment, leads to colon shortening. Therefore, colon length is a benchmark for severity of disease. After mice were killed, colon length was determined. DSS-administered and EC-fed mice featured a significantly longer colon as compared with DSS-administered, DSS-administered and EC-Mut-fed, as well as DSS-administered and LP-Mut-fed mice (Fig. 3C, Table 2). In line with this, LP-fed and DSS-administered mice revealed a significantly longer colon in comparison with DSS-administered, DSS-administered and EC-Mut-fed, as well as DSS-administered and LP-Mut-fed mice (Fig. 3C, Table 2).

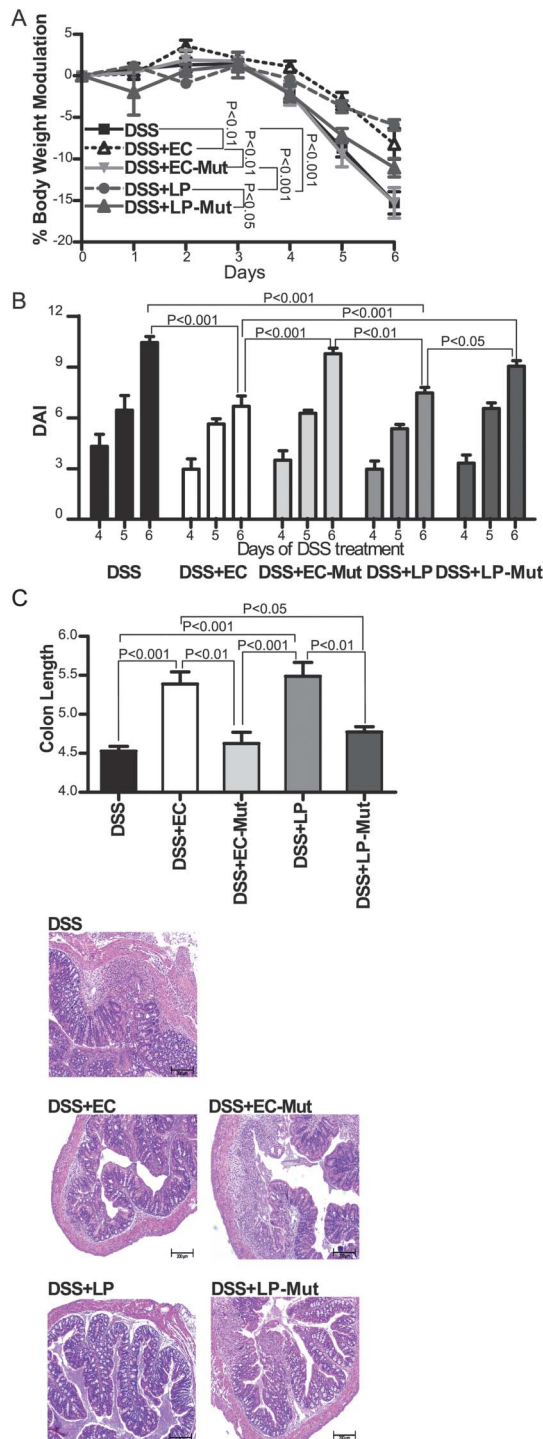


FIGURE 3. TLR2/4 signal induction attenuates symptoms of DSS colitis. Graphs represent (A) modulation of initial body weight (B) DAI (C) colon length, and (D) histological changes of DSS-administered [DSS, solid black line and squares (A), black bars (B and C) and (D)], DSS-administered and *E. coli* JM83-fed [DSS+EC, white triangles and black dashed line (A), white bars (B and C) and (D)], DSS-administered and *E. coli* JM83 Δ trb htrB_{pg}-fed [DSS+EC-

Mut (A), light gray downward triangles and solid line, light gray bars (B and C) and (D)], DSS-administered and *L. plantarum* WCFSI [DSS+LP, dark gray circles and dashed line (A), gray bars (B and C) and (D)], and DSS-administered and *L. plantarum* Δ dltX-D-fed mice [DSS+LP-Mut, dark gray solid line and triangles (A), dark gray bars (B and C) and (D)]. Significances were calculated using one-way analysis of variance and Tukey's multiple comparison test. Data represent at least 5 mice.

To evaluate the histological changes that are commonly observed in DSS-caused intestinal inflammation, colonic sections were made and scored for histological changes as previously described.²⁷ DSS-administered, DSS-administered and EC-Mut-fed, as well as DSS-administered and LP-Mut-fed mice (Fig. 3D, Table 2) exhibited greater leukocyte infiltrations, loss of goblet cells, epithelial disruption, hyperplasia of crypts, and ulcerations when compared with DSS-administered and EC-fed as well as DSS-administered and LP-fed mice (Fig. 3D, Table 2). Fecal colony forming units were determined to rule out that observed differences between WT and mutant bacteria in prevention of disease is a result of differential bacterial survival. Results demonstrate comparable amounts of colony forming units of *Enterobacteriaceae* (in log₁₀) in the feces of DSS-administered mice (7.4 ± 1.7), DSS-administered and EC-fed (7.6 ± 1.7), and DSS-administered and EC-Mut-fed mice (7.2 ± 2) (see Fig. A, Supplemental Digital Content 5, <http://links.lww.com/IBD/A752>). In contrast, colony forming units of lactobacilli (log₁₀) were significantly increased in DSS-administered and LP-fed (8.0 ± 0.2) and DSS-administered and LP-Mut-fed mice (8.6 ± 0.5) when compared with DSS-administered mice (7.0 ± 1.1) (see Fig. B, Supplemental Digital Content 6, <http://links.lww.com/IBD/A752>). Prevention of body weight loss, DAI, colon length loss, and histological changes in the colon after feeding of WT bacteria demonstrates a beneficial function of TLR2/4 signal cascade induction during DSS-caused intestinal inflammation.

To elucidate the prevention of DSS-induced disease by induction of the TLR2 or TLR4 signaling cascade, LPDCs were isolated. The influence of DCs on intestinal inflammation is not fully understood because depletion of DCs during DSS colitis was demonstrated to attenuate and exacerbate intestinal inflammation.^{20,21} Next, we addressed whether efficient versus malfunctioning TLR2/4 induction of signaling impacts on TLR2 and TLR4 expression on LPDCs. To analyze DCs only, flow cytometry analyses were restricted to CD11c⁺Lin⁻ cells (Fig. 4A). DSS-induced intestinal inflammation had no influence on the percent frequency of LPDCs because mice suffering from intense intestinal inflammation (DSS 1.6% ± 0.6%, DSS+EC-Mut 1.6% ± 0.5%, DSS+LP-Mut 1.6% ± 0.5%) exhibited comparable percentages as healthy mice (Mock 1.2% ± 0.5%) and mice, which were protected from inflammation (DSS+EC [2.2% ± 1.4%], DSS+LP [1.9% ± 1.0%]) (Fig. 4B). Untreated Mock mice exhibited a significantly reduced percentage of TLR2-expressing LPDCs as compared with DSS-administered,

TABLE 2. Symptoms of DSS-induced Disease Intensity

Treatment	Weight Modulation, %	DAI	Colon Length, cm	Histological Score
DSS	-15.3 ± 4.4	10.4 ± 1	4.5 ± 0.2	1.2 ± 0.6
DSS+EC	-8.2 ± 5.2 ^a	6.7 ± 1.9 ^b	5.4 ± 0.4 ^c	1.0 ± 0.8
DSS+EC-Mut	-15.3 ± 5.5	9.8 ± 1	4.7 ± 0.4	1.4 ± 0.5
DSS+LP	-5.9 ± 2.3 ^a	7.5 ± 1.1 ^b	5.5 ± 0.5 ^c	0.7 ± 0.5
DSS+LP-Mut	-10.5 ± 3.9	9.0 ± 1.1	4.8 ± 0.2	1.2 ± 0.9

Numbers indicate mean and SD of percent body weight modulation, DAI, colon length in centimeter, and histological scores of DSS-administered, DSS-administered and *E. coli* JM83-fed (DSS+EC), DSS-administered and *E. coli* JM83 Δ htrB htrB_{P_g-fed (DSS+EC-Mut), DSS-administered and *L. plantarum* WCFS1-fed (DSS+LP), as well as DSS-administered and *L. plantarum* Δ dltX-D-fed mice (DSS+LP-Mut).}

^aDSS+EC versus DSS and DSS+EC-Mut ($P < 0.01$), DSS+LP versus DSS+LP-Mut ($P < 0.05$), DSS and DSS+EC-Mut ($P < 0.001$).

^bDSS+EC versus DSS, DSS+EC-Mut, and DSS+LP-Mut ($P < 0.001$). DSS+LP versus DSS ($P < 0.001$), DSS+EC-Mut ($P < 0.01$), and DSS+LP-Mut ($P < 0.05$).

^cDSS+EC versus DSS ($P < 0.001$), DSS+EC-Mut ($P < 0.01$), and DSS+LP-Mut ($P < 0.05$). DSS+LP versus DSS, DSS+EC-Mut ($P < 0.001$), and DSS+LP-Mut ($P < 0.01$). Data represent at least 5 mice.

DSS-administered and LP-fed, as well as DSS-administered and LP-Mut-fed mice. Moreover, DSS-administered mice demonstrated a significantly decreased percentage of TLR2-positive LPDC as compared with DSS-administered and LP-Mut-fed mice. TLR2 surface expression of DCs is not influenced by ligand recognition.³⁰ In line with this, DSS+LP and DSS+LP-Mut mice exhibited comparable TLR2 expression (Fig. 4B).

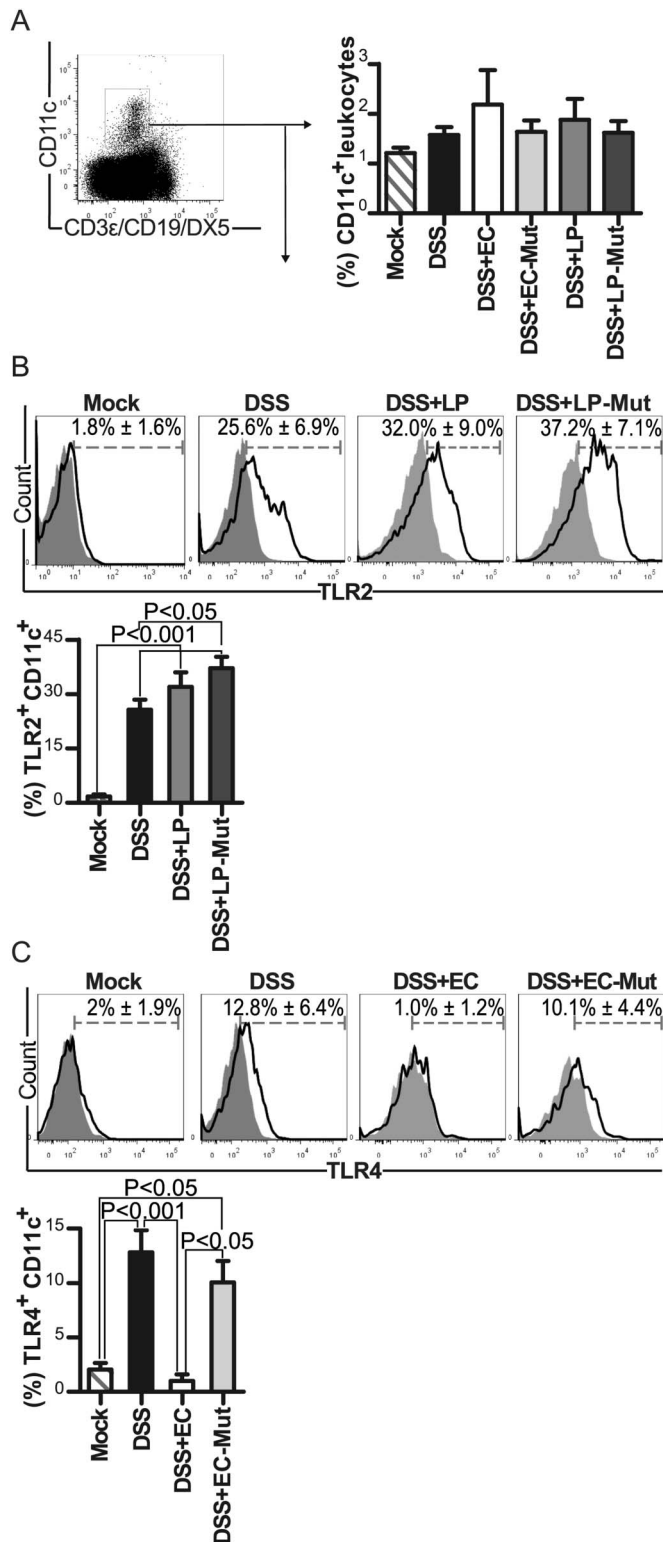
Untreated Mock mice as well as DSS-administered and EC-fed mice exhibited a significantly lower percentage of TLR4-positive LPDCs as compared with DSS-administered as well as DSS-administered and EC-Mut-fed mice (Fig. 4C).

Increased activation levels of LPDCs are connected to intestinal inflammation.¹¹ Therefore, we elucidated the expression of the activation marker (MHCII), the costimulatory molecules (CD40, CD80, and CD86), and the migration marker CCR7. Indeed, healthy mice (Mock) exhibited a significantly reduced state of activation when compared with DSS-administered, DSS-administered and EC-fed, DSS-administered and EC-Mut-fed, DSS-administered and LP-fed mice, as well as DSS-administered and LP-Mut-fed mice (Fig. 5A–E). Although DSS-induced intestinal inflammation led to a greater state of activation in LPDCs, the effect was even more pronounced after bacterial feeding, indicated by an significantly increased expression of markers in DSS-administered and EC-fed, DSS-administered and EC-Mut-fed, DSS-administered and LP-fed, as well as DSS-administered and LP-Mut-fed mice when compared with DSS-administered mice (Fig. 5A–E).

LPDCs of DSS-administered mice fed with mutant bacteria (EC-Mut, LP-Mut) and suffering from intense intestinal inflammation, exhibited a comparable state of activation as LPDCs of DSS-administered and WT bacteria fed mice (EC, LP), which did not exhibit symptoms of disease. These observations indicate that a differing state of LPDC activation does not underlie the TLR2/4 signal induction-mediated amelioration of disease.

The function of TLR2 or TLR4 signal induction during DSS-induced intestinal inflammation was more precisely

elucidated through an analysis of the composition of DC subsets using flow cytometry. CD103-expressing DCs were of especial interest because these cells are believed to be important in maintaining the intestinal homeostasis and in fulfilling anti-inflammatory functions.³¹ Flow cytometry analysis demonstrated that the frequency of CD103-expressing LPDCs in DSS-administered and EC-fed mice is significantly higher as compared with untreated Mock, DSS-administered, DSS-administered and EC-Mut-fed, as well as DSS-administered and LP-Mut-fed mice (Fig. 6A). Also, feeding of LP during DSS administration resulted in a significant increase in CD103-expressing LPDCs when compared with untreated Mock, DSS-administered, as well as DSS-administered and EC-Mut-fed mice (Fig. 6A). According to the increase in CD103-expressing cells, DSS-administered and EC-fed mice possessed a significantly decreased frequency of CD103-negative LPDCs as compared with untreated Mock, DSS-administered, DSS-administered and EC-Mut-fed, as well as DSS-administered and LP-Mut-fed mice (Fig. 6A). The same can be applied to DSS-administered and LP-fed mice, which exhibited a significant reduction in CD103-negative LPDC frequency when compared with untreated Mock, DSS-administered, as well as DSS-administered and EC-Mut-fed mice (Fig. 6A). To investigate the influence of bacterial feeding on general frequency of CD103-positive cells, MLN DCs were also analyzed by flow cytometry. DSS-administered mice revealed a significantly reduced percentage of CD103-expressing MLNDCs as compared with untreated Mock, DSS-administered and EC-fed, DSS-administered and EC-Mut-fed, as well as DSS-administered and LP-fed mice (Fig. 6B). DSS-administered and LP-Mut-fed mice also displayed a significantly reduced percentage of CD103-positive MLNDCs as compared with untreated Mock, DSS-administered and EC-fed, DSS-administered and EC-Mut-fed, as well as DSS-administered and LP-fed mice (Fig. 6B). Conversely, DSS-administered mice exhibited a significantly increased frequency of CD103-negative MLNDCs when compared with Mock, DSS-administered and EC-fed, DSS-administered and EC-Mut-fed, as



well as DSS-administered and LP-fed mice (Fig. 6B). Again, DSS-administered and LP-Mut-fed mice also demonstrated a significantly increased percentage of CD103-negative MLNDCs as compared with untreated Mock, DSS-administered and EC-fed, DSS-administered and EC-Mut-fed, as well as DSS-administered and LP-fed mice (Fig. 6B).

The fact that CD103-expressing DCs are only increased in mice in which disease was prevented (DSS+EC, DSS+LP) and not in mice with intestinal inflammation (DSS, DSS+EC-Mut, DSS+LP-Mut) indicates an anti-inflammatory function of these cells during inflammation.

Amelioration of WT Bacteria Relies on TLR2/4 Signal Induction in Hematopoietic Cells

To address whether successful signaling induction by WT bacteria has to happen in the hematopoietic compartment, we irradiated WT mice and transplanted these with bone marrow of TLR2/TLR4 double knockout mice (*tlr2/4*^{-/-} → WT) resulting in intact TLR-signaling in stromal cells only. We administered mice either DSS alone or we fed mice with wild-type EC or LP and administered DSS. Feeding of bacteria to mice lacking TLR2/4 on immune cells failed to prevent of loss of body weight (Fig. 7A, Table 3), signs of disease (Fig. 7B, Table 3), and histological changes (Fig. 7D, Table 3). Only colon length loss was decreased in DSS-administered and EC-fed *tlr2/4*^{-/-} → WT mice (Fig. 7C, Table 3). The absence of bacteria-mediated amelioration of disease demonstrates a crucial role for signal-induction in immune cells.

Our results clearly demonstrate that induction of the TLR2/4 signaling cascade resulted in amelioration of disease. In addition,

FIGURE 4. Bacterial feeding results in altered TLR expression of LPDCs. A, LPDCs were gated on CD3ε, CD19, and DX5-negative and CD11c-positive cells as indicated in exemplary depicted dot plot. Graph represents LPDC frequencies in percent of healthy (Mock, gray striped bar), DSS-administered (DSS, black bar), DSS-administered and *E. coli* JM83-fed (DSS+EC, white bar), DSS-administered and *E. coli* JM83 Δ *htrB htrB_{P_g}*-fed (DSS+EC-Mut, light gray bar), DSS-administered and *L. plantarum* WCFS1-fed (DSS+LP, gray bar), as well as DSS-administered and *L. plantarum* Δ *dltX-D*-fed mice (DSS+LP-Mut, dark gray bar). B, Histograms and graph represent TLR2 surface expression (open histograms) of LPDCs of healthy mice (Mock, gray striped bar), DSS-administered mice (DSS, black bars), DSS-administered and *L. plantarum* WCFS1-fed (DSS+LP, gray bar), as well as DSS-administered and *L. plantarum* Δ *dltX-D*-fed mice (DSS+LP-Mut, dark gray bar) with respective isotype controls (gray-filled histograms). C, Histograms and graph represent TLR4 surface expression (open histograms) of LPDCs of healthy mice (Mock, gray striped bar), DSS-administered mice (DSS, black bars), DSS-administered and *E. coli* JM83-fed (DSS+EC, white bar), DSS-administered and *E. coli* JM83 Δ *htrB htrB_{P_g}*-fed (DSS+EC-Mut, light gray bar) with respective isotype controls (gray-filled histograms). Numbers indicate mean surface expression and SD in percentage. LPDCs were gated on CD3ε, CD19, and DX5-negative and CD11c-positive cells as indicated in exemplary depicted dot plot. Significances were calculated using one-way analysis of variance and Tukey's multiple comparison test. Data represent at least 4 mice.

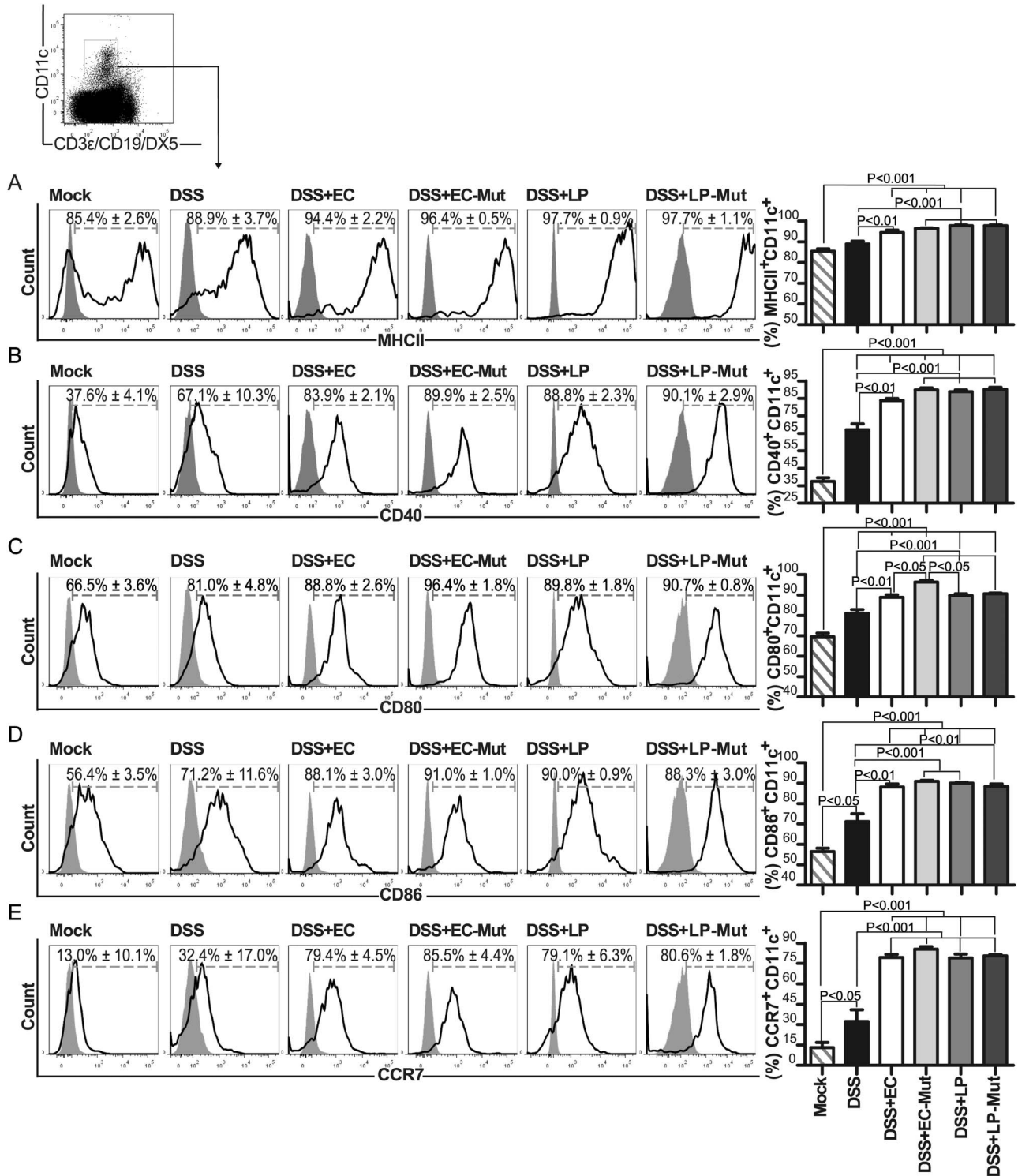


FIGURE 5. State of LPDC activation. LPDCs were gated on CD3ε, CD19, and DX5-negative and CD11c-positive cells as indicated in exemplary depicted dot plot. Histograms and graphs indicate MHC class II (MHCII), A, CD40, B, CD80, C, CD86, D, and CCR7, and (E), surface expression (open histograms) and respective fluorescence minus one control (gray-filled histograms) of healthy (Mock, gray striped bar), DSS-administered (DSS, black bar), DSS-administered and *E. coli* JM83-fed (DSS+EC, white bar), DSS-administered and *E. coli* JM83 Δ trbB trbP_g-fed (DSS+EC-Mut, light gray bar), DSS-administered and *L. plantarum* WCFS1-fed (DSS+LP, gray bar), as well as DSS-administered and *L. plantarum* Δ dltX-D-fed mice (DSS+LP-Mut, dark gray bar). Numbers indicate mean surface expression and SD in percent. Significances were calculated using one-way analysis of variance and Tukey's multiple comparison test. Data represent at least 4 mice.

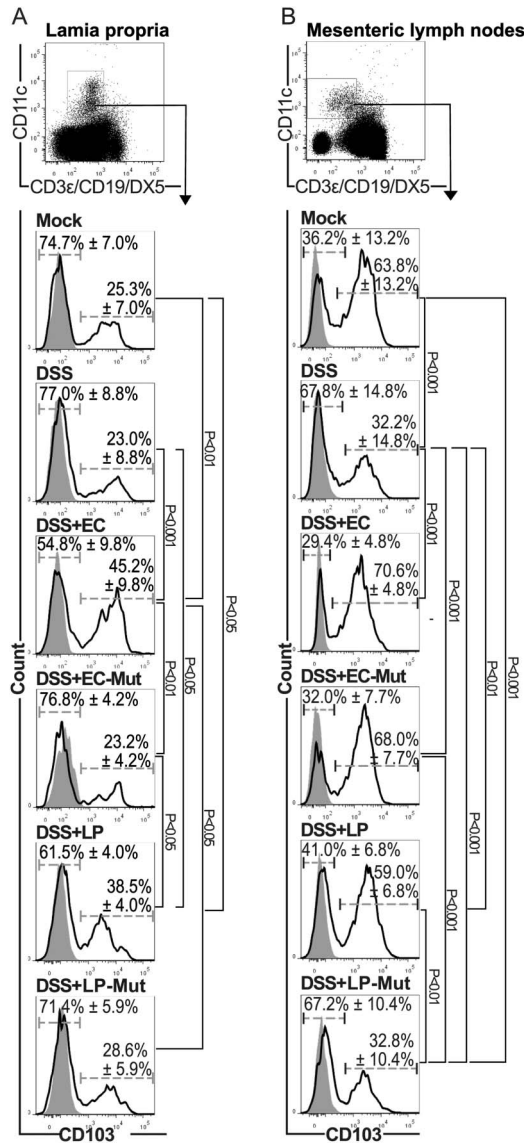


FIGURE 6. Frequencies of CD103⁺ LP and MLN DCs. A, LP and MLN DCs were gated on CD3 ϵ , CD19, and DX5-negative and CD11c-positive cells as indicated in exemplary depicted dot plots. Histograms indicate CD103-expressing LP (A) and MLN DCs (B) (open histogram) and respective fluorescence minus one control of healthy (Mock), DSS-administered (DSS), DSS-administered and *E. coli* JM83-fed (DSS+EC), DSS-administered and *E. coli* JM83 Δ *htrB htrB_{pg}-fed (DSS+EC-Mut), DSS-administered and *L. plantarum* WCFS1-fed (DSS+LP), as well as DSS-administered and *L. plantarum* Δ *dltX-D*-fed mice (DSS+LP-Mut). Numbers indicate mean surface expression and SD in percent of CD103-expressing LP (A) and MLN DCs (B) and CD103⁻ LP (A) and MLN DCs (B). Significances were calculated using one-way analysis of variance and Tukey's multiple comparison test. Data represent at least 4 mice.*

our data indicate that it is important in which cell type TLR2/4 signaling is initiated because the induction in epithelial cells seems to be detrimental, whereas induction in hematopoietic cells might be beneficial. However, efficient versus malfunctioning signal

induction had no influence on maturation of LPDCs, whereas LPDC subset composition was influenced. Thus, successful induction of the TLR2/4 cascade resulted in an increase in CD103-expressing DCs, which may ameliorate disease.

DISCUSSION

The fact that patients with IBD harbor an altered intestinal microbiota implies an active role of the microbiota in disease development.³² One influencing factor might be to what extent the resident microbiota is able to initiate TLR signaling. We only observed amelioration of DSS-induced intestinal inflammation by feeding mice WT bacteria, indicating that the initiation of beneficial pathways is mediated through the TLR2/4 signaling cascade in immune cells because this effect was absent in BMCM lacking TLR2/4 on hematopoietic cells.

Moreover, depletion of anaerobic bacteria resulted in amelioration of DSS-induced inflammation, whereas eradication of aerobic bacteria exhibited no effect.³³ This differential outcome might depend on the fact that anaerobic bacteria fail to elicit TLR responses,³⁴ whereas recognition of aerobic bacteria results in a strong induction of the TLR pathway. A previous study also observed TLR-mediated amelioration of disease by administration of TLR ligands to commensal depleted mice.¹⁷ In contrast to our experiment, this study does not include the complete microbiota in disease development and additionally antibiotic treatment itself is able to impact on the host's immune response.³⁵ To unravel the function of TLR signaling cascade in IBD, it is important to include the effect of the complete microbiota. Recognition of microbial-associated molecular patterns at once with TLR ligands are likely to shape signal induction, because, e.g., initiation of the NOD2 signal cascade after ligand recognition results in the employment of signaling molecules that also involved in TLR signal transduction.³⁶ In addition, changes in gut microbiota metabolites such as reduced amounts of short chain fatty acids³⁷ might influence the establishing TLR response and need to be considered.

Our experiments demonstrated that the lack of TLR2/4 cascade induction in stromal cells prevented DSS-induced symptoms of disease. By contrast, induction of TLR2/4 signal cascade in hematopoietic cells might be beneficial, as mice lacking the receptors here suffer from intestinal inflammation. Intestinal epithelial cells express TLR4 intracellular^{38,39}; therefore, signal-induction occurs exclusively intracellular. Previous work demonstrates that extracellular signal recognition results in signal transmission through Myd88, whereas recognition of TLR4 in endosomes results in signal transduction by Trif.⁴⁰ The differential employment of signaling pathways might be responsible for differing disease outcome. In contrast to our results, previous studies connect TLR responses to multiple beneficial functions in stromal cell types, e.g., follicle-associated epithelial cells sample luminal antigens with increasing frequency after TLR2 and TLR4 ligand administration⁴¹ and in Paneth cells ligand recognition results in secretion of anti-microbial compounds.⁴² Moreover, TLR signal

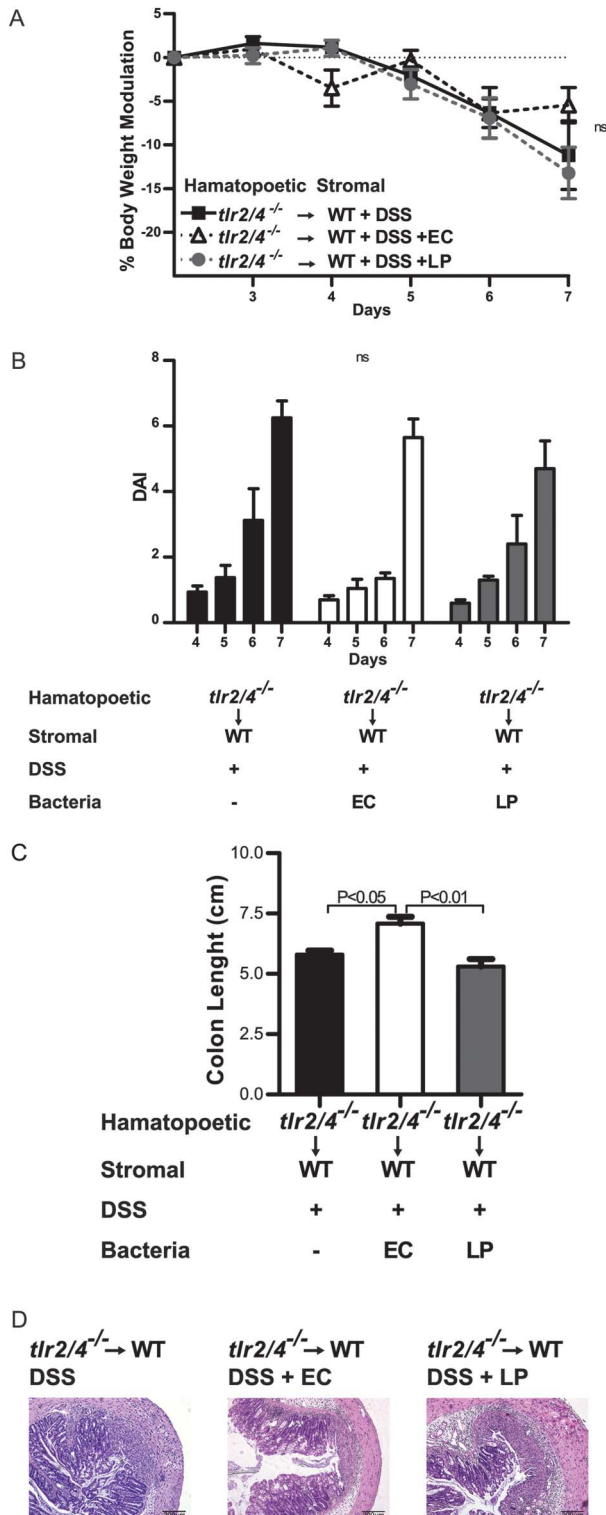


FIGURE 7. Lack of TLR2/4 signal induction on hematopoietic cells Abrogates bacteria-mediated protection. Graphs represent (A) modulation of initial body weight, (B) DAI, (C) colon length, and (D) histological changes of DSS-administered irradiated WT mice transplanted with bone marrow cells of $tlr2/4^{-/-}$ -deficient mice

cascade initiation in intestinal epithelial cells leads to an increase in intestinal barrier function by preventing inflammation by anti-inflammatory proliferator-activated receptor- γ ,⁴³ by maintaining tight junctions, preventing intestinal epithelial cell apoptosis,⁴⁴ and inducing intestinal epithelial cell growth.⁴⁵

DCs orchestrate immunity throughout the entire organism. For this reason, there is great interest in discovering to what extent DCs are involved in TLR signaling-mediated prevention of DSS-induced disease. The loss of the intestinal barrier function after DSS administration might allow LPDCs to gain greater access to luminal antigens. The increased antigen contact resulted in an enhanced expression of activation and migration markers on LPDCs as compared with healthy controls. In addition, feeding of bacteria increased the expression of maturation and migration markers compared with DSS-administered mice. The differences in the expression of these markers might depend on the fact that LPDCs better recognize fed bacteria than resident microbiota. Studies dealing with chronic intestinal inflammation models suggest that enhanced DC activation promotes disease development. In *il-2*-deficient mice *E. coli* monocolonization results in the development of colitis, whereas *Bacteroides vulgatus* monocolonized mice remained healthy.⁴⁶ LPDCs of *E. coli* monocolonized mice have an increased expression of activation markers compared with healthy germ-free and *B. vulgatus* monocolonized mice.¹¹ Yet, the state of DC activation, which is defined by the high expression of activation markers, does not always reflect immunologic potential. This difference is demonstrated by DCs that are able to induce proliferation of CD4⁺-naïve T cells but not the differentiation into effector T-helper cell types.⁴⁷ In addition, DCs rely on the expression of activation markers to fulfill their tolerogenic tasks.⁴⁸ The studies mentioned above lead us to the conclusion that despite the similar maturation states of LPDCs of bacterial-fed cohorts, cells might respond differently. Less severe intestinal inflammation in DSS-administered and WT bacteria-fed mice might depend on the initiation of altered immune responses by LPDCs as compared with DSS-administered and mutant bacteria-fed mice.

Indeed, in vitro stimulation of bone marrow-derived macrophages and DCs with TLR4 ligand demonstrates that upon LPS restimulation, genes are categorized as inducible and irresponsive.^{30,49,50} The potential to be responsive depends on a first stimulation, which mediates chromatin modifications. Proinflammatory genes compose large parts of the irresponsive class, whereas the inducible class hardly contains proinflammatory genes. Examples

($tlr2/4^{-/-} \rightarrow$ WT+DSS), black squares and black line (A), black bars (B and C), DSS-administered and *E. coli* JM83-fed irradiated WT mice transplanted with bone marrow cells of $tlr2/4^{-/-}$ -deficient mice ($tlr2/4^{-/-} \rightarrow$ WT+DSS+EC), white triangles and black dashed line (A), white bars (B and C), and DSS-administered and *L. plantarum* WCFS1-fed irradiated WT mice transplanted with bone marrow cells of $tlr2/4^{-/-}$ -deficient mice ($tlr2/4^{-/-} \rightarrow$ WT+DSS+LP), grey circles and grey dashed line (A), grey bars (B and C). Significances were calculated using one-way analysis of variance and Tukey's multiple comparison test. Data represent at least 4 mice.

TABLE 3. Symptoms of DSS-induced Disease Intensity of Bacteria-fed BMCM

Genotype	Bacterial Feeding	Weight Modulation, %	DAI	Colon Length, cm	Histological Score
Donor → Recipient					
<i>tlr2/4</i> ^{-/-} → WT		-11.2 ± 6.8	6.3 ± 1.0	5.8 ± 0.3	2.2 ± 0.6
<i>tlr2/4</i> ^{-/-} → WT	EC	-5.5 ± 4.0	5.6 ± 1.3	7.1 ± 0.6 ^a	1.2 ± 0.7
<i>tlr2/4</i> ^{-/-} → WT	LP	-13.2 ± 5.9	4.7 ± 1.9	5.3 ± 0.6	1.8 ± 0.8

Numbers indicate mean and SD of percent body weight modulation, DAI, colon length in centimeter, and histological scores of DSS-administered irradiated WT mice transplanted with bone marrow cells of *tlr2/4*^{-/-}-deficient mice (*tlr2/4*^{-/-} → WT+DSS), DSS-administered and *E. coli* JM83-fed irradiated WT mice transplanted with bone marrow cells of *tlr2/4*^{-/-}-deficient mice (*tlr2/4*^{-/-} → WT+DSS+EC), and DSS-administered and *L. plantarum* WCFS1-fed irradiated WT mice transplanted with bone marrow cells of *tlr2/4*^{-/-}-deficient mice (*tlr2/4*^{-/-} → WT+DSS+LP).

^a*tlr2/4*^{-/-} → WT+DSS+EC versus *tlr2/4*^{-/-} → WT+DSS ($P < 0.05$) and *tlr2/4*^{-/-} → WT+DSS+LP ($P < 0.01$). Data represent at least 4 mice.

of inducible genes are the TLR signaling inhibitor *irak-m* and the cathelicidin-related antimicrobial peptide.⁴⁹

Additionally, the categorization into inducible and irresponsive genes is shown by experiments using BMDCs. In this study, a high dose of TLR2 or TLR4 ligand leads to cell maturation and, upon restimulation, mature cells secrete IL-6 but not TNF- α .³⁰

Moreover, after TLR restimulation BMDCs secrete increased amounts of anti-inflammatory IL-10, whereas secretion of proinflammatory IL-12p40 is diminished.⁵⁰

The administration of DSS might first generate proinflammatory conditions. However, the additional feeding of WT bacteria may lead to a repetitive induction of the TLR2/4 signaling cascade in LPDCs, which might induce a change of cell type from pro- to anti-inflammatory, whereas LPDCs of DSS-administered and mutant bacteria-fed mice become activated and remain proinflammatory. This fact may contribute to stronger intestinal inflammation as compared with DSS-administered and WT bacteria-fed mice.

Besides DC maturation, the composition of LPDC subsets is important here. We observed an increase in CD103-expressing DCs in mice which were protected from DSS-induced inflammation. Accordingly, DSS administration results in more severe inflammation in mice which feature high percentages of CX₃CR1-positive and low percentages of CD103-positive LPDCs.⁵¹

Upon antigen contact, CD103-expressing cells migrate to the MLNs.⁵² Considering the high migratory capacity of CD103-expressing LPDCs, we conclude that TLR2/4 signal induction in DSS-administered and WT bacteria-fed mice results in great intestinal onsite development of CD103-expressing cells because these mice have high frequencies in both the LP and the MLNs. In contrast, homeostatic conditions in healthy mice require less onsite development and, paired with steady-state migration to MLNs, results in a low frequency of CD103⁺ LPDC.

In this model, the beneficial effect of CD103⁺ DCs might rely on their ability to induce regulatory T cells by the secretion of TGF- β and retinoic acid.⁵³ Moreover, CD103⁺ intestinal DCs express indoleamine-2,3-dioxygenase 1 (IDO1), which exerts an anti-inflammatory influence in the murine and human intestine.⁵⁴

We demonstrate that induction of the TLR2/4 signaling cascade resulted in amelioration of disease. Moreover, initiation of

TLR2/4 signaling seems to have differing functions depending on cell types. Our results indicate that TLR signal induction in hematopoietic cells might be beneficial, although detrimental in epithelial cells.

From these results, we conclude that during DSS-induced intestinal inflammation, recognition of TLRs may lead to the development of CD103-expressing LPDCs, which might be responsible for amelioration of intestinal inflammation by the induction of regulatory T cells.

Furthermore, during DSS administration, the employment of the TLR2/4 signaling pathway leads to maturation of LPDCs. Maturation may result in a proinflammatory phenotype of cells. However, later repetitive induction of the TLR2/4 signaling cascade might result in a program change from pro- to anti-inflammatory LPDCs.

The increase in CD103-expressing DCs and the anti-inflammatory DC phenotype have led us to the hypothesis that during inflammation, the upregulation of TLRs might function as a counterregulatory mechanism. This may happen to change the proinflammatory potential of the TLR signal cascade, which results in amelioration of disease by the induction of beneficial pathways.

The observed mechanisms might also account for patient with IBD to maintain the immune balance; however, counterregulatory functions of TLR cascade might be impaired because of genetic predisposition and microbiota composition.

ACKNOWLEDGMENTS

The authors wish to thank Richard P. Darveau, Department of Periodontics, University of Washington, for the *E. coli* strains used in this study.

REFERENCES

- Niess JH, Brand S, Gu X, et al. CX3CR1-mediated dendritic cell access to the intestinal lumen and bacterial clearance. *Science*. 2005;307:254–258.
- Lelouard H, Fallet M, de Bovis B, et al. Peyer's patch dendritic cells sample antigens by extending dendrites through M cell-specific transcellular pores. *Gastroenterology*. 2012;142:592–601 e593.
- Iwasaki A. Mucosal dendritic cells. *Annu Rev Immunol*. 2007;25:381–418.
- Kraehenbuhl JP, Neutra MR. Epithelial M cells: differentiation and function. *Annu Rev Cell Dev Biol*. 2000;16:301–332.

5. McDole JR, Wheeler LW, McDonald KG, et al. Goblet cells deliver luminal antigen to CD103+ dendritic cells in the small intestine. *Nature*. 2012;483:345–349.
6. Inaba K, Inaba M, Naito M, et al. Dendritic cell progenitors phagocytose particulates, including bacillus Calmette-Guerin organisms, and sensitize mice to mycobacterial antigens in vivo. *J Exp Med*. 1993;178:479–488.
7. Svensson M, Stockinger B, Wick MJ. Bone marrow-derived dendritic cells can process bacteria for MHC-I and MHC-II presentation to T cells. *J Immunol*. 1997;158:4229–4236.
8. Sallusto F, Cella M, Danieli C, et al. Dendritic cells use macropinocytosis and the mannose receptor to concentrate macromolecules in the major histocompatibility complex class II compartment: downregulation by cytokines and bacterial products. *J Exp Med*. 1995;182:389–400.
9. Pierre P, Turley SJ, Gatti E, et al. Developmental regulation of MHC class II transport in mouse dendritic cells. *Nature*. 1997;388:787–792.
10. Trombetta ES, Mellman I. Cell biology of antigen processing in vitro and in vivo. *Annu Rev Immunol*. 2005;23:975–1028.
11. Muller M, Fink K, Geisel J, et al. Intestinal colonization of IL-2 deficient mice with non-colitogenic *B. vulgatus* prevents DC maturation and T-cell polarization. *PLoS One*. 2008;3:e2376.
12. Kawai T, Akira S. The role of pattern-recognition receptors in innate immunity: update on Toll-like receptors. *Nat Immunol*. 2010;11:373–384.
13. Bron PA, van Baarlen P, Kleerebezem M. Emerging molecular insights into the interaction between probiotics and the host intestinal mucosa. *Nat Rev Microbiol*. 2012;10:66–78.
14. Cario E, Podolsky DK. Differential alteration in intestinal epithelial cell expression of toll-like receptor 3 (TLR3) and TLR4 in inflammatory bowel disease. *Infect Immun*. 2000;68:7010–7017.
15. Hausmann M, Kiessling S, Mestermann S, et al. Toll-like receptors 2 and 4 are up-regulated during intestinal inflammation. *Gastroenterology*. 2002;122:1987–2000.
16. Hart AL, Al-Hassi HO, Rigby RJ, et al. Characteristics of intestinal dendritic cells in inflammatory bowel diseases. *Gastroenterology*. 2005;129:50–65.
17. Rakoff-Nahoum S, Paglino J, Eslami-Varzaneh F, et al. Recognition of commensal microflora by toll-like receptors is required for intestinal homeostasis. *Cell*. 2004;118:229–241.
18. Perse M, Cerar A. Dextran sodium sulphate colitis mouse model: traps and tricks. *J Biomed Biotechnol*. 2012;2012:718617.
19. Melgar S, Karlsson L, Rehnstrom E, et al. Validation of murine dextran sulfate sodium-induced colitis using four therapeutic agents for human inflammatory bowel disease. *Int Immunopharmacol*. 2008;8:836–844.
20. Berndt BE, Zhang M, Chen GH, et al. The role of dendritic cells in the development of acute dextran sulfate sodium colitis. *J Immunol*. 2007;179:6255–6262.
21. Qualls JE, Tuna H, Kaplan AM, et al. Suppression of experimental colitis in mice by CD11c+ dendritic cells. *Inflamm Bowel Dis*. 2009;15:236–247.
22. Bron PA, Tomita S, van S II, et al. Lactobacillus plantarum possesses the capability for wall teichoic acid backbone alditol switching. *Microb Cell Fact*. 2012;11:123.
23. Grangette C, Nutten S, Palumbo E, et al. Enhanced antiinflammatory capacity of a Lactobacillus plantarum mutant synthesizing modified teichoic acids. *Proc Natl Acad Sci U S A*. 2005;102:10321–10326.
24. Bainbridge BW, Coats SR, Pham TT, et al. Expression of a Porphyromonas gingivalis lipid A palmitoyltransferase in Escherichia coli yields a chimeric lipid A with altered ability to stimulate interleukin-8 secretion. *Cell Microbiol*. 2006;8:120–129.
25. Park BS, Song DH, Kim HM, et al. The structural basis of lipopolysaccharide recognition by the TLR4-MD-2 complex. *Nature*. 2009;458:1191–1195.
26. Lambert JM, Bongers RS, Kleerebezem M. Cre-lox-based system for multiple gene deletions and selectable-marker removal in Lactobacillus plantarum. *Appl Environ Microbiol*. 2007;73:1126–1135.
27. Krajina T, Leithauser F, Reimann J. MHC class II-independent CD25+ CD4+ CD8alpha beta+ alpha beta T cells attenuate CD4+ T cell-induced transfer colitis. *Eur J Immunol*. 2004;34:705–714.
28. Wittmann A, Autenrieth IB, Frick JS. Plasmacytoid dendritic cells are crucial in bifidobacterium adolescentis-mediated inhibition of Yersinia enterocolitica infection. *PLoS One*. 2013;8:e71338.
29. Husebye H, Halaas O, Stenmark H, et al. Endocytic pathways regulate Toll-like receptor 4 signaling and link innate and adaptive immunity. *EMBO J*. 2006;25:683–692.
30. Geisel J, Kahl F, Muller M, et al. IL-6 and maturation govern TLR2 and TLR4 induced TLR agonist tolerance and cross-tolerance in dendritic cells. *J Immunol*. 2007;179:5811–5818.
31. Annacker O, Coombes JL, Malmstrom V, et al. Essential role for CD103 in the T cell-mediated regulation of experimental colitis. *J Exp Med*. 2005;202:1051–1061.
32. Frank DN, Pace NR. Gastrointestinal microbiology enters the metagenomics era. *Curropin Gastroenterol*. 2008;24:4–10.
33. Rath HC, Schultz M, Freitag R, et al. Different subsets of enteric bacteria induce and perpetuate experimental colitis in rats and mice. *Infect Immun*. 2001;69:2277–2285.
34. Martin M, Katz J, Vogel SN, et al. Differential induction of endotoxin tolerance by lipopolysaccharides derived from Porphyromonas gingivalis and Escherichia coli. *J Immunol*. 2001;167:5278–5285.
35. Tauber SC, Nau R. Immunomodulatory properties of antibiotics. *Curr Mol Pharmacol*. 2008;1:68–79.
36. Kaser A, Zeissig S, Blumberg RS. Inflammatory bowel disease. *Annu Rev Immunol*. 2010;28:573–621.
37. Machiels K, Joossens M, Sabino J, et al. A decrease of the butyrate-producing species Roseburia hominis and Faecalibacterium prausnitzii defines dysbiosis in patients with ulcerative colitis. *Gut*. 2014;63:1275–1283.
38. Hornef MW, Frisan T, Vandewalle A, et al. Toll-like receptor 4 resides in the Golgi apparatus and colocalizes with internalized lipopolysaccharide in intestinal epithelial cells. *J Exp Med*. 2002;195:559–570.
39. Hornef MW, Normark BH, Vandewalle A, et al. Intracellular recognition of lipopolysaccharide by toll-like receptor 4 in intestinal epithelial cells. *J Exp Med*. 2003;198:1225–1235.
40. Kagan JC, Su T, Horng T, et al. TRAM couples endocytosis of Toll-like receptor 4 to the induction of interferon-beta. *Nat Immunol*. 2008;9:361–368.
41. Chabot S, Wagner JS, Farrant S, et al. TLRs regulate the gatekeeping functions of the intestinal follicle-associated epithelium. *J Immunol*. 2006;176:4275–4283.
42. Vaishnava S, Behrendt CL, Ismail AS, et al. Paneth cells directly sense gut commensals and maintain homeostasis at the intestinal host-microbial interface. *Proc Natl Acad Sci U S A*. 2008;105:20858–20863.
43. Dubuquoy L, Jansson EA, Deeb S, et al. Impaired expression of peroxisome proliferator-activated receptor gamma in ulcerative colitis. *Gastroenterology*. 2003;124:1265–1276.
44. Cario E, Gerken G, Podolsky DK. Toll-like receptor 2 controls mucosal inflammation by regulating epithelial barrier function. *Gastroenterology*. 2007;132:1359–1374.
45. Fukata M, Chen A, Klepper A, et al. Cox-2 is regulated by Toll-like receptor-4 (TLR4) signaling: role in proliferation and apoptosis in the intestine. *Gastroenterology*. 2006;131:862–877.
46. Waidmann M, Bechtold O, Frick JS, et al. Bacteroides vulgatus protects against Escherichia coli-induced colitis in gnotobiotic interleukin-2-deficient mice. *Gastroenterology*. 2003;125:162–177.
47. Sporri R, Reis e Sousa C. Inflammatory mediators are insufficient for full dendritic cell activation and promote expansion of CD4+ T cell populations lacking helper function. *Nat Immunol*. 2005;6:163–170.
48. Reis e Sousa C. Dendritic cells in a mature age. *Nat Rev Immunol*. 2006;6:476–483.
49. Foster SL, Hargreaves DC, Medzhitov R. Gene-specific control of inflammation by TLR-induced chromatin modifications. *Nature*. 2007;447:972–978.
50. Yanagawa Y, Onoe K. Enhanced IL-10 production by TLR4- and TLR2-primed dendritic cells upon TLR restimulation. *J Immunol*. 2007;178:6173–6180.
51. Varol C, Vallon-Eberhard A, Elinav E, et al. Intestinal lamina propria dendritic cell subsets have different origin and functions. *Immunity*. 2009;31:502–512.
52. Bogunovic M, Ginhoux F, Helft J, et al. Origin of the lamina propria dendritic cell network. *Immunity*. 2009;31:513–525.
53. Coombes JL, Siddiqui KR, Rancibia-Carcamo CV, et al. A functionally specialized population of mucosal CD103+ DCs induces Foxp3+ regulatory T cells via a TGF-beta and retinoic acid-dependent mechanism. *J Exp Med*. 2007;204:1757–1764.
54. Matteoli G, Mazzini E, Iliev ID, et al. Gut CD103+ dendritic cells express indoleamine 2,3-dioxygenase which influences T regulatory/T effector cell balance and oral tolerance induction. *Gut*. 2010;59:595–604.